AAEC/E203

AAEC/E203

AUSTRALIAN ATOMIC ENERGY COMMISSION

RESEARCH ESTABLISHMENT
LUCAS HEIGHTS

A FEASIBILITY STUDY OF THE AUTOMATIC CONTROLS FOR A PEBBLE BED REACTOR POWER STATION

by

C.P. GILBERT

L.B. ACKLAND

November 1970

ISBN 0 642 99392 0

AUSTRALIAN ATOMIC ENERGY COMMISSION

RESEARCH ESTABLISHMENT

LUCAS HEIGHTS

A FEASIBILITY STUDY OF THE AUTOMATIC CONTROLS FOR A PEBBLE BED REACTOR POWER STATION

by

C. P. GILBERT

L. B. ACKLAND*

ABSTRACT

A conceptual automatic control system proposed for a Pebble Bed Reactor power station is examined to establish its feasibility over a wide range of operating conditions. Frequency response methods, making use of a digital computer, are used to design the various control loops, and the resulting system is examined on an analogue computer.

It is shown that the system could be made to work under all conditions, but that much improved operation would result if certain modifications were introduced.

*Now at Central Scientific Laboratory, State Electricity Commission of Victoria

National Library of Australia card number and ISBN 0 642 99392 0

PREFACE

This study formed part of a research project of the Australian Atomic Energy Commission to evaluate the prospects of a high temperature gas-cooled power reactor system based on the circulating pebble-bed concept.

The study was completed in 1966 but publication of the report was delayed when one author (C.P.G.) was posted overseas and the other (L.B.A.) left the service of the Commission. The work has now been reviewed by the authors and is issued to complete this part of the record of the study.

CONTENTS

(continued)

CONTENTS (continued)

(continued)

1. INTRODUCTION

In 1966 the Australian Atomic Energy Commission completed a feasibility study of a high temperature gas-cooled reactor system. A conceptual design of a 200 megawatt central power station was prepared (Ebeling and Hayes 1967) based on the pebble bed reactor concept (P.B.R.).

This report describes a computer study of the automatic control of the power station. The general arrangement of the control system originally proposed by the consultants* is shown in Figure 1. Heat is transferred from the reactor to the boiler by a closed carbon dioxide ('gas') coolant circuit, and from the boiler to the turbine by a closed steam/water circuit.

1.1 Scope of This Study

This is a feasibility study whose sole object is to show that a regulating system of the type shown in Figure 1 can be designed to give satisfactory operation, and no attempt is made to optimise the controls to give the best performance. Such optimisation would be quite pointless in view of the uncertainty in some of the equations and in much of the data on which the study is based, whereas the feasibility study simply has to show that satisfactory controls are possible.

There are three main automatic controllers:–

(1) Reactor outlet gas temperature controller, which moves the reactor control rods.

(2) Boiler outlet gas temperature controller, which adjusts the gas blower speed.

(3) Steam pressure controller, which varies the feed-water flow.

These should operate so that any disturbances to the desired operating levels are removed quickly and accurately with no excessive correcting action.

The equipment on the steam side of the boiler, particularly the turbine and governor, is largely conventional. It is not considered in detail in this study and can be approximated fairly crudely if the loading effect upon the boiler is accurately represented.

With minor exceptions the work concerns a linearised model and the results apply to small perturbations only, not to large transients. However, under normal operating conditions, no large transients will arise. Large changes can only enter the system during load changing as described in Section 1.3 and this is normally done so slowly that the actual 'disturbance' is quite small. The system has been examined for three values of temperature coefficient of reactivity, at 100%, 60% and 20% of full load, the latter being the minimum load at which automatic control would normally be attempted. Fault studies and station start-up and shut-down are not considered in this report.

1.2 The Three Controls

To protect the reactor and the boiler, the temperature of the reactor outlet gas has to be held constant at a reference temperature not exceeding 865 °C. This maximum value is used during full load operation, but a lower value is permissible at reduced load or for other reasons. Any error between the actual reactor outlet gas temperature and the reference temperature is used to adjust the position of the control rods and hence the heat generated in the core, so that the temperature error is reduced to zero.

The temperature of the gas leaving the boiler should also be held constant. Since the inlet and outlet temperatures are normally constant the rate of heat transfer to the boiler can only be varied by altering the mass-flow of the gas, which entails altering the speed of the blowers (circulators). Thus any error in boiler outlet gas temperature is used to control the blower speed in such a way that the temperature returns to its correct value.

*Babcock and Wilcox Australia Ltd.

The outlet pressure on the steam side of the boiler should be held at some fixed reference level depending on load conditions. Any pressure error is used to operate the feed-water valve and hence to vary the amount of water forced into the boiler by the feed pump. This returns the steam pressure to its desired value.

It was also originally proposed to make use of the flow error obtained by comparing the steam mass-flow measured close to the turbine throttle-valve with the feed-water mass-flow. Though not essential, the transient values of this error could be used to reduce the amplitude of the pressure fluctuations caused by load changes and other disturbances. For the reasons given in Section 1.5, this feature was not investigated. Since the boiler is of the once-through type there is no water/steam drum, and so no external means of measuring or controlling the water ('boiling') level. In fact, the effective water level is maintained in the correct region mainly by the arrangement of the boiler tubes themselves. Should too much steam be extracted and the pressure fall, the water level would tend to fall as steam was flashed off. However, since the heat transfer to steam is much less than that to water, a falling water level causes a reduction in heat input: this tends to prevent the fall in water level but accentuates the fall in pressure.

The pressure referred to above is that of the high-pressure, superheated steam, measured at the boiler outlet. Steam is also fed from the first stage of the turbine back to the boiler for reheating, and then returned to the second stage of the turbine. This reheat circuit, not shown in Figure 1, has no direct influence on the automatic control and has little effect on the transient loading of the boiler under the conditions examined here (see Section A2.7.4). Exhaust steam from the turbine is condensed and is then available for return to the boiler via the feed pump.

The two gas temperatures and the steam pressure are normally constant apart from slight continuous fluctuations (noise) and transient disturbances such as those due to load changing as described below.

The speed of the alternator may be held constant by a governor, which uses any speed error to operate the turbine throttle-valve and hence admit more or less steam. The power delivered by the alternator under these conditions depends only on the load connected to its terminals: this may be known as 'load following' operation. However, the speed (that is, frequency) of a base load station is often maintained solely by the alternator's self-synchronising action with the other stations with which it is in parallel. The alternator is assumed to be connected to an 'infinite bus', that is, a system which is so large that the station being examined can have no influence upon it. The power delivered is then determined simply by the setting of the throttle valve which is now disconnected from the governor. If the throttle is opened, more steam is admitted and there is a transient increase in alternator speed. This results in the alternator returning to its original speed but at a different phase (load) angle to the rest of the system, and thus is able to deliver the additional power corresponding to the increased steam flow. However, the throttle is normally left fully open, and so the station operates at constant load.

A change in station load has only one direct effect on the system of Figure 1, and that is to alter the setting of the throttle valve and thus change the steam flow.

1.3 Effect of a Load Change

The general mode of operation of the automatic controls can be illustrated by describing a change in station load. With the system operating in a steady state, a step increase in station load has the following effects. For the most part they are simultaneous and superimposed upon each other. Analogue computer results (Figure 47) show a load change of the type described below.

The opening of the throttle valve increases the steam flow, and hence the steam pressure falls as does the water level in the boiler. The pressure error causes an increased flow of feed water which tends to force the water level in the boiler to rise, but the resulting increase in heat transfer minimises this rise and increases the outlet pressure, until it approaches its previous value.

Since the water level has a large influence on the heat transfer it also has a large influence on the temperature of the gas leaving the boiler. This temperature rises slightly to begin with (correspond-

ing to the initial fall in water level) and then falls markedly as the feed flow is increased and more heat is transferred. The water level will only take up its correct position when both the boiler inlet and outlet gas temperatures and the steam pressure have returned to their normal values.

The fall in boiler outlet gas temperature causes an increase in gas flow and since this tends to remove more heat from the reactor, the reactor outlet gas temperature falls. This change is opposed by a withdrawal of the control rods, leading to increased heat generation, which sustains the original change in load. The final position of the rods depends upon the temperature coefficient of reactivity.

If the whole system is stable, it will eventually settle down to a new steady state with the two gas temperatures and the steam pressure at exactly their previous values, and the water level slightly higher than before. The gas and steam flows will both be larger than before, approximately in proportion to the load change, and the neutron power and the fuel temperature will both be increased.

1.4 Outline of the Study

The general procedure was as follows: First, the linearised differential equations describing the system were used to find the transfer functions of the various components, which were then combined into a control loop, allowing the particular controller to be designed using graphical frequency-response techniques. This work was based on the use of the digital programme LINCAN (Gilbert, unpublished AAEC report). The original linear differential equations and the newly designed controller were then simulated on an analogue computer and the transient behaviour examined for typical disturbances, giving a clear understanding of the system operation and a precise check on the digital calculations. Where a range of values of a given parameter had to be considered the above process was repeated several times.

First the reactor outlet gas temperature controller was designed, then the boiler outlet gas temperature controller, and finally the pressure controller. The interaction between these three systems was examined to various extents at the same time. The frequency response work is described in Section 2: only sufficient data to illustrate the general design process are given, but the basic transfer functions are listed in Appendix 3. The analogue models used to check the individual control loops are not described except to compare the linear and non-linear rod servo-mechanisms.

A complete analogue model representing the whole of the system was constructed and used to study typical (small) operating transients for the whole power station. The system had to be simplified slightly before it could be fitted onto the analogue computer, but so much was known about its behaviour at that stage that no loss in accuracy was involved (Appendix A2.3). The analogue model is described in Section 3, which also presents the transients recorded. These summarise the general dynamic performance of the system over a wide range of operating conditions.

In both Sections 2 and 3, the equations used to describe the systems are introduced with the minimum of discussion. However, the choice of equations, their derivation and the values used for their coefficients are discussed at some length in Appendix 2.

1.5 Accuracy and Reliability of Results

Three sources of error can be identified:

1. Errors in computation.

2. Incorrect data.

3. Unsuitable equations.

In this study, computation errors have been virtually eliminated since at least two completely separate computing methods have been used throughout. From the digital frequency-response results it was possible to predict graphically the gain and frequency at which a given closed loop should just become unstable. The analogue model was then given this value of gain, and the frequency of the resulting constant-amplitude oscillation measured. Any disagreement in these results indicated a

computation error which was found before work was continued. Final agreement within a few per cent was normal, the largest part of the error being associated in most cases with the graphical procedures, not the results themselves. Also, a few selected transients obtained from the analogue computer were recalculated digitally as a further check, and again close agreement was achieved. These checks were applied to the complete analogue model as well as to the individual control loops.

It was known when the study was started that much of the data was speculative, giving the possibility of error. In some cases, a range of values was investigated (for example, temperature coefficient of reactivity) and in others, a pessimistic value was used (for example, thermocouple time constants). To allow for any data changes not covered in these ways, care was taken to ensure that the control designs were not critically dependent upon data values and could easily be readjusted. It must be recalled that provided a closed loop system is stable its overall behaviour is not markedly affected by changes in the properties of the components of the loop (apart from those in the feedback path). Thus most components of a conservatively designed control loop may be changed by a factor of up to 2 without causing a gross change in the properties of the closed loop. In this respect then, the results relating to a closed loop system are much more accurate than might be supposed from a consideration of the possible errors in the data used to obtain them. In fact, many of the calculated transfer functions could have been simplified considerably without loss of accuracy, but at the time there was no method of simplification which did not require considerable labour and so the full transfer functions were used. Of the data used, those relating to the steam circuit are probably the least reliable, particularly for the lower values of load.

Only the third source of error, unsuitable equations, need be considered seriously. Discrepancies between the system to be described and the set of equations used to describe it (the model) are inevitable. Even if an accurate model is available, some simplification and linearisation is essential to keep the volume of computation within manageable limits. Appendix 2 provides comments on the equations used but the following general observation should be kept in mind.

In this study, point equations have been used, that is, all spatial effects have been neglected except that transportation delays are introduced to represent the effects of the low coolant velocity. The equations used to represent the reactor and its heat transfer are similar to those used satisfactorily in many previous control studies.

The boiler equations are of a well accepted form but unfortunately they had to be modified from a set relating to a drum-type boiler. The only important discrepancy is that the self-regulating property of the water level mentioned in Section 1.2 is ignored in the equations so that no effective mass balance is included in the steam/water circuit. This gave some inconsistencies in the values of the feed water flow and made it impossible to investigate the steam flow/feed flow comparison mentioned above. However, in practice a flow error would only be used if it improved the situation so its omission does not affect the validity of the overall conclusions of the study.

It is ironic that the most conventional part of the system (turbine, throttle valve etc.) proved the most difficult for which to obtain reliable equations and data. This is mainly because the boiler controls in a conventional power station are well understood and studies of the type being considered here are hardly justified. The only purpose of the equations describing this part of the system is to provide a realistic load for the boiler, that is, to permit the calculation of the steam flow in terms of the steam pressure. The equations do this adequately provided the temperature of the super-heated steam does not vary. It is almost certain that in a practical power station the degree of super-heat would be controlled in some way even if it did not have to be kept constant. However, in the system proposed in Figure 1 no means of temperature control is indicated and the temperature of the super-heated steam does vary. Where such variations cause inconsistencies in the results, a subsidiary load disturbance is introduced whose main result is to ensure that there is no sustained change in the steam temperature.

Even the most pessimistic assessment of the suitability of the equations representing the steam/water circuit would reveal that their general form is not inappropriate and that the magnitude of the time constants involved is of the correct order. This study shows that suitable controllers can

be designed under a range of conditions and there is little doubt that suitable, although possibly different, systems could be designed even if large changes were eventually found to be necessary in the steam-side equations.

2. DESIGN OF THE FEEDBACK CONTROLS

2.1 Description of the Reactor

The first control loop to be examined in detail is that associated with the regulation of the reactor outlet gas temperature. It operates by adjusting the control rods so as to vary the heat generated in the core. The components are shown in the top left-hand corner of Figure 2 to which the following discussion refers. All symbols are listed in Appendix 1 and the values of all equation coefficients are given in Appendix 2.

Since it has no direct influence on control, except for a slight change in gain, the by-pass flow around, rather than through the pebble bed is not considered separately from the main coolant flow. Also, the designs given in this section neglect the effect of temperature and flow variations introduced by the rest of the system except where indicated.

The reactivity, which determines the future heat generation (neutron power) in the reactor, is considered in three parts:

$$\rho = \rho_c + \rho_t + \rho_d \qquad (1)$$

The components on the right hand side of Equation 1 are associated respectively with the controller output (rod position), the reactor fuel temperature via the temperature coefficient of reactivity, and a reactivity disturbance which could be due, for instance, to a sudden change in the random assembly of the fuel balls. The perturbation in neutron power P_n about a fixed power level ${}_sP_n$ is given by the linearised neutron kinetics equations:

$$\frac{dP_n}{dt} = \frac{1}{\ell^*}\left[\rho\, {}_sP_n - \beta P_n\right] + \sum_{i=1}^{3} \lambda_i x_i \qquad (2)$$

$$\frac{dx_i}{dt} = -\lambda_i x_i + \frac{\beta i}{\ell^*} P_n \quad , \quad i = 1,2,3. \qquad (3)$$

The frequency response derived from these equations is given in Figure 3, which shows the ratio of normalised neutron power $P_n / {}_sP_n$ to reactivity ρ over the frequency range of interest.

The perturbations in fuel and coolant temperatures (T_f and T_c) resulting from a change in neutron power, together with those caused by gas flow changes and variations in the gas inlet temperature, are given by

$$\frac{dT_f}{dt} = AP_n - B(T_f - T_c) - G\,W_g \qquad (4)$$

$$\frac{dT_c}{dt} = C(T_f - T_c) - D(T_{co} - T_{ci}) - FW_g \qquad (5)$$

and

$$T_c = \frac{1}{2}(T_{co} + T_{ci}) \quad . \qquad (6)$$

The frequency response of T_f / P_n which is essentially a simple time constant of about 100 seconds (the fuel time constant) is shown in Figure 3.

Owing to the low gas velocities, the outlet gas temperature T_{co} does not change as soon as more heat enters the coolant but only after the heated gas has had time to flow out of the reactor. The resulting time delay is represented by an all-pass (Padé) transfer function so that the delayed reactor outlet gas temperature at the thermocouple T_{cod} is given by

$$\frac{T_{cod}}{T_{co}} = \frac{1-s\tau_r/2}{1+s\tau_r/2} , \tag{7}$$

giving the frequency response shown in Figure 3. The gain change compared with T_f is very small, but large phase lags caused by the delay are evident.

Changes in fuel temperature have a direct influence on the reactivity due to the temperature coefficient of reactivity α, thus

$$\rho_t = \alpha T_f . \tag{8}$$

When this work was being done, α was not known accurately and so the three values $-5\text{x}10^{-5}$, 0, and $+5\text{x}10^{-5}$ per °C were used. Results are given for all these values although the more accurate estimates now available show that $-5\text{x}10^{-5} < \alpha < 0$.

Figure 4, which gives the frequency responses relating outlet gas temperature to reactivity, shows the influence of the temperature coefficient of reactivity which effectively forms an inherent closed loop as shown in Figure 2. When α is zero, (curve 1), the response is simply the sum of curves 1 and 3 from Figure 3. A negative coefficient removes the high gains and the large phase lags which occur at low frequencies with $\alpha(0)$, resulting in curve 2 of Figure 4. The inherent closed loop is unstable with $\alpha(+)$, but as discussed below, this loop can be made stable if a flux signal is used for control purposes. T_{co}/ρ is then as shown in curve 3 of Figure 4. At high frequencies, the fuel temperature does not change significantly so the value of α has little effect.

2.2 Reactor Control – Flux Loop

All the components of the control loop so far described are essential parts of the reactor which the control designer cannot alter. Provided unavoidable practical limitations are kept in mind, the remaining components can be designed to suit the control requirements.

The actual mechanism which moves the control rods is first assumed to be a linear servomechanism which positions the rods and introduces reactivity ρ_c as demanded by a low power signal ρ_{cd}. The transfer function

$$\frac{\rho_c}{\rho_{cd}} = \frac{1}{(1+s)(1+s)} \tag{9}$$

has two one-second time constants which represent a mechanical time lag associated with the inertia of the moving parts, and the time constant of the final power amplifier. A more practical type of rod servo is considered briefly in Section 2.4.

As mentioned above, with $\alpha(+)$, the uncontrolled reactor is unstable. An increase in flux raises the fuel temperature which in turn increases the reactivity and leads to a further increase in flux. It is possible to rectify this situation by detecting the increase in flux (power), or the associated temperature rise, and using it to drive the control rods so as to decrease the total reactivity. By this means, the effective temperature coefficient can be given any desired value (all the time the equipment associated with the control loop is working). The time lags associated with a temperature change and its measurement would make it necessary to use phase advance if a temperature signal were to be used for stabilisation purposes. This is not desirable in practice owing to possible overloading and noise difficulties and so flux is measured in this case as shown in Figure 2. The reactivity change demanded by a given flux (power) perturbation is

$$\frac{\rho_f}{P_n} = \frac{h}{1 + sk} \tag{10}$$

and the total demanded rod reactivity is

$$\rho_{cd} = \rho_e - \rho_f \ . \tag{11}$$

With the flux path connected, and using the values given in Appendix A2.5, the frequency response of Figure 4, curve 3, was obtained, and this is used in all future work when the temperature coefficient of reactivity is positive. For the other values of α the flux stabilising path is not used, although it would improve the control characteristics significantly with $\alpha(0)$.

2.3 The Reactor Outlet Gas Temperature Controller

Since the design process is common for all values of α and all load levels, unless there are special features to be emphasised only the full load case with $\alpha = -5 \times 10^{-5}$ per °C which is thought to be the one most likely to be of interest, is described in this section.

The measured value of the reactor outlet gas temperature at the thermocouple output T_{com} is given by

$$\frac{T_{com}}{T_{cod}} = \frac{1}{1 + s\tau_t} \ , \tag{12}$$

where τ_t is the thermocouple time constant, and the error between the actual temperature and the reference temperature, (see Figure 2) which would be represented by a voltage in practice, is

$$T_{he} = T_{hr} - T_{com} \ . \tag{13}$$

The frequency response T_{cod}/ρ at full load for negative α is shown in Figure 5. It is identical to the corresponding curve in Figure 4 but the effects of the rod servo and the thermocouple are also shown, giving T_{com}/ρ_{cd}. Thus, every component is taken into account except the controller itself. For comparison, the curves for 60% and 20% load are shown. The main change in performance with load level is the slower heat transfer due to lower gas speeds, both in the reactor and in the thermocouple.

A proportional-plus-integral controller is used, having the transfer function

$$\frac{\rho_e}{T_{he}} = g_h \frac{(1 + s\tau_h)}{s\tau_h} \ . \tag{14}$$

The frequency response is shown in Figure 6 with g_h given the arbitrary value of 316/°C (50 dB) and $\tau_h = 10$ sec. The integral term gives a very high gain at low frequencies and hence zero steady state temperature error for any setting of the temperature reference, despite changes in the steady operating levels of the power, inlet gas temperature or gas flow, or any changes in the reactor properties. The 90° phase lag associated with the integral term is not important at low frequencies, and at medium and high frequencies the proportional term predominates and no phase lag is introduced.

The frequency response T_{com}/ρ_{cd} is transferred from Figure 5 to Figure 6 (curve 2) and is there combined with the controller response to give the complete open loop frequency response (curve 3). Figure 6 then shows that with $g_h = 10^{-5}$/°C (–100 dB) and $\tau_h = 10$ sec., the phase and gain margins are 78° and 12 dB respectively. The gain scale of the complete open loop is then that shown on the right, and the transient behaviour is illustrated in Figure 10.

In fact, such a controller must be adequately stable over a range of values of gain, since the effective gain of the system will vary during operation (even at a given power level) in a manner which is not under the designer's control. For instance,

(1) the rod effectiveness (reactivity per unit displacement) varies with rod insertion, and

(2) if a non-linear rod servo is used (as is likely) the effective gain will be different for signals of different amplitudes.

For the case with $\alpha(-)$, provided the gain does not exceed the values specified in Appendix 2, no direct problems will arise, but the temperature correction will be much slower if the gain is reduced excessively and interaction with the boiler could give instability. The case with $\alpha(+)$ is similar except that the gain of the flux loop may also vary (see Section 2.4).

The $\alpha(0)$ case is different because there is no internal feed-back loop. Figure 7 (curve 2) shows that the phase lag of the complete open loop including the controller approaches 180° at low frequencies, and so a low gain will give a very poor transient response as well as being slow. The present full load design has an acceptable gain range of 5 to 1 for the reactor on its own which is adequate, but it is probable that if α were very close to zero in practice, the flux loop would be used to improve the control characteristics.

Although the reactor on its own could be controlled satisfactorily under all conditions using the methods described above, it was later found (Section 2.5) that owing to interaction with the boiler, instability could not be prevented at 20% load with zero temperature coefficient. For this one case, phase advance had to be introduced and the controller of Equation 14 was replaced by

$$\frac{\rho_e}{T_{he}} = g_h \cdot \frac{1 + s\tau_h}{s\tau_h} \cdot \frac{1 + 71s}{1 + 18s} \qquad (15)$$

Figure 7 shows the open loop response without the controller (curve 3), and with it (curve 4).

In all cases, with the controller in place, what becomes important is the frequency response seen by the rest of the system, when there are changes in the gas inlet temperature and gas flow, that is, the closed-loop frequency responses $\frac{T_{cod}}{T_{ci}}$ and $\frac{T_{cod}}{W_g}$. Typical values are shown in Figure 8 (100% load, $\alpha(-)$). The gain approaches zero at low frequencies of course, because, given time, the controller removes any error in outlet gas temperature caused by T_{ci} or W_g. This helps to reduce interaction between the various control loops provided the controller is not too slow.

2.4 Non-Linear Rod Drive

In practice it is unlikely that a linear servo-mechanism of the type described by Equation 9 would be used to position the control rods. It would be far more convenient to have a drive motor capable of being run in either direction at some fixed speed corresponding to the maximum rate of rod removal permitted by safety considerations. The static characteristics of the system would then be as shown in Figure 9a. Large temperature errors would switch the motor on and cause the rods to move with the maximum velocity, but there would be a dead zone such that for small errors, that is, when

$$-a° < T_{he} < a° \quad ,$$

the rods would be stationary. A dead zone is essential in practice, (1) to prevent continuous small oscillations, by allowing the motor to stop when $T_{he} \to 0$; and (2) because noise in the thermocouple signal would cause continuous erratic motor switching, resulting in excessive component wear. However, if the dead zone is too large, excessive power transients are caused by quite small disturbances since the temperature error can rise to a° before any correcting action is taken. Usually, the dead zone is adjusted in a given situation so that occasional noise peaks just cause rod operation as in the figure.

The describing function of the static characteristic of Figure 9a (that is, the plot of 'gain' to a sinusoidal signal as a function of signal amplitude) is shown in Figure 9b together with its effective value in the presence of noise. This shows that some gain is available even with small temperature errors if a is correctly adjusted.

A controller of this type was designed as an alternative to the linear system discussed in Section 2.3 for the full load case with $\alpha(-)$. The maximum rate of change of reactivity was taken as 2×10^{-5}/sec and artificial noise was used to just penetrate the dead zone of $\pm 0.5\,^{\circ}C$. Equation 9 was replaced by

$$\frac{\rho_c'}{\rho_{cd}} = \frac{1}{s} \cdot \frac{1}{1+s} \quad , \tag{16}$$

which gave a velocity proportional to the relay output after a time lag of one second representing the inertia and friction of the mechanism. The blocks of Figure 9c replaced the relevant parts of Figure 2.

The controller was a simple gain g_h' instead of that given by Equation 14. The value of gain was not critical, but was taken as 1.5×10^{-6} (sec $^{\circ}C)^{-1}$. Transient responses taken from an analogue model of the reactor only are shown in Figures 10, 11 and 12. The first illustrates the behaviour of the linear controller described in Section 2.3, and the other two that of the non-linear controller: the latter have a periodic 'dither' signal applied to represent the effect of noise.

A $10\,^{\circ}C$ step in temperature reference is imposed in Figures 10 and 11. Although the linear controller gives a peak of rod velocity approaching 4×10^{-5}/sec compared with a maximum of only 1.2×10^{-5}/sec for the non-linear controller, the response of the latter is not significantly worse.

The detailed behaviour of the non-linear controller depends upon the size of the disturbance. For instance the $5\,^{\circ}C$ step in temperature reference illustrated in Figure 12 shows a closer resemblance to the linear case (Figure 10) than to the non-linear case with a $10\,^{\circ}C$ step (Figure 11).

Since the general character of these responses was the same, the linear controller was used in all subsequent calculations because it was so much easier to handle theoretically. However, it is clear that similar results could have been obtained using the non-linear rod servo. In any case, comparison of Figures 31 and 40 for the analogue model of the complete system, show that the overall behaviour is largely unaffected by the type of controller used so long as it is of suitable design.

Similar non-linear controllers could have been designed for the other values of temperature coefficient of reactivity. The only significant difference would have been that with $\alpha(+)$, a given noise level would have required a smaller dead zone than in the case described, resulting in more frequent erratic rod movements. This is because a certain minimum gain is essential for the flux loop to keep the system stable. Under these circumstances, equipment wear would be worse, but the resulting temperature and flux transients would be essentially the same as those given by the linear system.

2.5 The Control of the Boiler Outlet Gas Temperature

There are six boilers and six blowers in the proposed power station (Ebeling and Hayes 1967) but for control purposes these have been combined into one equivalent boiler and one equivalent blower.

Any change in reactor outlet gas temperature introduced by the reactor will effectively move along the hot gas duct at the same speed as the gas stream and enter the boiler. Subsequently, it will emerge from the boiler in modified form and will return to the reactor via the cold gas duct and the blower (Figure 1). At the reactor, this temperature change will form an inlet gas temperature disturbance and will cause a further change in outlet gas temperature. The dominant features of this inherent feedback loop are the transportation delays in the hot gas duct, the boiler and the cold gas duct, and other effects introduced by the boiler (see Figure 2).

The effect of the blower is negligible from this point of view, and the boiler properties are discussed below. For simplicity, the delay in the boiler is considered as two equal delays at input and output, the former being included with the hot gas duct delay. The equations used to represent the delays are:

$$\frac{T_{g0}}{T_{cod}} = \frac{1 - s\tau_1/2}{1 + s\tau_1/2} \tag{17}$$

$$\frac{T_{gout}}{T_{g4}} = \frac{1 - s\tau_2/2}{1 + s\tau_2/2} \tag{18}$$

$$\frac{T_{ci}}{T_{gout}} = \frac{1 - s\tau_3/2 + s^2\tau_3^2/9.1 - s^3\tau_3^3/78.6 + s^4\tau_3^4/1420}{1 + s\tau_3/2 + s^2\tau_3^2/9.1 + s^3\tau_3^3/78.6 + s^4\tau_3^4/1420} \tag{19}$$

As discussed in Appendix 2, these equations give pessimistic stability results, but even so the effect of feedback via the cold gas duct was found to be so small that it was neglected in the frequency-response designs although included in the final analogue model.

The boiler equations dealing with both the gas and steam sides together, are:

$$\frac{dT_{m1}}{dt} = \phi_1 T_{g0} + \phi_2 T_2 + \phi_3 T_{m1} + \phi_4 W_g + \phi_5 W_2 \tag{20}$$

$$\frac{dT_{m2}}{dt} = \phi_6 T_{g0} + \phi_7 T_4 + \phi_8 T_{m1} + \phi_9 T_{m2} + \phi_{10} W_g + \phi_{11} W_2 \tag{21}$$

$$\frac{dT_{m3}}{dt} = \phi_{12} T_{g2} + \phi_{13} T_4 + \phi_{14} T_{m3} + \phi_{15} W_g \tag{22}$$

$$\frac{dT_{m4}}{dt} = \phi_{16} T_{m4} + \phi_{17} T_{g2} + \phi_{18} T_{m3} + \phi_{19} T_6 + \phi_{20} W_g + \phi_{21} W_4 \tag{23}$$

$$T_{g2} = \phi_{22} T_{g0} + \phi_{23} T_{m1} + \phi_{24} T_{m2} + \phi_{25} W_g \tag{24}$$

$$T_{g4} = \phi_{26} T_{g2} + \phi_{27} T_{m3} + \phi_{28} T_{m4} + \phi_{29} W_g \tag{25}$$

$$\frac{dT_2}{dt} = \phi_{30} T_{m2} + \phi_{31} T_4 + \phi_{32} T_2 + \phi_{33} W_2 \tag{26}$$

$$\frac{dT_4}{dt} = \phi_{34} T_{m3} + \phi_{35} T_4 + \phi_{36} T_6 + \phi_{37} W_2 \tag{27}$$

$$\frac{dT_6}{dt} = \phi_{38} T_{m4} + \phi_{39} T_6 + \phi_{40} W_4 \tag{28}$$

$$P = \gamma T_4 \quad . \tag{29}$$

Figure 13 shows the frequency response T_{gout}/W_g which is the response concerned in the present control loop. Relatively small differences exist between the characteristics at the various load levels, but the delays due to the low gas velocities have a major effect.

The thermocouple used to measure the boiler outlet gas temperature is similar to that used at the reactor ourlet, and so the measured temperature is

$$\frac{T_{gom}}{T_{gout}} = \frac{1}{1 + s\tau_t} \quad . \tag{30}$$

Figure 2 shows that the error in the boiler outlet gas temperature is

$$T_{ce} = T_{cr} - T_{gom} \quad . \tag{31}$$

The blower, which is a variable speed gas circulator, is assumed to produce a mass flow proportional to a demand signal W'_g . A time constant of 30 seconds is associated with the inertia of the rotating parts, and so the gas mass-flow is

$$\frac{W_g}{W'_g} = \frac{1}{1 + 30s} \quad . \tag{32}$$

It should be noted that a flow change is introduced simultaneously throughout the whole gas circuit, and is not propagated round the system with the speed of the gas flow as are temperature changes. In the block diagram of Figure 2 then, the blower operates directly on the heat transfer properties of the reactor and the boiler. Thus, a change in blower speed not only produces the wanted change in boiler outlet temperature but also causes a variation in the boiler inlet temperature, which the reactor outlet temperature controller reduces to zero only after a significant time.

The latter effect can be ignored only if the reactor outlet gas temperature controller operates quickly enough. For this reason the integral term in that controller (τ_h) must not be too large, particularly when the temperature coefficient of reactivity is positive. As an example, if the value of τ_h given in Appendix 2 for the 100% load $\alpha(+)$ case is increased by a factor of ten times, instability results even when the gain g_h is correctly adjusted. At 20% load, adjustment of τ_h alone is not sufficient to prevent instability with $\alpha(0)$ and the controller has to be speeded up by the use of phase advance as mentioned below (Equation 15).

Figure 14 shows the full load response T_{gout}/W_g again, and also shows the effect of including the other components progressively, that is, the thermocouple, the blower and the controller. The latter is of the same form as the reactor outlet temperature controller, and

$$\frac{W'_g}{T_{ce}} = g_c \frac{(1 + s\tau_c)}{s\tau_c} \quad . \tag{33}$$

With $g_c = 1.59 \times 10^5$ lb/hr/°C and $\tau_c = 100$, the phase margin is 36° and the gain margin 12 dB (Figure 14). As for the reactor outlet gas temperature control loop, no sustained temperature error results from any disturbance to the system or any change in system properties, provided the loop remains stable.

2.6 Pressure Control Loop

Referring to Figure 2 the gas flow to the boiler is determined by the boiler outlet gas temperature controller, and the inlet gas temperature by the reactor outlet gas temperature controller. Before the steam pressure can be calculated, the feed-water and steam flows must both be known. The feed flow is adjusted by the pressure controller, whose design is discussed in this section. The steam flow W_2 can be found by regarding the steam ducts, the throttle valve and the turbine as an impedance forming a load on the boiler to which the pressure P is applied.

In Section 1.1 it was stated that there are two ways in which the alternator speed can be controlled, the resulting incremental loads on the boiler being quite different. Since the governor-controlled type of operation was found to be the less stable of the two, it is the only one to be examined here. In Section A2.7 it is shown that the equations relating pressure and flow are

$$\frac{dW_2}{dt} = \frac{1}{M}(P - P_2) \tag{34}$$

$$\frac{dP_2}{dt} = \frac{1}{C_1}(W_2 - Q_2) \tag{35}$$

$$Q_2 = \frac{1}{R_H}(P_2 - P_3) \tag{36}$$

$$\frac{dP_3}{dt} = \frac{1}{C_2}(Q_2 - P_3/R_B) \quad , \tag{37}$$

and a typical frequency response is shown in Figure 15.

With the steam-duct loop connected and the boiler outlet gas temperature controller operating, the frequency response P/W_4 of the boiler at full load is as shown in Figure 16. The feed-water valve has a time constant of 5 seconds and so the relationship between the actual feed flow and the demanded feed flow is

$$\frac{W_4}{W_4'} = \frac{1}{1+5s} \quad . \tag{38}$$

This has only a slight effect at the frequencies at which the control design is performed.

The pressure controller shown in Figure 2 is of the same type as those used before, and so

$$\frac{W_4'}{P_e} = g_p \frac{(1 + s\tau_p)}{s\tau_p} \quad , \tag{39}$$

where the error between the actual pressure and the reference value is given by

$$P_e = P_r - P \quad . \tag{40}$$

Figure 16 shows that with $g_p = 794$ lb/hr/p.s.i. and $\tau_p = 100$ sec. the gain and phase margins are 10 dB and 56° respectively.

The effect of the steam duct and turbine becomes increasingly important as the load is reduced, the two part-load cases being unstable in the absence of the pressure controller. (A small pressure disturbance increases slowly but at an increasing rate). If the controller is used, but the gain is too low, slow sinusoidal oscillations build up. The minimum period for this type of behaviour, which corresponds to the minimum gain for stability, is about 7½ hours for a 60% load, so that in the case of controller breakdown, manual correction would be quite straightforward. Figure 17 shows the 60% load frequency responses equivalent to the 100% case of Figure 16.

3. THE ANALOGUE MODEL

3.1 General

The set of transfer functions and differential equations representing the dynamic behaviour of the reactor and plant were used to derive an analogue model, which was set up on a PACE 231R computer. The full set of first order differential equations used on the analogue is given in Appendix 4. Although some of the transfer functions, such as single lags, are sufficiently well known not to require

expansion into the differential equations prior to modelling, the full expansion was needed for the Fortran programme with which the checking runs were made on the digital computer. Further, the calculation of complete static checks requires the full expansion.

For convenience the model has been drawn in three sections (Figures 18, 19, 20) corresponding to more or less related sections of the power station which are discussed more fully below.

3.2 Circuit Description

3.2.1 The reactor and reactor control loop (Figure 18)

Equations 1 to 17 are modelled in this section, which consists of the reactor core in both nuclear and thermodynamic sections, the reactor and hot gas duct delays, reactor outlet gas temperature controller, and control rod servos. The reactor kinetics circuit contains four time constants, and Equations 2 and 3 have been modified to the form

$$\frac{dP_n}{dt} = \frac{1}{\ell^*}\left[{}_sP_n\,\rho - \beta P_n + \sum_{i=1}^{3}\beta_i X_i\right]$$

$$\frac{dX_i}{dt} = -\lambda_i X_i + \lambda_i P_n$$

where $$X = \frac{\lambda \ell^*}{\beta} x$$

which is more convenient for representation since all parameters appear directly in the model; the delayed neutron concentrations are not required explicitly. Lack of equipment prevented using the more accurate

$$\frac{dX_i}{dt} = \lambda_i[P_n - X_i]$$

but for these studies the effect of the kinetics is not as critical as for wide range transients. The fairly small value of ℓ^* implies a high loop gain in the kinetic section, and this was achieved by decreasing the integrating capacitor by a factor of 10. The heat transfer equations for the core are represented by the circuits associated with integrators 90 and 91, inputs from the blower (gas flow) and cold gas duct inlet temperature variations being obtained from Section 3. Fuel temperature coefficients of 0 and $\pm 5 \times 10^{-5}$ are introduced by SW20, the flux feedback path is introduced through SW10, and the gain and time constant for the reactor controller are set by Q25 and Q17. When dealing with low gains (as in the 20% model) some re-arrangement of the circuit was necessary to prevent overloading of the controller integral term, but these changes have not been shown on the circuit. Because it was required for output presentation, the rate of change of reactivity introduced by the control rods was derived explicitly on the model.

3.2.2 The boiler (Figure 19)

The rearranged boiler equations (20 to 29) are modelled without any controls, and form a minimum equipment representation. Although they are not entirely satisfactory because of a number of rather low coefficient values, any significant improvement would have required the use of excessive equipment. The difficulty simply lies in the inherently long time constants associated with the boiler operation, and for the low power runs the whole model was time scaled up by a factor of 10, resulting in a reduced computation time and an increased accuracy.

3.2.3 The boiler controllers, steam duct, and turbine (Figure 20)

Included in this section are the delays associated with the passage of the gas through the boiler and through the return duct to the reactor; the measurement of boiler outlet temperature and its control

via the feed valve; and the steam duct and turbine equations representing the load on the boiler. As with the reactor gas delays, Padé approximations have been used for both boiler and cold gas duct.

The rest of this section is straightforward, although the rather high gains associated with the steam duct resonance meant that the steam flow term (W_2) was rather noisy. When used for recording, this signal was taken through a 1 second lag which removed the high frequency components while not degrading the recorded trace.

As is customary, some of the fixed coefficients which appear separately in the list of analogue equations have been grouped together for convenience in the model, and in these cases the potentiometer listing (Appendix 4) gives the combined value and its derivation.

3.3 Computer Scaling

(a) Amplitude

The model was produced using machine unit scaling, so that 1 M.U. = 100 volts and each variable was normalised to its maximum expected value. This scaling method produces computer outputs which can be regarded as normalised physical quantities. A list of the maxima used is given in Table 1 of Appendix 4. Some early studies with the reactor model alone used maxima which were changed with mean power level in order to optimise coefficients. However, the set of boiler equations was received with existing fixed scale units and consequently some parts of the model have fixed maxima which become rather too large for use in the low power runs. Some loss of accuracy results from this but the effect is not serious. For the final model whose circuit diagrams are presented here, all scales remain fixed except for those temperatures associated with the reactor gas flows and reactor core.

(b) Time

The runs on the 100% model were performed in real time but for the lower power models, particularly the 20% one, the inherently long time constants associated with the much reduced gas flows meant that computation times became excessively long, and many of the coefficients became too low for reasonable accuracy in setting-up. Both the 60% and 20% runs were therefore made at ten times real time. All time scaling was performed by effectively decreasing the integrator time constants. This was done by changing the integrating capacitors except for that part of the model representing the boiler, where the opportunity was taken to improve many of the coefficient values.

(c) Equipment Limitations

The set of equations to be modelled contained some thirtythree time constants whereas the PACE 231R has provision for only thirty integrators. Consequently, some use was made of passive elements in conjunction with normal summers to provide the additional time constants. Although operationally rather inconvenient, the overall accuracy of the model was not impaired.

3.4 Non-Linear Controller

The circuit shown in Figure 21 gives details of the non-linear reactor controller used for some of the 100% studies. The temperature error, T_{he}, from the reactor outlet gas was examined by comparators M0 and M1, adjusted to give a dead band equivalent to $\pm 0.5\,^{\circ}C$, and the relay contacts associated with each comparator provided the correctly phased input to drive the rod servo motor (represented by 70 and 60) up or down. Hence, after the time lag associated with the servo itself, the rods were driven at their maximum speed in the required direction as determined by the sign of the temperature error. The value of the rod speed was governed by Q17. To provide a more effective control, and also to make the model more realistic, some artificial noise was introduced into the temperature error signal. The resulting wave form was then used as an input to the comparators and the subsequent small oscillations of the rod drive when the temperature error was small effectively reduced the temperature offset to a very low value.

3.5 Results

3.5.1 General comments

With an analogue model of the complexity of that shown in Figures 18, 19 and 20, many tests could be performed and great care had to be exercised in selecting suitable records for presentation here.

To begin with, apart from those relating to the non-linear rod servo, no results are given for the models of individual sections of the system. Similarly, although the complete model was checked for stability as indicated by the frequency response work, none of the results are shown here. Next, the number of points at which disturbances could be applied were restricted to those at which inputs could be expected in practice, that is,

1. Reactivity disturbance ρ_d
2. Reactor outlet gas temperature reference T_{hr}
3. Boiler outlet gas temperature reference T_{cr}
4. Steam pressure reference P_r
5. Turbine (that is, alternator) load.

Even then, with three load levels to be considered, and three values of α, a minimum of 45 records would result even if only one form of disturbance (that is, step, ramp etc.,) was applied and if only one time scale was considered. In fact, many of the records taken had no features of particular interest, and to reduce the bulk of this report only about half the records actually examined are presented here. The aim is to illustrate the general performance of the system, rather than to attempt a complete description of any one aspect.

Thus, since the reactor characteristics become less important as the input disturbance moves towards the turbine end of the model, where the system responses are much slower than those of the reactor, only those results involving changes in ρ_d and T_{hr} are shown for all three values of α. Changes involving T_{cr}, P_r and load are shown only with $\alpha(-)$, the corresponding $\alpha(+)$ and $\alpha(0)$ cases being very similar.

Output Variables

To facilitate comparison between differing runs, an attempt was made to keep most of the significant variables on display on all records, and to vary the choice of only one or two, depending upon the particular disturbance. Accordingly, the channels indicated below always show the same variable (though not necessarily to the same scale):

CHANNEL NO.	1	2	3	4	5	6	7	8
VARIABLE	P_n	T_f	T_{go}			W_g	P	

Channel 1 is at the top of each set of results and channel 8 at the bottom. Channel 8 is used for the error signal corresponding to the disturbance, or the effective load change, or the total reactivity of the system, whichever is appropriate for a particular run.

Scaling

Although the use of a linearised model means that only the relative magnitudes of disturbance and response are of importance, for the sake of ease of comparison, some effort has been made to provide equally scaled plots of the same output variable for similar runs. Also, disturbances for similar runs have been normalised to equal values. In the case of the load changes, the magnitude of the change is approximately the same percentage of the steady state load level. However, because the model

response often changes significantly as the operating conditions are altered, it has been necessary to increase the scale of some output plots to show sufficient detail. The amplitude scaling is shown on each set of results for each output channel and is always given in physical units, or where applicable, a dimensionless ratio. Because all runs are deviations from the steady state, all output traces have a centre zero.

Time Scales

The wide range of time constants in the original system and the variation of these with steady state power level made it rather difficult to display satisfactorily all the detailed time behaviour on one output trace and also to keep the time scales the same for all power runs. Since for the most part, the shorter time constants are associated with the reactor while the longer ones are associated with the boiler, it has been possible to speed up the recorder for at least some of those runs more closely associated with the reactor behaviour and thus display rather more detail than would otherwise have been the case. Generally, the time scales for the low power runs are longer than for the others, and for these, the whole model was time scaled to avoid excessive computation time. All runs are shown in real time, and are marked in seconds per unit length of chart. The start of each transient is also indicated.

3.5.2 Arrangement of Figures

	Figure	Power Level %	Disturbance	α
Group 1	22	100	Step of + 1 x 10^{-4} in ρ_d	–
	23	100	"	0
	24	100	"	+
	25	60	"	–
	26	60	"	0
	27	60	"	+
	28	20	"	–
	29	20	"	0
	30	20	"	+
Group 2	31	100	Step of + 2 °C in T_{hr}	–
	32	100	"	0
	33	100	"	+
	34	60	"	–
	35	60	"	0
	36	60	"	+
	37	20	"	–
	38	20	"	0
	39	20	"	+
	40*	100	Step of + 5 °C in T_{hr}	–

* ON–OFF Reactor Controller

(continued)

	Figure	Power Level %	Disturbance	α
Group 3	41	100	Step of + 1°C in T_{cr}	–
	42	60	"	–
	43	20	"	–
Group 4	44	100	Step of + 100 psi in P_r	–
	45	60	"	–
	46	20	"	–
Group 5	47	100	Step of + 1% in load	–
	48	100	Ramp 1% in 4000 secs	–
	49	60	Step of + 1%	–
	50	60	Ramp 1% in 5000 secs	–
	51	20	Step of + 1%	–
	52	20	Ramp 1% in 10000 secs	–

3.5.3 Discussion

Group 1 Reactivity Step Figures 22 to 30

The first group of figures shows the effects of a step change of 1×10^{-4} in the reactivity of the core at each of the three levels of operation, with each of the three values of α.

At each power level, the behaviour of the core is determined primarily by the temperature coefficient; the initial power surge is more or less rapidly reduced, either directly for α(–) or α(+) (using the direct flux feedback) or indirectly for α(0) through the control of the reactor outlet gas temperature.

The transient rise in reactor outlet temperature (T_{go}) causes an initial rise in both boiler outlet gas temperature and steam pressure. Subsequent controller action reduces the gas and feed water flows, leading to a slow fall in steam pressure.

Since the time scales of the records were chosen to show the reactor performance clearly, there is not sufficient time in some cases for the records to show the eventual return to zero of the pressure and flow variations.

In all six cases involving α(–) or α(+), the power output from the reactor is returned to its steady level so rapidly that there is little energy transferred to the boiler and steam sections; consequently there is little disturbance to the secondary side despite the relatively large value of reactivity step involved, and the differences in response are due largely to the differences in time constants associated with the slower coolant flows as the power level drops (Figures 23, 26, and 29). (Note that there are different time scales).

With α(0), the control is rather slower, since the rods do not act to reduce the power surge until the thermocouple in the gas steam is able to respond. Hence the magnitude and duration of the surge is greater, much more energy is transferred to the boiler, and the changes which occur are considerably larger. For example, the pressure changes at 20% load rise from about 10 psi for α(–) or α(+) to nearly 150 psi for α(0). Such changes, in this case amounting to about 15% of the steady pressure level may or may not be acceptable; they could be reduced readily by using the direct flux feedback for temperature coefficients approaching zero.

Only in one case (100%, $\alpha(+)$, Figure 24) does the required rate of change of reactivity become larger than the maximum (2×10^{-5}/sec) permitted by the design, but since the initial step of 1×10^{-4} is arbitrary and rather large, no loss of performance from the limitation would be expected in practice. High rod rates are to be expected in this case, since the control reactivity has to oppose the disturbance and also counteract the effects of any fluctuations in fuel temperature, and thus has to change at a rate at least equivalent to the fuel temperature variations.

Group 2 Reactor Outlet Gas Temperature Reference Step (Figures 31 to 40)

The runs of the second group of figures show the response of the system to a step change of 2 °C in the reference level for the reactor outlet gas temperature. As with Group 1, all combinations of steady power level and temperature coefficient are examined, since here also it is primarily the behaviour of the reactor which determines the behaviour of the system, although α has much less effect on the overall result.

Following an increase in the temperature reference, the control rods are temporarily withdrawn to raise the reactor power, their subsequent motion and final position depending upon α. Both fuel and reactor gas outlet temperature rise (the latter by exactly 2 °C) and the gas flow is reduced to prevent a corresponding rise in the boiler outlet gas temperature, thus maintaining a constant power transfer to the boiler. A small change in steam pressure is removed by a reduction in the feedwater flow: since the power is unchanged, this indicates that the temperature of the superheated steam has increased slightly.

In the final example in this group, (Figure 40), the controller regulating the reactor outlet gas temperature has been replaced by the non-linear relay controller described in Section 2.4. Although the disturbance is larger than that in Figure 31 (normalising of the non-linear run is not possible) the general forms of the transients for both are very similar, and it is evident that from the point of view of the system it is immaterial which controller was used.

Group 3 Boiler Outlet Gas Reference Step (Figures 41, 42 and 43)

The results of the two previous groups of figures have indicated that the form of the transients measured on the model is largely determined by the position at which the disturbance is introduced, and in general, as the primary disturbance occurs further from the reactor so do the characteristics of the reactor become less important. In other words, the effect of the direct control of the reactor by the rods tends to produce a "standard" reactor whose external behaviour is largely independent of any internal differences.

Accordingly, the effects of a change in the reference temperature for the boiler outlet gas are shown only for the $\alpha(-)$ case. Although not shown, additional runs confirm this essential independence of behaviour of the value of α.

When the reference temperature is increased (by 1 °C for the results shown here) the immediate effect is to produce an increase in gas flow through the circuit, so as to increase the boiler outlet gas temperature. The reactor core temperatures initially fall, but are subsequently increased by a temporary rise in reactor power, and the rise in inlet gas temperature; the final average fuel temperature is a little higher than before the change. On the steam side, the initial drop in heat transferred from the gas [$T_{g0} - T_{gout} < 0$] causes a drop in steam pressure, but this is eventually restored by changes in the feed flow; the relative slowness of this action leads to a certain amount of overshoot, which becomes more marked as the time constants increase with lower load values, but this is unavoidable because of the physical behaviour of the system components. Again, an increase in steam temperature is indicated.

Group 4 Pressure Reference Step (Figures 44, 45 and 46

The three runs in this group of figures show the response of the system to a step increase in the reference steam pressure of 100 psi. As in Group 3 the transients are examined for a reactor with $\alpha(-)$ operating at the three steady power levels.

The pressure error causes an initial increase in feed water flow (not shown), so that the increased heat transfer drops the outlet gas temperature on the primary side of the boiler. This drop is reflected in the reactor temperatures, and these are corrected by the reactor controller; it also produces an immediate increase in gas flow (W_g) and this supplies the additional heat needed to bring the steam pressure up to the new level.

These records are more difficult to interpret owing to the interaction of two effects, and while the speed of one (the governor) is substantially independent of load level, that of the other becomes progressively slower as load is reduced. Under constant power output conditions, a rise in steam pressure is accompanied by a reduction in steam flow, due to the governor action described in Section A2.7.1. However, in this case the positive pressure error increases the feedwater flow in order to raise the pressure to its new reference level. Because of these two opposing effects large differences exist in the transient responses for the different load levels.

In the 20% case the gain of the pressure controller is so low that the pressure error first increases, but is finally reduced by the integral action.

Group 5 Load Changes (Figures 47–52)

There are three pairs of results in this Group, each referring to one of the three operating levels of a reactor with $\alpha(-)$.

For each level, a change in station load was produced at the turbine end of the model, either as a step, or more realistically, a ramp terminating at the same final load level as the step.

In each case a load change of 1% was used, the duration of the ramps being

100% Model	4000 seconds
60%	5000 "
20%	10,000 "

The general behaviour of the system to a step load change can be seen by referring to Figure 47. The removal of more steam from the boiler (an increase in steamflow W_2) causes the steam pressure to fall, so opening the feed valve to admit more water. Consequently the gas flowing from the boiler has more heat exhausted from it, and this in turn produces a drop in temperature, causing both gas flow and reactor power to increase until eventually the required increase in power is produced in the reactor core. Since the core outlet temperature and boiler outlet temperature both return to their original levels, the increased power is transferred by an increased gas flow through the boiler, and appears as an increased steam flow at the original pressure level.

The results at all three power levels are quite similar, though as anticipated the general slowness with which the controls can act at the lowest power level leads to transient disturbances which persist for a long time.

When the disturbance is changed to a ramp, the response is such that there is little difference between the results at the three power levels; during the ramp, the controlled variables are offset by an amount depending upon the actual rate of change, and then return to their correct levels.

The smooth changes illustrated in these runs are typical of those expected under normal operating conditions.

4. CONCLUSIONS AND RECOMMENDATIONS

Control of a power station based on a proposed pebble bed reactor system has been examined extensively. The system has no unusual dynamic features and no difficulty was experienced in designing effective automatic controls except at low power levels (less than 30% of full load). While the system could be controlled at these power levels, the response was so slow that it is doubtful if it would be of much value in practice.

Although much of the information used in deriving the model was of a preliminary nature, and would almost certainly be subject to change, there is no reason to suppose that automatic control would become significantly more difficult, even if the parameters were changed by a factor of as much as two.

The proposed system has two main defects which should be kept in mind when future systems are specified. First no provision is made for controlling the temperature of the super-heated steam. While this is not objectionable from a theoretical point of view, it would not be acceptable in practice, owing to the possibility of excessive temperatures in the super-heater and turbine. Automatic temperature control is quite feasible: for instance the steam temperature could be used to adjust the reactor outlet gas temperature reference level, but such a system would alter the boiler dynamics and thus possibly invalidate some of the work in this study. The second major defect is the lack of any means of adjusting the reactor power directly from incoming load changes. As the system stands, the reactor power cannot be changed until the load disturbance has propagated through the system by way of changes in pressure and temperature, all of which ideally should remain constant. If signals indicating a load change were fed directly to the reactor, the transient disturbance to the system would be much smaller and would decay more quickly. The flow error system mentioned in Section 1.2 is one way in which this could be achieved.

Although the flux feedback loop was used in these studies only when the temperature coefficient of the reactor was positive, it is evident that it should also be used not only when the effective coefficient is zero, but also when it is negative if it is likely to change appreciably during operation.

In this connection, it should also be noted that while it would be reasonable to change the gain and time constants of the controllers with changing load level, major changes of their form would not be possible. In practice, this might mean a less than optimum control at the lowest levels of operation where the need for an alternative form of controller would be most marked.

5. REFERENCES

Campbell, D.P. (1958). – Process Dynamics. John Wiley and Sons Inc. New York.

Denton, W.H., Robinson, C.H. and Tibbs, R.S. (1963). – The heat transfer and pressure loss in fluid flow through randomly packed spheres. AERE–R 4346.

Ebeling, D.R. and Hayes, J.E. (1967). – The engineering design and analysis of a beryllia-moderated Pebble Bed Reactor. Mech. and Chem. Eng. Trans. Institution of Engineers, Australia MC3 (1): 119–137.

APPENDIX 1

LIST OF SYMBOLS

All variables are perturbations about a steady state level unless preceded by the subscript s. Thus T_{co} is a perturbation about ${}_sT_{co}$.

All coefficients are incremental values, and the normal units are °C, seconds, psi, lb/hr and cm. Reactivity ρ and power P_n are ratios, ${}_sP_n$ being set at unity for each power level.

Coefficients	Variables	Nomenclature
A °C/sec		rate of change of T_f per unit P_n
a °C		dead zone of non linear rod controller
B sec^{-1}		rate of change of T_f per unit difference $(T_c - T_f)$
C sec^{-1}		rate of change of T_c per unit difference $(T_f - T_c)$
C_1 (lb/hr) $(psi/sec)^{-1}$		'Capacitance' associated with the steam duct
C_2 (lb/hr) $(psi/sec)^{-1}$		'Capacitance' associated with the throttle valve time constant
D sec^{-1}		rate of change of T_c per unit difference $(T_{co} - T_{ci})$
	D_i	concentration of the i^{th} group of delayed neutron emitters
d cm		distance between two points in a gas circuit
d_i		Padé constants for cold gas duct delay, i = 1–4
F (°C/sec) $(lb/hr)^{-1}$		rate of change of T_c per unit W_g
G (°C/sec) $(lb/hr)^{-1}$		rate of change of T_f per unit W_g
g		unspecified gain
g_c (lb/hr)/°C		gain of boiler outlet gas temperature controller
g_h $°C^{-1}$		gain of reactor outlet gas temperature controller
g_h' $(sec\ °C)^{-1}$		gain of non-linear hot gas temperature controller
g_p (lb/hr)/psi		gain of steam pressure controller
h $(kW\ thermal)^{-1}$		gain of flux filter
k sec		flux filter time constant
K_i		constants in heat transfer analogue equations
ℓ^* sec		mean prompt neutron lifetime
M(psi)sec$(lb/hr)^{-1}$		'inductance' associated with steam duct
	P psi	boiler outlet pressure

(continued)

Coefficients	Variables	Nomenclature
	P_n	normalised neutron power (flux)
	P_e psi	pressure error
	P_r psi	pressure reference
	P_2, P_3 psi	pressures arising in the steam duct equations
	Q_2 lb/hr	steam mass flow at throttle valve
R_B psi(lb/hr)$^{-1}$		effective throttle valve 'resistance'
R_H psi(lb/hr)$^{-1}$		effective turbine 'resistance'
	s	Laplace operator
	T_{ce} °C	boiler outlet gas temperature error
	T_{ci} °C	gas temperature at reactor inlet
	T_{co} °C	gas temperature at reactor outlet (with no delay)
	T_{cod} °C	delayed gas temperature at reactor outlet
	T_{com} °C	measured value of T_{cod}
	T_{cr} °C	boiler outlet gas temperature reference
	T_f °C	average fuel temperature
	T_{gom} °C	measured value of T_{gout}
	T_{gout} °C	delayed value of T_{g4}
	T_{g0} °C	gas temperature at boiler inlet
	T_{g1} to T_{g3} °C	gas temperature within the boiler
	$\bar{T}_{g1}$ to $\bar{T}_{g4}$ °C	average gas temperature within the boiler
	T_{g4} °C	gas temperature at boiler outlet
	T_{he} °C	reactor outlet gas temperature error
	T_{hr} °C	reactor outlet gas temperature reference
	$\bar{T}_{m1}$ to $\bar{T}_{m4}$ °C	average metal temperatures within the boiler
	T_1 to T_7 °C	steam and water temperature within the boiler
	T_4 °C	steam saturation temperature
	$\bar{T}_1$ to $\bar{T}_7$ °C	average steam and water temperatures within the boiler
	t sec	time

(continued)

Coefficients	Variables	Nomenclature
	v cm/sec	gas velocity
	W_g lb/hr	mass-flow of coolant gas
	W'_g lb/hr	demanded gas flow
	W_{s1} lb/hr	steam flow within the boiler
	W_2 lb/hr	steam flow external to the boiler
	W_4 lb/hr	feed-water flow
	W'_4 lb/hr	demanded feedwater flow
	x_i	concentration of delayed neutron emitters, $i = 1,2,3$
	X_i	normalised concentration of delayed neutron emitters
α °C^{-1}		temperature coefficient of reactivity
β		sum of delayed neutron fractions $\Sigma \beta_i$
β_i		delayed neutron fractions, $i = 1,2,3$
γ psi/°C		relationship of pressure to saturation temperature
λ_i sec^{-1}		decay rate of delayed neutron emitters, $i = 1,2,3$
	ρ	total reactivity
	ρ_c	reactivity introduced by control rods
	ρ_{cd}	total demanded reactivity
	ρ_d	reactivity disturbance
	ρ_e	reactivity demanded by controller
	ρ_f	reactivity demanded by flux filter
	ρ_t	reactivity due to fuel temperature changes
τ sec		unspecified time
τ_b		time constant of main gas circulator
τ_c sec		integral time constant of boiler outlet gas temperature controller
τ_f		time constant of feed water valve
τ_h sec		integral time constant of reactor outlet gas temperature controller

(continued)

Coefficients	Variables	Nomenclature
τ_p sec		integral time constant of steam pressure controller
τ_r, sec		effective gas delay in reactor
τ_t sec		thermocouple time constant
τ_1 sec		delay in hot gas duct and first half of boiler
τ_2 sec		delay in second half of boiler
τ_3 sec		delay in cold gas duct and plenum
ϕ_n sec^{-1}; (°C/sec)(lb/hr)$^{-1}$		boiler equation coefficients, n = 1,....40

APPENDIX 2

DERIVATION OF THE MODEL

A2.1 The Reactor (Equations 1 to 6)

A2.1.1 General

The source of energy for the whole plant is the fissile material of the fuel in the reactor core. The fission energy appears as heat within each fuel ball, which is in turn transferred to the coolant gas flowing upwards through the core between the packed balls.

In the actual reactor, the rate at which heat is produced within any given ball and the rate at which heat is transferred to the gas varies widely throughout the core, so that no two sections will be alike in temperature, coolant properties and so on. To provide a model in which these individual variations were all represented would be not only unrealistic in view of the preliminary nature of the parameters which are available but also impractical because of the excessive complication of the resulting calculations. Consequently, an average model has been adopted in which the overall properties are assumed to apply at all points throughout the core.

A2.1.2 Neutron Kinetics (Equations 2 and 3)

The time behaviour of the fission process has been represented by the standard form of the neutron kinetics equations:

$$\frac{dn}{dt} = \frac{\rho - \beta}{\ell^*} n + \Sigma \lambda_i D_i$$

$$\frac{dD_i}{dt} = \frac{\beta_i n}{\ell^*} - \lambda_i D_i \quad ,$$

where n represents the neutron density and $\lambda_i D_i$ is the contribution from the delayed neutron emitters. The heat produced in the fuel has been assumed proportional to the neutron density and n may be replaced by $({}_sP_n + P_n)$ where ${}_sP_n$ is the steady state power level and P_n is the variation from this. Substituting for n and putting x_i for the perturbation in D_i, gives, after linearising, Equations 2 and 3.

For studies involving large uncontrolled departures from criticality, it is necessary to know accurately the values of ℓ^*, β_i and λ_i, and to provide an adequate simulation of the delayed neutron groups since they play a significant part in determining the changes in the neutron population during any transient. In these control studies however, the importance of the groups is considerably reduced by the external control feedback, so that it is possible to reduce the number of groups considered without loss of accuracy.

Three have been used, the relative abundance and decay constants for each being shown in following Table:

PROMPT NEUTRON LIFETIME $\ell^* = 2 \times 10^{-4}$ sec

GROUP	FRACTION β	DECAY CONSTANT λ
1	0.1352×10^{-2}	$0.2920\ sec^{-1}$
2	0.1000×10^{-2}	$0.0360\ sec^{-1}$
3	0.0170×10^{-2}	$0.0020\ sec^{-1}$

These values were derived from a more comprehensive set of 12 groups suggested by Nicholls (unpublished AAEC report), which included a number of photoneutron groups from the Be (γ,n) reaction. Some weight was given to these longer lived contributions in deriving Group 3 above, but in the present studies their effect is virtually negligible.

A2.1.3 Reactivities and Reactor Control (Equation 1)

In any reactor there are many different ways in which the effective multiplication constant of the fissile assembly may be varied, not all of which are directly available for control purposes. In these studies, all reactivities have been divided into two main groups. The first, called "control rod reactivity", represents the normal method (of whatever kind, such as absorber or fuel movement) by which the reactor power level is to be raised or lowered by a control signal during normal running. The second, called "temperature reactivity", represents the internal mechanisms such as variation in fission or absorption cross section with neutron energy over which the operator has no direct control. The magnitudes of these internal effects are not well known at this stage so it was assumed that they are all directly a function of fuel ball temperature, and a range of values from $\alpha = 5 \times 10^{-5}$ per °C through zero to -5×10^{-5} per °C was used.

The total values of control reactivity available or necessary depend generally on the predictions of large transient studies and, except possibly for demanded reactivity rates of change, do not place any real limits on these small perturbation studies. However, in Section 2.4, dealing with a simple on/off rod controller, the asymptotic rates of reactivity removal or addition used were chosen to be the maximum permitted by the reference design (see A2.4.3). Reactivity changes have been assumed to be linear with rod movement and independent of each other. When required, a disturbance ρ_d (Equation 1) has been added to that produced by the control ρ_c and the temperature coefficient ρ_t. The nature of such a disturbance need not be postulated as it is used simply to demonstrate the system response.

A2.1.4 Heat Transfer in the Reactor Core (Equations 4,5,6)

The complex relationships which determine the way in which the energy produced within the fuel is eventually transferred to the gas leaving the reactor cannot be at all accurately set up within the physical limits imposed by the model. Fortunately, within the framework of the existing study, such detail is not necessary and it has been possible to make use of drastic simplifications without losing the essential characteristics of the reactor system. These characteristics are:

1. The reactor core contains a large number of oxide balls in each of which the heat producing fuel particles are more or less evenly distributed.

2. The majority of the external surface of each fuel ball is exposed to the coolant gas as it passes through the reactor core.

3. The coolant gas consequently becomes heated to an extent dependent upon the parameters of the oxide and coolant and the heat transfer relationship existing at the oxide – coolant interface.

Accordingly, the fuel and coolant properties have been averaged over the whole volume of the core, whose steady state behaviour may then be described by the two equations:

$$\begin{pmatrix}\text{heat increase}\\ \text{in fuel}\end{pmatrix} = \begin{pmatrix}\text{fission energy}\\ \text{released}\end{pmatrix} - \begin{pmatrix}\text{heat transferred}\\ \text{to coolant}\end{pmatrix}$$

$$\begin{pmatrix}\text{heat increase}\\ \text{in coolant}\end{pmatrix} = \begin{pmatrix}\text{heat transferred}\\ \text{from fuel}\end{pmatrix} + \begin{pmatrix}\text{heat brought}\\ \text{into core}\end{pmatrix} - \begin{pmatrix}\text{heat taken out}\\ \text{from core}\end{pmatrix},$$

from which, by expansion, the primary heat transfer equations for the reactor core used in these studies were obtained:

$$(1-v)\, V_T \rho_f\, C_f \frac{dT_f}{dt} = E - h_{fc} \frac{3(1-v)}{r_b} V_T (\bar{T}_f - \bar{T}_c)$$

$$v\, V_T \rho_c C_c \frac{d\bar{T}_c}{dt} = h_{fc} \frac{3(1-v)}{r_b} V_T (T_f - \bar{T}_c) + W_g C_c (T_{ci} - T_{co}) ,$$

where

v	=	voidage of packed bed
V_T	=	total core volume
ρ	=	density of fuel and coolant, as subscripted
C	=	specific heat of fuel and coolant, as subscripted
T_f	=	average fuel temperature
$\bar{T}_c$	=	average coolant temperature = $\frac{1}{2}(T_{ci} + T_{co})$
h_{fc}	=	average heat transfer coefficient between fuel and coolant
r_b	=	ball radius
W_g	=	coolant mass flow
T_{ci}, T_{co}	=	coolant inlet and outlet temperatures
E	=	power produced in the core.

In particular, $\frac{3(1-v)V_T}{r_b}$ represents the heat transfer surface available in the core, that is, the surface area of the fuel balls, and h_{fc} is the heat transfer coefficient at this surface.

This coefficient has been taken from Denton et al. (1963) and is assumed to be in the form:

$$h_{fc} = 0.58\, G\, C_c \left(\frac{2Gr_b}{\mu_c}\right)^{-0.3} \left(\frac{C_c \mu_c}{k_c}\right)^{-0.7}$$

where as before the gas properties μ_c (viscocity) and k_c (thermal conductivity) are assumed constant about a given steady state condition. The mass velocity G is derived from the bulk mass flow W_g and the reactor cross-section area is derived from the mean core diameter.

In arriving at the two equations above, it should be noted that several important details of the core have been ignored, or erased in the averaging process. Some of these, which might be included in any more detailed study of the transient behaviour are:

(1) It has been assumed that all the fuel balls produce the same amount of heat, thus ignoring both the non-uniformity of the fuel-oxide structure in each ball, and the variations in neutron flux (and hence fission rate) throughout the core.

(2) The ball temperature remains constant throughout the ball volume and around the ball surface. The thermal conductivity of the oxide is thus assumed to be infinite, while negligible contact area between the balls is assumed. Hence the existence of temperature variations and heat transfer variations within the core are ignored.

(3) All properties of fuel and coolant are assumed to remain constant during a transient. Actually, all the gas properties vary fairly considerably with temperature, so that, for example, heat transfer will appreciably alter from core bottom to core top. Fuel property changes are less marked, although the oxide conductivity varies.

(4) All gas on entering the core immediately assumes the average coolant temperature (the mean of T_{ci} and T_{co}) at which temperature the gas properties are estimated and at which the heat is transferred from the fuel balls to the gas.

One disadvantage of this averaging technique is that changes in the temperature of the incoming gas (T_{ci}) appear instantly at the outlet with opposite sign. In practice this will not occur, as the nature of the ball packing ensures that the outlet gas temperature is determined largely by the temperature of the balls. It should be noted that this is a defect in the method of representation, and that the addition of delay terms (as discussed below) to the existing model only delays the observed outlet changes without altering their character. In the present work, fortunately, the effect on the stability of the system is slight, because the feedback path via the gas duct is of little importance.

Some preliminary studies (Nicholls, unpublished AAEC report) used a reactor model in which the core was divided by horizontal planes into four sections so that some variations of parameters and heat transfer up the core was possible. The delay terms which were used between each section still permitted input disturbances to propagate straight through the core, but the results did show that averaging over the whole core would produce acceptable results.

By combining fixed terms, the equations above become,

$$\frac{d\overline{T}_f}{dt} = a_1 E - a_2 W_g^{0.7} (T_f - \overline{T}_c)$$

$$\frac{d\overline{T}_c}{dt} = a_3 W_g^{0.7} (T_f - \overline{T}_c) + a_4 W_g (T_{ci} - T_{co}) ,$$

where the a_1 to a_4 represent the combined fuel, coolant and reactor properties.

For each steady state power level about which perturbations were examined, the fuel and coolant properties were derived to satisfy the heat balance. Variation of coolant properties with temperature were linearised and a digital programme written to estimate the steady state values, resulting in the linearised equations 4 and 5 of Section 2.1, whose coefficients are as follows:

Load	A	B	C	D	F	G
100%	3.48	5.76×10^{-2}	8.87	1.11	1.33×10^{3}	21.6
60%	2.094	3.98×10^{-2}	6.11	0.673	1.44×10^{3}	21.2
20%	0.702	1.85×10^{-2}	2.84	0.223	1.44×10^{3}	20.9

A2.2 Measurement of Gas Temperature (Equations 12 and 30)

To provide input signals for the gas temperature controllers the gas temperature at reactor outlet and boiler outlet must be measured. Because of the low gas velocities, these measurements present some difficulties, of which the one of most concern here is the speed with which the measuring device can respond to changes in the temperature of the gas flowing past it.

It has been assumed that some form of thermocouple will be used and its response will depend primarily on its physical construction and on the speed of the gas at the measuring point. At a given location, an increase in gas flow past the thermocouple will decrease the response time. An increase in thermocouple dimensions will increase the Reynolds' number, which tends to decrease the response time, but owing to the increased thermal mass and increased conduction, the response time will in fact be increased.

For bare (or plain sheathed) thermocouples of workable dimensions, the response times at the low flows which are associated with part load operation will become quite long, in addition to which there will be a significantly lower final indicated temperature. One solution would be to use some form of aspirated thermocouple which would produce both a faster response and one which would be essentially independent of bulk coolant flow. The actual response times which have been used in these studies are:

LOAD	100%	60%	20%
τ_t sec	5	8	25

These are pessimistic, particularly the part load values, since the hot reference would probably be reduced, allowing higher gas velocities (see also Section A2.3).

A2.3 Transportation Delays (Equations 7, 17, 19, and 18)

Since the coolant gas flows at a relatively low speed, a change in gas temperature caused at a given point will not reach a distant point until a certain time has elapsed. The size of the delay is given by $\tau = d/v$ where d is the distance between the two points and v is the gas velocity. Such delays are represented by all-pass (Padé) transfer functions, which give the correct gain representation of a perfect delay, and a correct phase representation up to some limiting frequency. This frequency can be raised to any desired extent by increasing the order of the transfer functions, or by using more of them. No longitudinal mixing occurs in a pure delay, whereas a considerable amount of mixing occurs in the ducts, especially in the cold duct which in fact consists of all space within the concrete pressure vessel which is not otherwise occupied. As a result, the amplitude of any temperature change emerging from a duct will be smaller than that indicated by the equations given below, and its phase lag will be less. However, the all-pass transfer functions are used because they are convenient on both digital and analogue computers and because they give pessimistic stability results. Padé-type approximations can be formulated for all orders of s but for convenience, only first order

$$\frac{1 - s\tau/2}{1 + s\tau/2}$$

or fourth order $$\frac{1 - s\tau/2 + s^2\tau^2/9.1 - s^3\tau^3/78.6 + s^4\tau^4/1420}{1 + s\tau/2 + s^2\tau^2/9.1 + s^3\tau^3/78.6 + s^4\tau^4/1420}$$

transfer functions are employed, in which τ is the required delay in seconds. The following full load data from the reference design allow the delays to be found:

Coolant transit time in core,	1 second
Coolant transit time in hot plenum,	2.7 seconds
Coolant transit time in boilers,	7.4 seconds
Coolant transit time in cold duct,	17.6 seconds
Coolant transit time in cold plenum,	3.4 seconds.

The location of the 'point reactor' is assumed to be half-way along the core and so the delay to the exit is only half the core transit time. If the thermocouple is assumed to be half-way through the hot plenum, the approximate delay between the reactor and the thermocouple (τ_r) would be $\frac{1}{2}(1 + 2.7)$. The value used was 2 seconds, of which 1.5 seconds may be associated with the plenum. The delay from the thermocouple to half-way through the boiler is then approximately

$$(2.7 - 1.5) + \frac{7.4}{2} = 4.9 \text{ sec.}$$

the value used being τ_1 = 4 seconds. The rest of the boiler delay was introduced by τ_2 = 3 seconds, which assumes that the outlet gas thermocouple is close to the boiler gas exit. The cold gas duct and cold plenum which form the least defined part of the gas circuit was taken to be τ_3 = 24 seconds. The effect of temperature changes propagated along the cold gas duct has been found to be of little significance, but the other delays are important components of their respective control loops.

It was assumed that the delays would be inversely proportional to load due to the lower gas velocities. This is a pessimistic assumption since the reference level of the reactor outlet gas temperature controller would almost certainly be reduced with load, allowing higher gas velocities than those considered and hence smaller delays. The values used (in seconds) are given in the following Table.

DELAY	ORDER		LOAD %		
	A	B	100	60	20
τ_r – point reactor to 'hot' thermocouple	1	1	2	3	10
τ_1 – 'hot' thermocouple to point boiler	4	1	4	7	20
τ_2 – point boiler to 'cold' thermocouple	4	1	3	5	15
τ_3 – cold gas duct	16	4	24	40	125

In the initial frequency response design work, the bandwidth to be investigated was unknown. Thus a wider bandwidth than was essential was used, the order of the Padé sections being listed in line A of the above Table. When the final analogue model was formed, some reduction in complexity was essential; since the bandwidth required of the delay circuits was well known by that time; the circuits were simplified as indicated in line B of the Table. This was the only simplification introduced into the final analogue model, and Equations 7, 17, 19 and 18 are stated in the simplified form.

A2.4 Actuators (Equations 9, 16, 32 and 38)

A2.4.1 Definitions

The term 'actuator' is used to describe the power amplifying equipment which accepts a low level signal from a controller and causes a proportional change in some system variable. (Reactivity, gas flow or feed-water flow). The performance of the actuator itself is independent of the station load and the value of α.

A2.4.2 Linear Rod Servo-Mechanisms (Equation 9)

In the reactor outlet gas temperature-control loop the actuator consists of the control rods and their driving mechanisms. It is assumed that in the steady state a given controller output causes a given change in reactivity, that is, that the given controller signal causes a given rod position and that there is a linear relationship between rod position and reactivity. (The constant of proportionality forms only one component of the value of g_h). Time constants are associated with the inertia and friction of the moving parts (one second), and with the final stage of the power amplifier, such as the field circuit of a d.c. motor (one second). Time constants of this size could easily be achieved, but in any case Figure 5 shows that they could be significantly larger before there was any serious degradation in control performance.

A2.4.3 Non-Linear Rod Drive (Equation 16)

A more typical actuator consists of a constant speed motor which can be switched on and off by the controller so as to drive the rods in the appropriate direction (see Figure 9). Because the controller output causes a rod velocity, not a rod position as in the previous case, the actuator provides an operation which is similar to integration and it is for this reason that no integral term is required in the controller itself (Figure 9c). The maximum permitted rate of change of reactivity was calculated from the data of the reference design as follows:

Worth of control absorbers,	1%
Effective length,	4 feet
Maximum velocity,	0.5 feet per minute
Time for full insertion,	8 minutes.

Therefore the maximum rate is 1% in 8 minutes which is only slightly larger than 2×10^{-5}/sec, the value used in these studies. In practice a total rod worth of less than 0.2% would be adequate for fine control provided faster actuators could be used to maintain the existing insertion rate..

The fact that a stable system could be designed, does not of itself imply that such a system would satisfactorily control a disturbance of arbitrarily large amplitude. However, in a number of the results taken from the complete linear analogue model, reactivity rate is recorded. If this is less than 2×10^{-5}/sec for most of the time, it is reasonably safe to assume that a non-linear controller would be adequate for the disturbance considered. Since the linear results can be scaled up, the size of disturbance which could be controlled without exceeding 2×10^{-5}/sec can be estimated very easily. It does not necessarily follow that because the linear controller demands rates greater than the above value for a given disturbance, a suitable non-linear controller cannot be designed (see for instance, Figures 10 and 11).

While from every other point of view it is desirable that the noise level at the thermocouple output should be as low as possible, it is not very important from the control design view point since the dead zone can be adjusted to suit any given noise level. In this study the dead zone was made $\pm$ 0.5 °C and the peak to peak noise level was slightly larger.

A non-linear control loop was examined only for the full load case with $\alpha(-)$. The controller gain was designed using describing function techniques and was subsequently modified in the light of the analogue results. The value finally used for Figures 11, 12 and 40 was $g'_h = 1.5 \times 10^{-6}$ (sec °C)$^{-1}$.

Figure 9b shows that if the noise penetrates the dead zone sufficiently often, the effective dead zone is zero, and there is some gain available no matter how small the error. This is essential when the temperature coefficient of reactivity is positive, since a zero gain controller allows instability to grow until limited by the normal actuator operation outside the dead zone. The result is that the temperature error moves backwards and forwards across the dead zone continuously, but larger oscillations do not build up, (a limit cycle).

A2.4.4 Blowers (Equation 32)

It was assumed that the blower speed and hence the gas mass flow would change from one level to another exponentially with a time constant of thirty seconds. The inertia of the gas in the coolant circuit can be ignored. It is now clear from the reference design that this value was pessimistic, although not excessively so. However, the blower performance is a significant element in the stability of the boiler outlet gas control loop (Figure 14) and even small improvements can be expected to allow faster control.

A2.4.5 Feed Valve (Equation 38)

Again, the change in flow from one level to another was assumed to be exponential, but in this case the inertia of the valve mechanism itself is small compared with the inertia of the water to be accelerated. A time constant of 5 seconds was arbitrarily chosen to represent this effect, but Figure 16 shows that this value could be increased by a factor of 10 before it had any significant effect on the pressure control loop.

A2.5 Controllers (Equations 10, 14, 15, 33 and 39)

With two exceptions (Equations 10 and 15) the basic controller transfer functions are all of the form

$$\frac{g(1 + s\tau)}{s\tau} = g\,(1 + 1/s\tau)$$

(see Figure 6 curve 1 for instance).

At frequencies which are less than $1/\tau$ radians per second, the integral term predominates giving a phase lag of 90° and a very high gain (theoretically infinite at zero frequency). For a temperature controller this ensures a zero error in the steady state between the measured value of the temperature and the temperature reference, and so the accuracy of control is determined only by the absolute accuracy of the thermocouple. It is doubtful if extreme accuracy is required. The same comments apply to the pressure control system and the pressure measuring transducer. At frequencies higher than $1/\tau$ radians per second, the integral term becomes negligible and the controller is effectively a simple gain term g. The values given in the following Tables were used.

Reactor Outlet Gas Controller Constants

TEMP. COEFF. α	–		0		+	
LOAD %	g_h	τ_h	g_h	τ_h	g_h	τ_h
100	1×10^{-5}	10	6×10^{-6}	10^3	1.0×10^{-5}	10
60	7.94×10^{-6}	10	2.8×10^{-6}	10^3	3.16×10^{-5}	10
20	1.58×10^{-6}	10	$*6.31 \times 10^{-6}$	* 500	1.94×10^{-4}	100

* In conjunction with phase advance

Boiler Outlet Gas, and Pressure Controller Constants

LOAD %	g_c	τ_c	g_P	τ_P
100	159×10^3	100	794	100
60	50×10^3	100	270	1250
20	8.7×10^3	100	16	2500

It must be stressed that the above values have not been optimised and are critical only in one or two cases. In general, g was made as large and τ as small as stability conditions allowed since this gave the fastest response obtainable under the given conditions and reduced the risk of instability due to interaction. However, wherever possible τ for any one controller was retained at the same value for the three power levels, since this would simplify the eventual controller construction. In all cases, faster response could have been achieved (using phase advance for example or the flux loop) but again for the sake of simplicity, this was only done where it was essential as in the two cases described below relating to the reactor outlet gas temperature controller.

At 20% load with $\alpha(0)$, the reactor outlet gas temperature controller was too slow to prevent instability caused by interaction with the boiler. Two octaves of phase advance gave a sufficient improvement and so the standard controller was modified by the inclusion of

$$\frac{1 + 71s}{1 + 18s}$$

as in Equation 15 (see Figure 7).

Special measures also had to be taken at all load levels to prevent instability when the temperature coefficient of reactivity was positive. If the method described above had been used, so much phase advance would have been necessary that there would have been a serious risk of overloading due to excessive noise. The method used avoided this risk entirely. By measuring flux, a signal was obtained which had not been subjected to the phase lags involved in the heat transfer and temperature measurement, and so required no phase advance. Thus a temperature change could be anticipated by measuring the flux change which was the cause of the temperature change.

To avoid a resonance associated with the rod servo, a low pass filter had to be used before the flux signal was suitable to adjust the control rod position. Such a filter would also ensure that in a practical system any noise which might be present in the flux signal would be removed. The transfer function of the flux path (Equation 10) is $h/(1 + sk)$. Provided it exceeded some minimum value (equivalent to the value of α) the size of the gain h could have been chosen from a wide range. In fact it was chosen so that the low frequency behaviour of the system was similar to the case with $\alpha(-)$. Similarly the value of the time constant k was not critical and was given the minimum value consistent with the suppression of the servo resonance (see Figure 4 in the region of 0.1 radians per second). The values used were h = 0.04 units ρ/kW thermal, and k = 50 seconds.

A2.6 Boiler Equations (Equations 20 – 29)

Originally a conventional boiler was designed for use with the P.B.R. and a set of linearised equations was formulated to describe its dynamic behaviour (Longrigg, unpublished AAEC report). At a later stage it was decided to use a once-through boiler and the equations given by Longrigg were modified by the author. Three sets of equations were supplied (Appendix 6) with coefficients relating to 100%, 60% and 30% of full load power level. These are scaled equations stated in volts/°F and volts/lb/hr. In fact, the final set of equations has been used to represent the 20% load behaviour and in view of the number of other approximations involved, the additional error is not thought to be of overriding importance. A partial description of the symbols for the original boiler equations is included in Appendix 1.

The equations of Appendix 6 were not suitable for direct analogue computation for two reasons:

(1) A number of simultaneous algebraic equations were present which would have given rise to algebraic loops in the analogue circuit.

(2) Excessive equipment would have been required owing to the large number of variables calculated explicitly. (Ideally the only variables of interest for control purposes are T_{go}, T_{g4}, T_4 (that is, P), W_2, W_4, and W_g).

For these reasons the equations were re-arranged and a number of variables eliminated resulting in Equations 20 – 28 stated in °C and lb/hr. It should be pointed out that no approximation was involved in this rearrangement but the resulting analogue circuit was more compact and free from algebraic loops. The coefficients are listed in Table A1.

Equation 29 evaluates the steam pressure from $P = \gamma T_4$, where T_4 is the saturation temperature. The value of γ obtained from steam tables is 28.8 psi/°C at full load and 20 psi/°C at both part load conditions. This is because the steam pressure is reduced from the full load value of 2400 psi to 1500 psi for part-load operation.

A2.7 The Steam System (Equations 34 – 37)

A2.7.1 Governor operation

It is only necessary to represent the steam ducts, throttle valve and turbine sufficiently accurately to provide the correct load for the boiler. As was mentioned in Section 1.2 the turbine speed may be controlled in two basic ways corresponding to base-load (constant load) operation or governor-controlled (load following) operation. In the case of a base-load station (governor inoperative) an increase in pressure causes an increase in volumetric flow (Figure 53 curve A), resulting in an increased

TABLE A1

BOILER COEFFICIENTS

Load	ϕ_1	ϕ_2	ϕ_3	ϕ_4	ϕ_5
100%	0.0863	0.137	-0.224	4.49×10^{-6}	-3.74×10^{-5}
60%	0.0630	0.0633	-0.126	4.25×10^{-6}	-4.03×10^{-5}
20%	0.0403	0.0283	-0.0685	4.35×10^{-6}	-4.11×10^{-5}

Load	ϕ_6	ϕ_7	ϕ_8	ϕ_9	ϕ_{10}
100%	0.0167	0.026	5.08×10^{-3}	-0.0488	1.35×10^{-6}
60%	0.0121	0.0067	4.60×10^{-3}	-0.0234	1.41×10^{-6}
20%	0.0058	0.0029	3.10×10^{-3}	-0.0120	1.16×10^{-6}

Load	ϕ_{11}	ϕ_{12}	ϕ_{13}	ϕ_{14}	ϕ_{15}
100%	-7.03×10^{-6}	0.0298	1.03	-1.06	1.69×10^{-6}
60%	-7.56×10^{-6}	0.0235	1.03	-1.05	1.32×10^{-6}
20%	-7.56×10^{-6}	0.0150	1.03	-1.04	1.25×10^{-6}

Load	ϕ_{16}	ϕ_{17}	ϕ_{18}	ϕ_{19}	ϕ_{20}
100%	-0.469	0.0119	0.0205	0.219	1.42×10^{-6}
60%	-0.193	0.0139	0.0093	0.085	1.55×10^{-6}
20%	-0.101	0.0057	0.0096	0.043	1.59×10^{-6}

Load	ϕ_{21}	ϕ_{22}	ϕ_{23}	ϕ_{24}	ϕ_{25}
100%	-5.54×10^{-6}	0.272	0.0825	0.645	1.64×10^{-5}
60%	-7.43×10^{-6}	0.0345	0.0132	0.953	2.31×10^{-5}
20%	-8.95×10^{-6}	-0.141	-0.0745	1.215	2.75×10^{-5}

Load	ϕ_{26}	ϕ_{27}	ϕ_{28}	ϕ_{29}	ϕ_{30}
100%	0.0857	0.148	0.767	1.07×10^{-5}	0.282
60%	0.0745	0.109	0.817	1.47×10^{-5}	0.173
20%	0.0662	0.110	0.824	2.95×10^{-5}	0.087

Load	ϕ_{31}	ϕ_{32}	ϕ_{33}	ϕ_{34}	ϕ_{35}
100%	-0.110	-0.250	-7.72×10^{-7}	0.547	-0.579
60%	-0.0696	-0.150	-8.88×10^{-7}	0.416	-0.428
20%	-0.0354	-0.075	-10.0×10^{-7}	0.341	-0.346

Load	ϕ_{36}	ϕ_{37}	ϕ_{38}	ϕ_{39}	ϕ_{40}
100%	0.0316	-6.46×10^{-6}	0.802	-0.464	-3.00×10^{-6}
60%	0.0119	-6.45×10^{-6}	0.312	-0.181	-1.22×10^{-5}
20%	0.0049	-6.45×10^{-6}	0.158	-0.091	-2.33×10^{-5}

power output from the alternator. Apart from a transient the speed does not change from that determined by the infinite bus, but the load angle is increased.

When the alternator operates on its own, with the governor as the only speed regulating mechanism (load following), an increase in pressure tends to cause the flow and the speed to rise. The rise in speed is prevented by the governor which closes the throttle valve and hence reduces the steam flow. A new steady state is reached with the speed virtually unchanged, the pressure higher than before, and the flow lower than before as shown in Figure 53 (cruve B). Thus, when the governor is operating, the turbine and throttle valve together appear to have a negative incremental resistance. This is reasonable since the alternator, having a constant voltage and an unchanged load, is forced by the governor to operate at constant speed, and hence at constant power. This implies that the product of pressure and volumetric flow is approximately constant giving the characteristic of Figure 53. Since it is the more difficult to stabilise, only governor-controlled operation is examined here.

The methods described by Campbell (1958) are used to represent the boiler load as an impedance relating flow to pressure, the main components being shown in Figure 54a. It is assumed that the turbine itself acts as a pure resistance and that the ducts can be represented by pure reactances corresponding to the inertia and compressibility of the steam. There are three separate duct circuits; one for high pressure steam; one for the re-heat inlet to the boiler; and one for the re-heat outlet from the boiler.

A2.7.2 Steam Ducts

The steam 'ducts' consist of the main components shown in Figure 54b. The risers (10 inch pipes) bring the steam to ground level from the boilers. There are two risers for each steam circuit from each of the six boilers, giving a total of 36 risers, each 100 ft long. The twelve risers in each circuit terminate in a header which consists of a pipe running completely round the whole structure, the circumference being about 350 ft. The header diameters are 18 inches (high pressure), 20 inches (re-heat inlet), and 24 inches (re-heat outlet). Each of the three headers is connected to the turbine via two 18 inch diameter pipes, 450 ft long.

A2.7.3 Turbine

Results of some heat rate tests performed on a turbo-alternator at Pyrmont Power Station in 1963 were made available by the Electricity Commission of N.S.W. Although the unit was not of the type proposed for use with the P.B.R., the values of incremental resistance, that is, $\frac{\Delta \text{ Pressure}}{\Delta \text{ Flow}}$, derived from the experimental results, were the most realistic which could be obtained at the time. The values include the effect of the governor and so give the slope of curve B of Figure 53. Curve A was assumed to be a straight line passing through the origin and hence its slope could be deduced from the static operating level in each case.

A2.7.4 Complete Steam Circuit (Equations 34 – 37)

It is assumed that:

(1) The change in operating pressure from 2400 p.s.i. at full load to 1500 p.s.i. at part load only affects the properties of the high pressure duct, not the re-heat ducts.

(2) The positive incremental resistance corresponding to slope A can be divided between the high-pressure, intermediate-pressure and low-pressure sections of the turbine in the same ratio as the power produced by the three sections.

(3) The negative incremental resistance corresponding to slope B of Figure 53 can be associated entirely with the throttle valve.

(4) The governor and throttle valve have a time constant of 5 seconds, that is, for frequencies above about 0.2 radians per second (30 seconds-cycle) the effectiveness of the governor declines and with increasing frequency the system gradually changes from slope B to slope A.

Calculations have shown that at the frequencies of interest each complete duct can be considered as a single filter section and so the basic equivalent circuit is as shown in Figure 54c. R_H is 0.3 of the resistance associated with the slope A and corresponds to the incremental resistance of the high pressure section of the turbine. The remaining 0.7 of this resistance is introduced by R_L which represents the intermediate pressure and low pressure sections of the turbine. R_B is a (negative) resistance representing the governor action (slope B) and is shunted by C_2 to remove its effect at high frequencies. Q_2 is the steam flow at the throttle valve and differs from W_2 under transient conditions. Investigation has shown that:

(1) At low frequencies the effect of R_L and the re-heat duct is negligible since $|R_B| >> R_L$.

(2) At high frequencies R_L can again be neglected due to the shunting effects of the re-heat ducts.

Thus the equivalent circuit can be re-arranged and reduced to that of Figure 54d without loss of accuracy over the frequency range of interest. Equations 34 – 37 in fact describe this circuit, P_2 and P_3 being pressures which arise in the circuit. Although formulated in terms of volumetric flow, at any given pressure the equations may be rescaled to give the mass flow of steam and in the following table the component values are presented in this form.

Components of Steam Circuit Analogue

Load	M	C_1	C_2	R_H	R_B
100%	3.68×10^{-6}	1.34×10^{4}	0.398×10^{3}	4.72×10^{-4}	-12.6×10^{-3}
60%	3.68×10^{-6}	1.47×10^{4}	0.806×10^{3}	4.66×10^{-4}	-6.21×10^{-3}
20%	9.2×10^{-6}	0.586×10^{4}	0.323×10^{3}	11.6×10^{-4}	-15.5×10^{-3}

The frequency response of the equivalent circuit is shown in Figure 15. At low frequencies, the governor has time to operate completely and so the frequency response corresponds to slope B of Figure 53. The flow changes are very small but there is a phase shift of 180°. At higher frequencies, the governor does not have time to operate fully; there is a transition region between slopes B and A of Figure 53 since at high frequencies the governor does not have time to operate at all. Over the transition range, the flow changes get larger, but the phase shift is reduced. The overall behaviour at high frequencies is dominated by a resonance in the high pressure steam duct. The calculations neglect all frictional effects on the steam so the resonance is much sharper than would be expected in practice. In any case, the resonance is above the frequency range of interest in this study.

APPENDIX 3

BASIC TRANSFER FUNCTIONS

Only the transfer functions which are not given in Section 2 are listed here, that is, those relating to the neutron kinetics, reactor heat transfer, boiler and steam duct.

All coefficients are given in Fortran format E11.4, that is, +a.bcdeE+fg represents $a.bcde \times 10^{+fg}$. Each transfer function consists of the ratio of two polynomials in s, the denominator being given first, and then the numerator. The integer preceding each set of coefficients is the number of coefficients in the following polynomial. Thus

```
 6
a       b       c       d       e
f
 3
g       h       j
```

represents

$$\frac{g + hs + js^2}{a + bs + cs^2 + ds^3 + es^4 + fs^5}$$

The transfer functions are labelled with symbols which are the closest to those of Figure 2 which could be obtained on a standard digital computer output. The units are those specified in Section A2.6 of Appendix 2.

NEUTRON KINETICS

P_n/ρ

```
 5
+0.0000E+00    0.2472E-05    0.4033E-03    0.2586E-02    +0.2000E-03
 4
 0.2102E-04    0.1117E-01    0.3300E-00    0.1000E+01
```

REACTOR HEAT TRANSFER

FULL LOAD

T_{cod}/P_n

```
 4
 0.1279E+00    0.1128E+02    0.1215E+02    0.1000E+01
 2
 0.6174E+02   -0.6174E+02
```

T_{cod}/T_{ci}

```
 4
 0.1279E+00    0.1128E+02    0.1215E+02    0.1000E+01
 4
 0.1279E+00   -0.6835E+01    0.5708E+01    0.1000E+01
```

T_{cod}/W_g

```
 4
 0.1025E+07    0.9043E+08    0.9741E+08    0.8017E+07
 3
-0.6112E+02   -0.2425E+03    0.3037E+03
```

T_f / P_n

3
0.1279E+00 0.1115E+02 0.1000E+01
2
0.1930E–02 0.1740E–03

T_f / T_{ci}

3
0.1279E+00 0.1115E+02 0.1000E+01
1
0.6394E–05

T_f / W_g

3
0.1025E+07 0.8939E+08 0.8017E+07
2
–0.1801E–02 –0.1230E–03

0.6 FULL LOAD

T_{cod} / P_n

4
0.5357E–01 0.7576E+01 0.1224E+02 0.1500E+01
2
0.2559E+02 –0.3838E+02

T_{cod} / T_{ci}

4
0.5357E–01 0.7576E+01 0.1224E+02 0.1500E+01
4
0.5357E–01 –0.4884E+01 0.6206E+01 0.1500E+01

T_{cod} / W_g

4
0.2577E+06 0.3644E+08 0.5887E+08 0.7215E+07
3
–0.2561E+02 –0.1602E+03 0.2979E+03

T_f / P_n

3
0.5357E–01 0.7496E+01 0.1000E+01
2
0.7806E–03 0.1047E–03

T_f / T_{ci}

3
0.5357E–01 0.7496E+01 0.1000E+01
1
0.2679E–05

T_f / W_g

3
0.2577E+06 0.3606E+08 0.4810E+07
2
–0.7377E–03 –0.7244E–04

0.2 FULL LOAD

T_{cod}/P_n

4
0.8251E–02 0.3346E+01 0.1752E+02 0.5000E+01
2
0.3987E+01 –0.1994E+02

T_{cod}/T_{ci}

4
0.8251E–02 0.3346E+01 0.1752E+02 0.5000E+01
4
0.8251E–02 –0.2454E+01 0.1106E+02 0.5000E+01

T_{cod}/W_g

4
0.1323E+05 0.5364E+07 0.2808E+08 0.8015E+07
3
–0.3944E+01 –0.4636E+02 0.3304E +03

T_f/P_n

3
0.8251E–02 0.3304E+01 0.1000E+01
2
0.1153E–03 0.3510E–04

T_f/T_{ci}

3
0.8251E–02 0.3304E+01 0.1000E+01
1
0.4125E–06

T_f/W_g

3
0.1323E+05 0.5296E+07 0.1603E+07
2
–0.1093E–03 –0.2396E–04

BOILER

FULL LOAD

T_{g4}/T_{go}

8
0.3031E–05 0.3956E–03 0.1393E–01 0.1965E+00 0.1169E+01 0.3045E+01
0.3095E +01 0.1000E +01
8
0.9390E–06 0.4874E–04 0.9395E–03 0.8580E–02 0.3892E–01 0.8490E–01
0.7735E–01 0.2331E–01

T_{g4}/W_g

8
0.2406E–01 0.3140E+01 0.1106E+03 0.1560E+04 0.9280E+04 0.2417E+05
0.2457E+05 0.7938E+04
8
0.1667E–05 0.1085E–03 0.2558E–02 0.2727E–01 0.1378E+00 0.3244E+00
0.3083E+00 0.9533E–01

T_{g4}/W_4

8
0.2406E-01 0.3140E+01 0.1106E+03 0.1560E+04 0.9280E+04 0.2417E+05
0.2457E+05 0.7938E+04
8
-0.2937E-05 -0.1816E-03 -0.3521E-02 -0.2505E-01 -0.7601E-01 -0.9278E-01
-0.3382E-01

T_{g4}/W_2

8
0.2406E-01 0.3140E+01 0.1106E+03 0.1560E+04 0.9280E+04 0.2417E+05
0.2457E+05 0.7938E+04
8
-0.3933E-05 -0.1569E-03 -0.2099E-02 -0.1183E-01 -0.2860E-01 -0.2423E-01
-0.5187E-02

P/T_{g0}

8
0.3031E-05 0.3956E-03 0.1393E-01 0.1965E+00 0.1169E+01 0.3045E+01
0.3095E+01 0.1000E+01
7
0.4421E-04 0.1526E-02 0.1839E-01 0.9317E-01 0.1967E+00 0.1277E+00

P/W_g

8
0.2406E-01 0.3140E+01 0.1106E+03 0.1560E+04 0.9280E+04 0.2417E+05
0.2457E+05 0.7938E+04
7
0.6915E-04 0.2723E-02 0.3528E-01 0.1873E+00 0.4101E+00 0.2723E+00

P/W_4

8
0.2406E-01 0.3140E+01 0.1106E+03 0.1560E+04 0.9280E+04 0.2417E+05
0.2457E+05 0.7938E+04
7
-0.1140E-03 -0.3724E-02 -0.2873E-01 -0.8078E-01 -0.7667E-01 -0.2167E-01

P/W_2

8
0.2406E-01 0.3140E+01 0.1106E+03 0.1560E+04 0.9280E+04 0.2417E+05
0.2457E+05 0.7938E+04
7
-0.2477E-03 -0.1106E-01 -0.1771E+00 -0.1139E+01 -0.3211E+01 -0.3718E+01
-0.1478E+01

0.6 FULL LOAD

T_{g4}/T_{g0}

8
0.1803E-04 0.4915E-02 0.3525E+00 0.9747E+01 0.1081E+03 0.5173E+03
0.9551E+03 0.4427E+03
8
0.9700E-05 0.7396E-03 0.1850E-01 0.2044E+00 0.1111E+01 0.2978E+01
0.3587E+01 0.1362E+01

T_{g4}/W_g

8
0.1431E+00 0.3902E+02 0.2798E+04 0.7737E+05 0.8581E+06 0.4106E+07
0.7582E+07 0.3514E+07

(continued)

T_{g4}/W_g (continued)

8
0.2320E-04 0.2767E-02 0.1191E+00 0.2270E+01 0.2029E+02 0.8428E+02
0.1398E+03 0.6180E+02

T_{g4}/W_4

8
0.1431E+00 0.3902E+02 0.2798E+04 0.7737E+05 0.8581E+06 0.4106E+07
0.7582E+07 0.3514E+07
8
-0.6578E-04 -0.8440E-02 -0.3260E+00 -0.4172E+01 -0.2173E+02 -0.4291E+02
-0.2042E+02

T_{g4}/W_2

8
0.1431E+00 0.3902E+02 0.2798E+04 0.7737E+05 0.8581E+06 0.4106E+07
0.7582E+07 0.3514E+07
8
-0.7955E-04 -0.5960E-02 -0.1395E+00 -0.1342E+01 -0.5588E+01 -0.8492E+01
-0.2392E+01

P/T_{go}

8
0.1803E-04 0.4915E-02 0.3525E+00 0.9747E+01 0.1081E+03 0.5173E+03
0.9551E+03 0.4427E+03
7
0.3022E-03 0.1400E-01 0.1959E+00 0.1172E+01 0.3106E+01 0.3002E+01

P/W_g

8
0.1431E+00 0.3902E+02 0.2798E+04 0.7737E+05 0.8581E+06 0.4106E+07
0.7582E+07 0.3514E+07
7
0.6348E-03 0.4424E-01 0.9858E+00 0.9296E+01 0.3830E+02 0.5464E+02

P/W_4

8
0.1431E+00 0.3902E+02 0.2798E+04 0.7737E+05 0.8581E+06 0.4106E+07
0.7582E+07 0.3514E+07
7
-0.1629E-02 -0.1111E+00 -0.1620E+01 -0.8806E+01 -0.1774E+02 -0.1020E+02

P/W_2

8
0.1431E+00 0.3902E+02 0.2798E+04 0.7737E+05 0.8581E+06 0.4106E+07
0.7582E+07 0.3514E+07
7
-0.3020E-02 -0.2376E+00 -0.6892E+01 -0.7916E+02 -0.3944E+03 -0.7850E+03
-0.4546E+03

0.2 FULL LOAD

T_{g4}/T_{go}

8
0.4791E-06 0.2742E-03 0.3884E-01 0.2067E+01 0.4347E+02 0.3879E+03
0.1265E+04 0.7274E+03
8
0.2979E-06 0.3067E-04 0.5192E-03 -0.1429E-01 -0.4660E+00 -0.4167E+01
-0.1226E+02 -0.6788E+01

T_{g4}/W_g

8
0.3803E-02 0.2177E+01 0.3083E+03 0.1641E+05 0.3451E+06 0.3079E+07
0.1004E+08 0.5774E+07
8
0.1251E-05 0.2819E-03 0.2332E-01 0.8509E+00 0.1443E+02 0.1116E+03
0.3244E+03 0.1809E+03

T_{g4}/W_4

8
0.3803E-02 0.2177E+01 0.3083E+03 0.1641E+05 0.3451E+06 0.3079E+07
0.1004E+08 0.5774E+07
8
-0.5179E-05 -0.1378E-02 -0.1060E+00 -0.2528E+01 -0.2347E+02 -0.7486E+02
-0.4279E+02

T_{g4}/W_2

8
0.3803E-02 0.2177E+01 0.3083E+03 0.1641E+05 0.3451E+06 0.3079E+07
0.1004E+08 0.5774E+07
8
-0.5910E-05 -0.7906E-03 -0.3127E-01 -0.5074E+00 -0.3532E+01 -0.8665E+01
-0.2352E+01

P/T_{g0}

8
0.4791E-06 0.2742E-03 0.3884E-01 0.2067E+01 0.4347E+02 0.3879E+03
0.1265E+04 0.7274E+03
7
0.9166E-05 0.5166E-03 -0.2468E-02 -0.2964E+00 -0.3368E+01 -0.1055E+02

P/W_g

8
0.3803E-02 0.2177E+01 0.3083E+03 0.1641E+05 0.3451E+06 0.3079E+07
0.1004E+08 0.5774E+07
7
0.3316E-04 0.4190E-02 0.1697E+00 0.2988E+01 0.2352E+02 0.6534E+02

P/W_4

8
0.3803E-02 0.2177E+01 0.3083E+03 0.1641E+05 0.3451E+06 0.3079E+07
0.1004E+08 0.5774E+07
7
-0.1197E-03 -0.1620E-01 -0.4584E+00 -0.4814E+01 -0.1801E+02 -0.1322E+02

P/W_2

8
0.3803E-02 0.2177E+01 0.3083E+03 0.1641E+05 0.3451E+06 0.3079E+07
0.1004E+08 0.5774E+07
7
-0.2096E-03 -0.2970E-01 -0.1565E+01 -0.3326E+02 -0.3042E+03 -0.1040E+04
-0.7466E+03

STEAM DUCT

W_2/P

FULL LOAD

4
+0.5210E+00 +0.1016E+00 +0.2639E-01 +0.5000E-02
3
-4.3100E+01 +7.2000E+03 +1.3680E+03

0.6 FULL LOAD

W_2/P

4
+0.1366E+00 +0.5529E-01 +0.7837E-02 +0.3000E-02
3
-2.3810E+01 +2.1330E+03 +0.8150E+03

0.2 FULL LOAD

W_2/P

4
+0.1366E+00 +0.5529E-01 +0.7837E-02 +0.3000E-02
3
-0.9530E+01 +0.8540E+03 +0.3260E+03

APPENDIX 4

ANALOGUE MODEL EQUATIONS

Symbols not listed in Appendix 1 refer to variables which arise in the analogue circuit and can be identified in Figures 18, 19 and 20.

(1) Neutron Kinetics

$$\frac{dP_n}{dt} = \frac{1}{\ell^*}\left[\rho - \beta P_n + \sum_{i=1}^{3} \beta_i X_i\right]$$

$$\frac{dX_i}{dt} = \lambda_i (P_n - X_i) .$$

(2) Reactor Core Heat Transfer

$$\frac{dT_f}{dt} = A P_n - B(T_f - T_c) - GW_g$$

$$\frac{dT_c}{dt} = C(T_f - T_c) - 2D(T_c - T_{co}) - FW_g$$

$$T_{co} = 2T_c - T_{ci} .$$

(3) Reactor and Hot Duct Delays

$$\frac{dT_{coo}}{dt} = \frac{2}{\tau_r}(T_{cod} - T_{co})$$

$$T_{cod} = -(T_{co} + T_{coo})$$

$$\frac{dT_{g0d}}{dt} = \frac{2}{\tau_1}(T_{g0} - T_{cod})$$

$$T_{g0} = -(T_{cod} - T_{g0d}) .$$

(4) Reactor Outlet Gas Thermocouple and Reactor Controller

$$\frac{dT_{com}}{dt} = \frac{1}{\tau_t}(T_{cod} - T_{com})$$

$$T_{he} = T_{hr} - T_{com}$$

$$\frac{dT_{ee}}{dt} = \frac{T_{he}}{\tau_h}$$

$$\rho_e = g_h (T_{he} + T_{ee}) .$$

20% Model, $\alpha = 0$ $\quad T_{fe} = T_{he} + T_{ce}$

$$\frac{dT_{ge}}{dt} = t_{h2}\left(t_{fe} - \frac{\rho_e}{g_h}\right)$$

$$\rho_e = g_h(t_{h1} T_{fe} + T_{ge})$$

$$\frac{dP_{nn}}{dt} = \frac{1}{k}(P_n - P_{nn})$$

$$\rho_f = hP_{nn}$$

$$\rho_{cd} = \rho_e - \rho_f .$$

(5) Control Rod Servos and Temperature Coefficient of Reactivity

$$\frac{d\rho_{cc}}{dt} = \rho_{cd} - \rho_{ce}$$

$$\frac{d\rho_e}{dt} = \rho_{cc} - \rho_c$$

$$\rho_t = \alpha T_f$$

$$\rho = \rho_c + \rho_t + \rho_d .$$

(6) Boiler

$$\frac{dT_{m1}}{dt} = \phi_1 T_{go} + \phi_2 T_2 + \phi_3 T_{m1} + \phi_4 W_g + \phi_5 W_2$$

$$\frac{dT_{m2}}{dt} = \phi_6 T_{go} + \phi_7 T_4 + \phi_8 T_{m1} + \phi_9 T_{m2} + \phi_{10} W_g + \phi_{11} W_2$$

$$\frac{dT_{m3}}{dt} = \phi_{12} T_{g2} + \phi_{13} T_4 + \phi_{14} T_{m3} + \phi_{15} W_g$$

$$\frac{dT_{m4}}{dt} = \phi_{16} T_{m4} + \phi_{17} T_{g2} + \phi_{18} T_{m3} + \phi_{19} T_6 + \phi_{20} W_g + \phi_{21} W_4$$

$$T_{g2} = \phi_{22} T_{go} + \phi_{23} T_{m1} + \phi_{24} T_{m2} + \phi_{25} W_g$$

$$T_{g4} = \phi_{26} T_{g2} + \phi_{27} T_{m3} + \phi_{28} T_{m4} + \phi_{29} W_g$$

$$\frac{dT_2}{dt} = \phi_{30} T_{m2} + \phi_{31} T_4 + \phi_{32} T_2 + \phi_{33} W_2$$

$$\frac{dT_4}{dt} = \phi_{34} T_{m3} + \phi_{35} T_4 + \phi_{36} T_6 + \phi_{37} W_2$$

$$\frac{dT_6}{dt} = \phi_{38} T_{m4} + \phi_{39} T_6 + \phi_{40} W_g$$

(7) Boiler Delay and Cold Duct Delay

$$\frac{dT_{g4d}}{dt} = \frac{2}{\tau_2}(T_{gout} - T_{g4})$$

$$T_{gout} = -(T_{g4} + T_{g4d})$$

$$\frac{dT_{d1}}{dt} = -\frac{1}{\tau_3}(T_{gout} - T_{ci})$$

$$\frac{dT_{d2}}{dt} = \frac{1}{\tau_3}(T_{gout} + T_{ci} + d_1 T_{d1})$$

$$\frac{dT_{d3}}{dt} = \frac{1}{\tau_3}(T_{gout} - T_{ci} + d_2 T_{d2})$$

$$\frac{dT_{d4}}{dt} = \frac{1}{\tau_3}(T_{gout} + T_{ci} + d_3 T_{d3})$$

$$T_{ci} = T_{gout} + d_4 T_{d4} .$$

(8) Boiler Outlet Gas Thermocouple, Flow Controller and Blower

$$\frac{dT_{gom}}{dt} = \frac{1}{\tau_t}(T_{gout} - T_{gom})$$

$$T_{ce} = T_{cr} - T_{gom}$$

$$\frac{dT_{cc}}{dt} = \frac{T_{ce}}{\tau_c}$$

$$W_g' = g_c(T_{cc} + T_{ce})$$

$$\frac{dW_g}{dt} = \frac{1}{\tau_b}(W_g' - W_g) .$$

(9) Pressure Controller and Feed Valve

$$P = \gamma T_4$$

$$P_e = P_r - P$$

$$\frac{dP_{ee}}{dt} = \frac{P_e}{\tau_t}$$

$$W_4' = g_p(P_e + P_{ee})$$

$$\frac{dW_4}{dt} = \frac{1}{\tau_f}(W_4' - W_4) .$$

(10) Steam Duct and Turbine

$$\frac{dW_2}{dt} = \frac{1}{M_1}(P - P_2)$$

$$\frac{dP_2}{dt} = \frac{1}{C_1}(W_2 - q_2)$$

$$q_2 = \frac{1}{R_H}(P_2 - P_3)$$

$$\frac{dP_3}{dt} = \frac{1}{C_2}\left(q_2 - \frac{P_3}{R_B}\right)$$

TABLE 1

SCALING MAXIMA

(1) Fixed Maxima

Variable	Maximum
P_n	0.1
P_{nn}	0.1
ρ (all subscripts)	0.001
X_i	0.1
W_g	5×10^5 lb/hr
W_4	5×10^5 lb/hr
W_2	5×10^4 lb/hr
q_2	5×10^4 lb/hr
P	2000 p.s.i.
P_2	200 p.s.i.
P_3	200 p.s.i.
T_{mi} i = 1,4	100 °F
T_2, T_4, T_6	100 °F
T_{g2}	100 °F

(2) Variable Maxima

Variable	Maximum		
	100%	60%	20%
All other T	50 °C	25 °C	10 °C

TABLE 2

COEFFICIENT POTENTIOMETER SETTINGS

(Problem P.B.R. Date 6.6.66)

* Into 10×

† Sign Change

POT	VAR	S.C.	100%	60%	20%	VALUE	100%	60%	20%
P 00									
01									
02									
03									
04	Cold Duct $1/\tau_{CD}$		0385	0233	0074				
05	Cold Duct $1/\tau_{CD}$		0385	0233	0074				
06		2000*							
07	(T_{cr}/T_m)								
08	Thermoc. $1/\tau_T$		2000	1250	0400				
09		8280							
10	DC_c		3322	2009	0640				
11	$(DC_d - 10)$	8066*							
12							1061	2951	1475*
13	Blower	0333							
14	Feed Valve	2000							
15	$\gamma/20$		8000	5550	5550				
16		1000							
17	$(\rho_d/0.001)$								
18	$100/\tau_P$		1.0000	0200	0400				
19									
20							0777	0284	0073
21							0150	0054	0010
22							0337	0363	0370
23							0063	0068	0068
24							0404	0382	0392
25							8522	1814*	4575*
26							2820	1725	0874
27							0007	0008	0009

(continued)

TABLE 2 (continued)

POT	VAR	S.C.	100%	60%	20%	VALUE	100%	60%	20%
P 28							2448	0155	†0254
29							0825	0132	†0745
30							1060*	1054*	1045*
31							0128	0140	0143
32							1030*	1030*	1030*
33							0205	0093	0096
34							0298	0235	0150
35							8020	3120	1582
36							5470	4164	3405
37							0270	1100	2100
38							0121	0127	0104
39							0316	0119	0049
40	$(1/\ell^*) \times 10^{-4}$	5000*							
41	$100\ \beta_1$	1352							
42	λ_3	0020							
43	λ_1	2920							
44	λ_2	0360							
45	$100\ \beta_2$	1000							
46	$100\ \beta_3$	0170							
47	$100\ C_3$		3388	6794	1706*				
48	$0.1\ C_4$		8773*	6135*	2844*				
49	C_6		2235	4469	1117*				
Q00	Reactor Delay		1.0000	6667	2000				
01	Hot Duct Delay		5000	2857	1000				
02	Boiler Delay		6667	4000	1333				
03									
04	DC_b		1750	1058	0337				
05	Boiler Delay		6667	4000	1333				
06	$(1/C_2 R_B)$		1999	1998	1998				
07	$(250/C_2)$		6281	3102	3102				
08	$(0.0004/R_H)$		8475*	8584*	8584*				

(continued)

TABLE 2 (continued)

POT	VAR	S.C.	100%	60%	20%	VALUE	100%	60%	20%
Q09	$(2500/C_1)$		1870	1697	1697				
10	$(P_r/2000)$								
11	Cold Duct Delay		0385	0233	0074				
12							0952	1656	3678
13	$(T_{mg}/5.10^5)/30$		5292*	8348	0582				
14			6350	2160	1270				
15		1000							
16		2000				α– ve	1.0000	1.0000	1.0000
17	$10/\tau_h$ ⟶				⟶	α = 0	0100	0100	0200
18	(T_{hr}/T_m)					α + ve	1.0000	1.0000	0.1000
19	Thermo.		2000	1250	0400				
20							2243	1263	0685
21							0488	0234	0120
22							1370	0633	0283
23							0051	0046	0031
24		α– ve	5000	1985	0158		0260	0067	0029
25	Cont. Gain ⟶	α = 0	3000	0705	3150				
26		α + ve	5000	7900	1.9400		2500	1500	0750
27							1100	0696	0354
28							1473	2078	2476
29							6450	9528	1215*
30							0152	0119	0112
31							4694	1932	1013
32							0119	0139	0057
33							0500	0670	0810
34							2190	0850	0430
35							4636	1806	0910
36							5786	4283	3455
37							0058	0058	0058
38	Reactor Delay		1.0000	6667	2000				
39	Hot Duct Delay		5000	2857	1000				
40							1644	2420	6128

(continued)

TABLE 2 (continued)

POT	VAR	S.C.	100%	60%	20%	VALUE	100%	60%	20%
Q 41	λ_1	2920							
42	$10^3 T_m \alpha_T$		2500*	1250*	5000				
43	$100 \beta_T$	2522							
44	DC_a		0769	0465	0148				
45	λ_2	0360							
46	λ_3	0020							
47	$100 C_1$		6970	8386	7020				
48	$10 C_2$		5700	3997	1861				
49	$0.1 C_5$		2244*	1347*	4486				

APPENDIX 5

DIGITAL CHECKING OF THE ANALOGUE TRANSIENTS

In order to achieve a final confirmation of the analogue results, several selected runs were duplicated in the 7040 digital computer using numerical integration techniques.

A FORTRAN version of the complete set of unscaled first order differential equations (Appendix 4) was arranged to permit the parameters relevant to each power level to be readily changed, and this then formed a sub-routine in the general computing programme.

The integration routines generally used fourth order Runge-Kutta methods, in which the step length required was chosen either from a consideration of the time constants involved or by automatic processes, these providing, when applicable, a marked reduction in computing time.

Because of the wide range of time constants in the model, long computations were required by the digital programme, limiting its use to the simulation of fairly short transient times.

Figure 55 shows an analogue transient with the corresponding digital results superimposed. The close agreement is typical of the results obtained, the only significant error being due to the restricted writing speed of the recorder used.

APPENDIX 6

BOILER EQUATIONS

(Linearised equations describing approximately the dynamic behaviour of the Lucas Heights designed ERS 251 steam boiler, converted to run as a once-through unit)

(a) FULL LOAD

Scale Factors:

All temperatures	1 volt = 10 °F
All steam and water flows	1 volt = 5×10^3 lb/hr
Gas flow	1 volt = 5×10^4 lb/hr

Time scale = real time

Reheater

$$\frac{d\bar{T}_{m1}}{dt} = .0965\,\bar{T}_{g1} + .455\,\bar{T}_1 - .5515\,\bar{T}_{m1} + .0378\,W_g - .0298\,W_2$$

$$T_{g1} = T_{go} - .261\,(\bar{T}_{g1} - \bar{T}_{m1}) + .0658\,W_g$$

$$\bar{T}_{g1} = .545\,T_{go} + .455\,T_{g1}$$

$$T_1 = T_2 + 4.25\,(\bar{T}_{m1} - \bar{T}_1) - .053\,W_2$$

$$\bar{T}_1 = .545\,T_1 + .455\,T_2$$

$$\frac{dT_2}{dt} = 0.172\,T_3 - 0.25\,T_2$$

Superheater

$$\frac{d\bar{T}_{m2}}{dt} = .0302\,\bar{T}_{g2} + .415\,\bar{T}_3 - .4452\,\bar{T}_{m2} + .00915\,W_g - .005375\,W_2$$

$$T_{g2} = T_{g1} - .893\,(\bar{T}_{g2} - \bar{T}_{m2}) + .175\,W_g$$

$$\bar{T}_{g2} = .571\,T_{g1} + .429\,T_{g2}$$

$$T_3 = T_4 + 25.6\,(\bar{T}_{m2} - \bar{T}_3) - .063\,W_2$$

$$\bar{T}_3 = .571\,T_3 + .429\,T_4$$

Evaporator

$$\frac{d\bar{T}_{m3}}{dt} = .0525\,\bar{T}_{g3} + 1.03\,T_4 - 1.0825\,\bar{T}_{m3} + .0119\,W_g$$

$$T_{g3} = T_{g2} - 1.1\,(\bar{T}_{g3} - \bar{T}_{m3}) + .161\,W_g$$

$$\bar{T}_{g3} = .326\,T_{g2} + .674\,T_{g3}$$

$$W_{s1} = 94.0\,(\bar{T}_{m3} - T_4) - 5.42\,(T_4 - T_8)$$

$$\frac{dT_4}{dt} = .00582\,(W_{s1} - W_2)$$

Economiser

$$\frac{d\bar{T}_{m4}}{dt} = .0525\ \bar{T}_{g4} + .437\ \bar{T}_6 - .4895\ \bar{T}_{m4} + .00785\ W_g - .005\ W_4$$

$$T_{g4} = T_{g3} - 1.245\ (\bar{T}_{g4} - \bar{T}_{m4}) + .12\ W_g$$

$$\frac{d\bar{T}_6}{dt} = .401\ (\bar{T}_{m4} - \bar{T}_6) - .0313\ (T_6 - T_7) - .00135\ W_4$$

$$\bar{T}_{g4} = .5\ T_{g3} + .5\ T_{g4}$$

$$T_6 = 2\ \bar{T}_6 - T_7$$

Input information required:

Gas side	W_g, T_{go}
Steam side	W_4, T_7, W_2, T_2

(b) 60% FULL–LOAD

Scale Factors etc. as for full–load equations.

Reheater

$$\frac{d\bar{T}_{m1}}{dt} = .0721\ \bar{T}_{g1} + .23\ \bar{T}_1 - .3021\ \bar{T}_{m1} + .035\ W_g - .032\ W_2$$

$$T_{g1} = T_{go} - .317\ (\bar{T}_{g1} - \bar{T}_{m1}) + .11\ W_g$$

$$\bar{T}_{g1} = .545\ T_{go} + .455\ T_{g1}$$

$$T_1 = T_2 + 4.83\ (\bar{T}_{m1} - \bar{T}_1) - .124\ W_2$$

$$\bar{T}_1 = .545\ T_1 + .455\ T_2$$

Superheater

$$\frac{d\bar{T}_{m2}}{dt} = .0282\ \bar{T}_{g2} + .155\ \bar{T}_3 - .1832\ \bar{T}_{m2} + .00855\ W_g - .00605\ W_2$$

$$T_{g2} = T_{g1} - 1.61\ (\bar{T}_{g2} - \bar{T}_{m2}) + .3435\ W_g$$

$$\bar{T}_{g2} = .571\ T_{g1} + .429\ T_{g2}$$

$$T_3 = T_4 + 38.6\ (\bar{T}_{m2} - \bar{T}_3) - .172\ W_2$$

$$\bar{T}_3 = .571\ T_3 + .429\ T_4$$

Evaporator

$$\frac{d\bar{T}_{m3}}{dt} = .0392\ \bar{T}_{g3} + 1.03\ T_4 - 1.0692\ \bar{T}_{m3} + .00935\ W_g$$

$$T_{g3} = T_{g2} - .99\ (\bar{T}_{g3} - \bar{T}_{m3}) + .1585\ W_g$$

$$\bar{T}_{g3} = .326\ T_{g2} + .674\ T_{g3}$$

$$W_{s1} = 71.8\ (\bar{T}_{m3} - T_4) - 2.06\ (T_4 - T_6)$$

$$\frac{dT_4}{dt} = .00582\ (W_{s1} - W_2)$$

Economiser

$$\frac{d\bar{T}_{m4}}{dt} = .0392\ \bar{T}_{g4} + .17\ \bar{T}_6 - .2092\ \bar{T}_{m4} + .0102\ W_g - .0067\ W_4$$

$$T_{g4} = T_{g3} - 1.28\ (\bar{T}_{g4} - \bar{T}_{m4}) + .195\ W_g$$

$$\frac{d\bar{T}_6}{dt} = .156\ (\bar{T}_{m4} - \bar{T}_6) - .0123\ (T_6 - T_7) - .00545\ W_4$$

$$\bar{T}_{g4} = .5\ T_{g3} + .5\ T_{g4}$$

$$T_6 = 2\ \bar{T}_6 - T_7$$

$$\frac{dT_2}{dt} = .103\ T_3 - .15\ T_2$$

(c) 30% FULL-LOAD

Scale Factors etc. as for full-load equations

Reheater

$$\frac{d\bar{T}_{m1}}{dt} = .0478\ \bar{T}_{g1} + .113\ \bar{T}_1 - .1608\ \bar{T}_{m1} + .0345\ W_g - .0325\ W_2$$

$$T_{g1} = T_{g0} - .41\ (\bar{T}_{g1} - \bar{T}_{m1}) + .257\ W_g$$

$$\bar{T}_{g1} = .545\ T_{g0} + .455\ T_{g1}$$

$$T_1 = T_2 + 5.5\ (\bar{T}_{m1} - \bar{T}_1) - .2925\ W_2$$

$$\bar{T}_1 = .545\ T_1 + .455\ T_2$$

Superheater

$$\frac{d\bar{T}_{m2}}{dt} = .0187\ \bar{T}_{g2} + .073\ \bar{T}_3 - .0917\ \bar{T}_{m2} + .0062\ W_g - .0061\ W_2$$

$$T_{g2} = T_{g1} - 2.54\ (\bar{T}_{g2} - \bar{T}_{m2}) + .615\ W_g$$

$$\bar{T}_{g2} = .571\ T_{g1} + .429\ T_{g2}$$

$$T_3 = T_4 + 42.0\ (\bar{T}_{m2} - \bar{T}_3) - .435\ W_2$$

$$\bar{T}_3 = .571\ T_3 + .429\ T_4$$

Evaporator

$$\frac{d\bar{T}_{m3}}{dt} = .026\ \bar{T}_{g3} + 1.03\ T_4 - 1.056\ \bar{T}_{m3} + .00865\ W_g$$

$$T_{g3} = T_{g2} - 1.08\ (\bar{T}_{g3} - \bar{T}_{m3}) + .25\ W_g$$

$$\bar{T}_{g3} = .326\ T_{g2} + .674\ T_{g3}$$

$$W_{s1} = 58.7\ (\bar{T}_{m3} - T_4) - .843(T_4 - T_6)$$

$$\frac{dT_4}{dt} = .00582\ (W_{s1} - W_2)$$

Economiser

$$\frac{d\bar{T}_{m4}}{dt} = .026\ \bar{T}_{g4} + .086\ \bar{T}_{6} - .112\ \bar{T}_{m4} + .009\ W_g - .0081\ W_4$$

$$T_{g4} = T_{g3} - 1.4\ (\bar{T}_{g4} - \bar{T}_{m4}) + .408\ W_g$$

$$\frac{d\bar{T}_{6}}{dt} = .0791\ (\bar{T}_{m4} - \bar{T}_{6}) - .00595\ (T_{6} - T_{7}) - .0105\ W_4$$

$$\bar{T}_{g4} = .5\ T_{g3} + .5\ T_{g4}$$

$$T_{6} = 2\ \bar{T}_{6} - T_{7}$$

$$\frac{dT_2}{dt} = .052\ T_3 - .075\ T_2$$

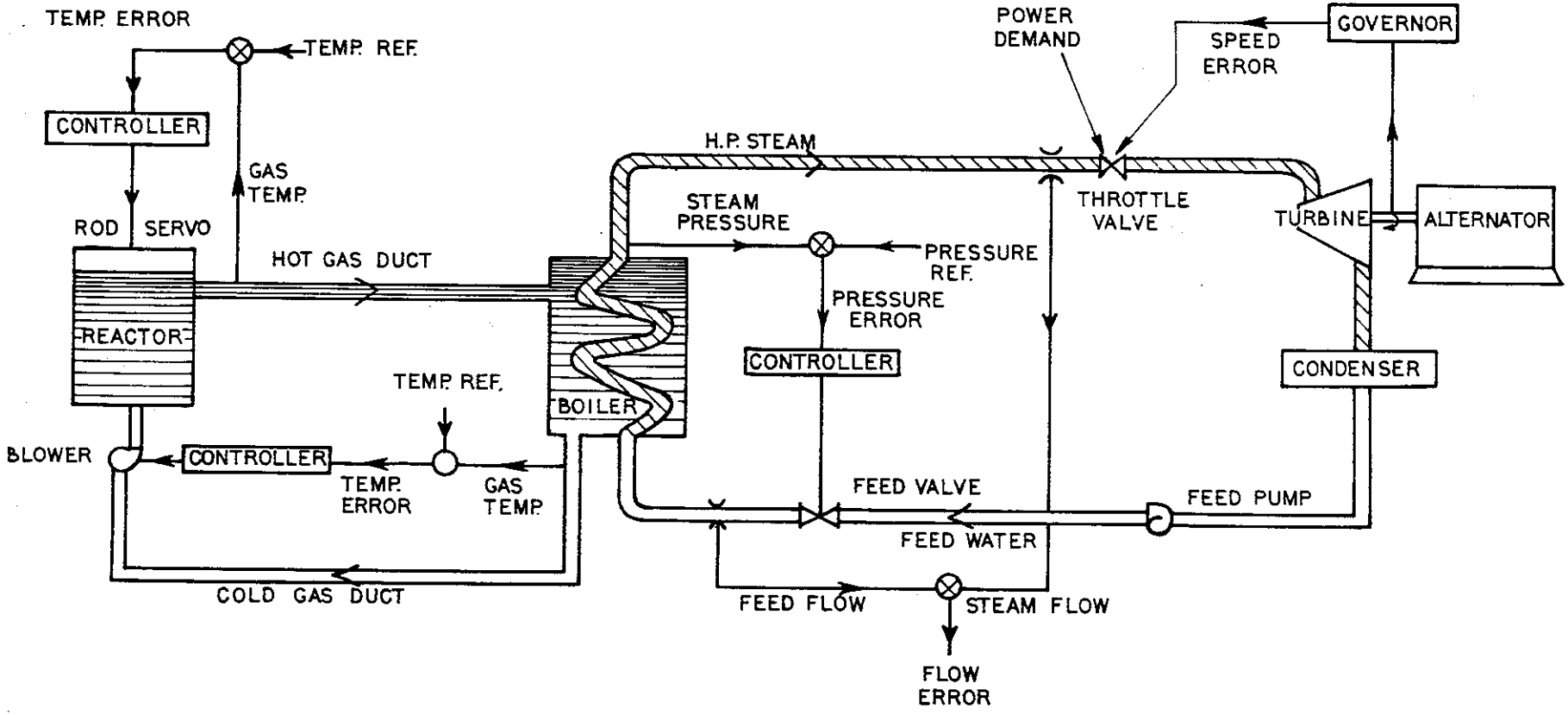

FIGURE 1. CONTROL SYSTEM FOR A PEBBLE BED REACTOR POWER STATION

(From a preliminary proposal by Babcock and Wilcox Ltd.)

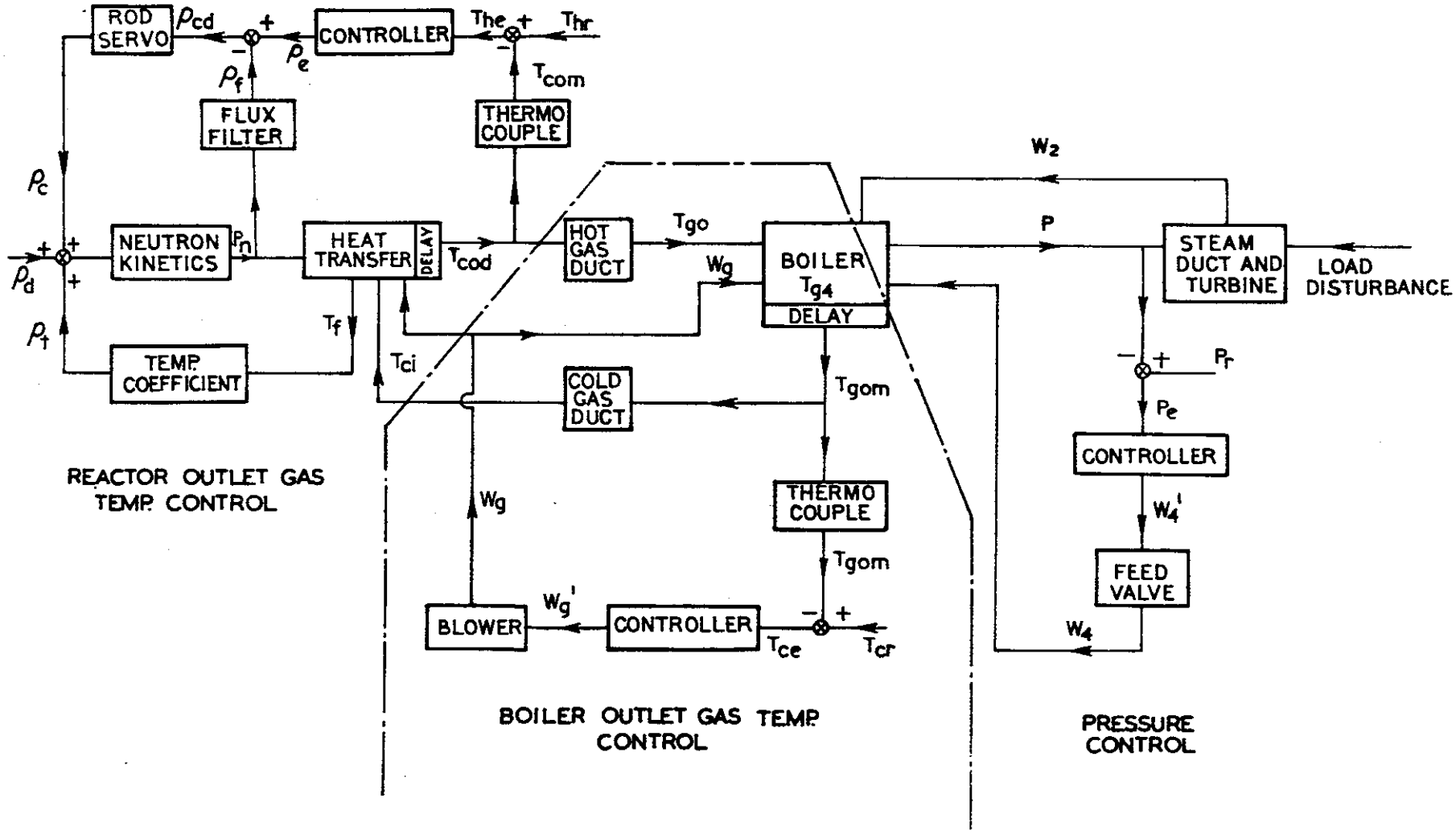

FIGURE 2. BLOCK DIAGRAM OF CONTROL SYSTEM FOR A PEBBLE BED REACTOR POWER STATION

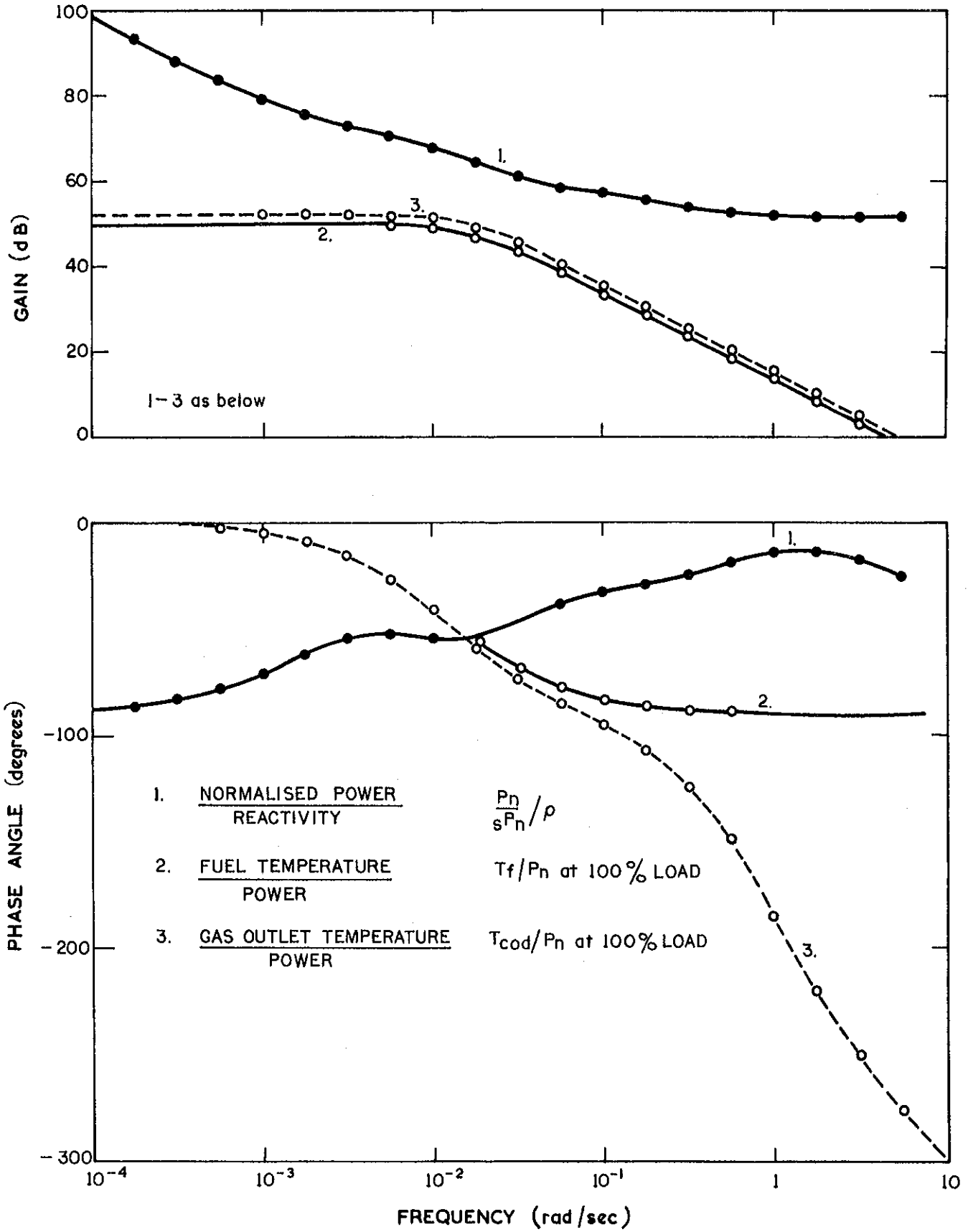

FIGURE 3. FREQUENCY RESPONSES OF THE REACTOR

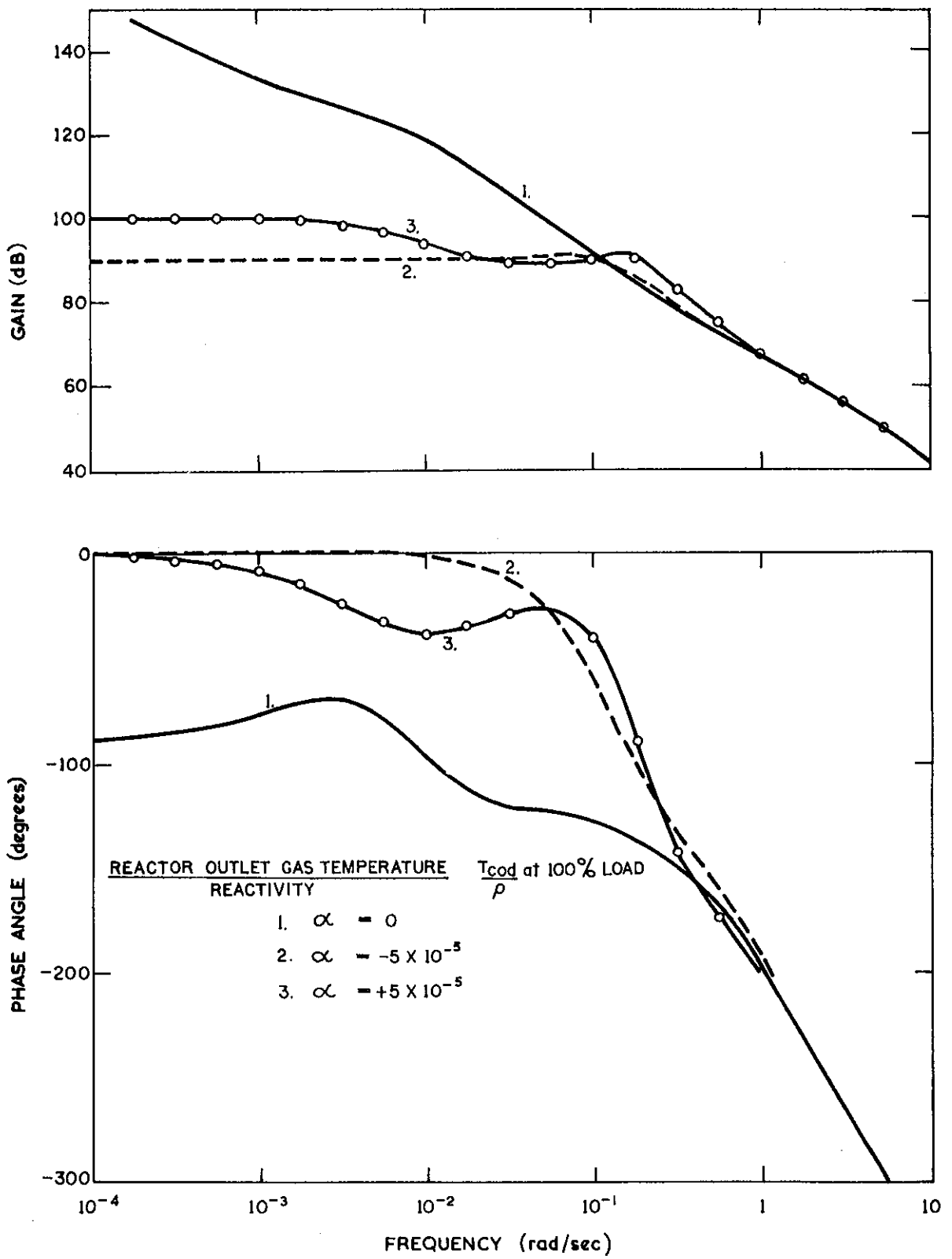

FIGURE 4. FREQUENCY RESPONSES OF THE REACTOR

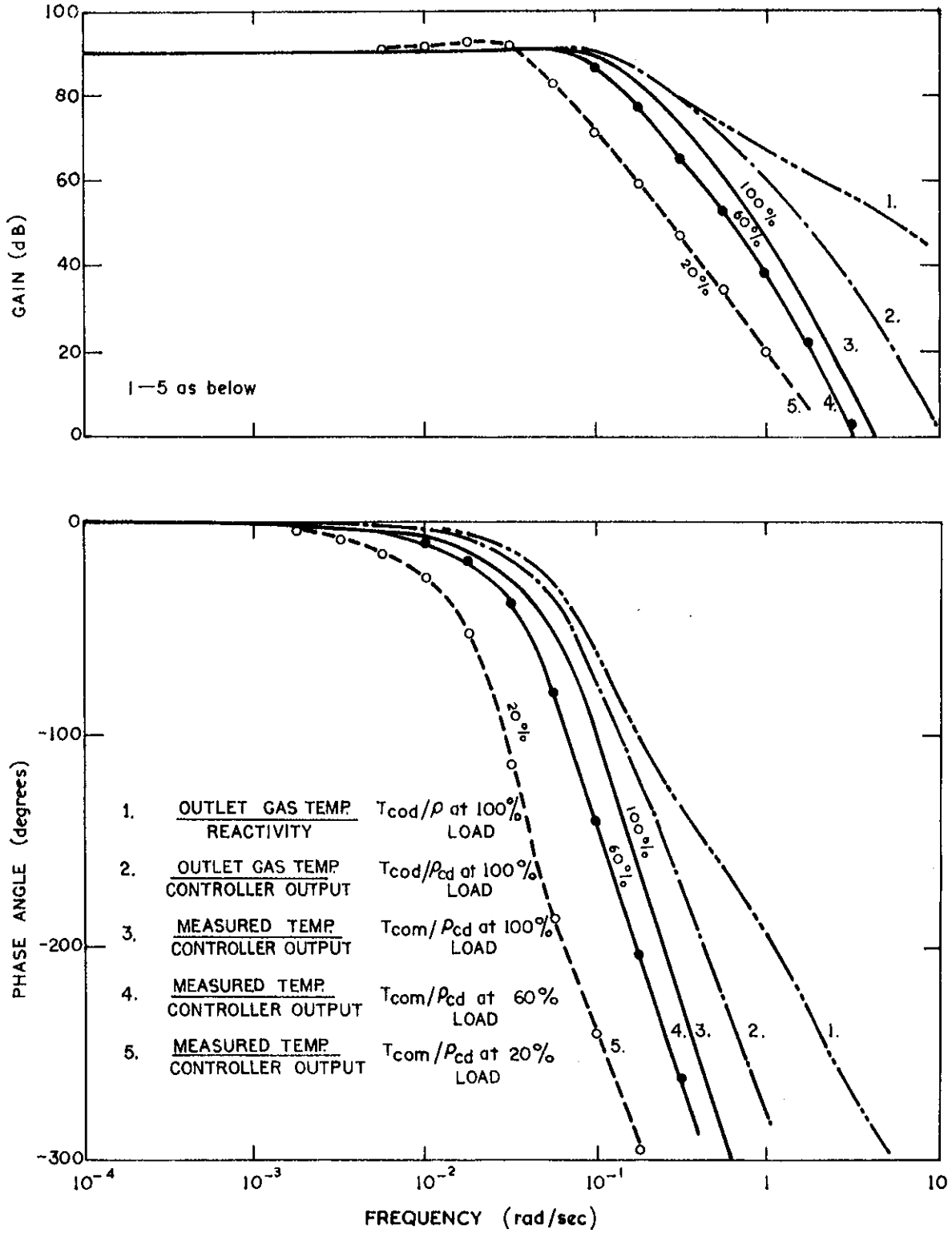

FIGURE 5. FREQUENCY RESPONSE OF REACTOR OUTLET GAS TEMPERATURE CONTROL LOOP WITH NEGATIVE TEMPERATURE COEFFICIENT (α-)

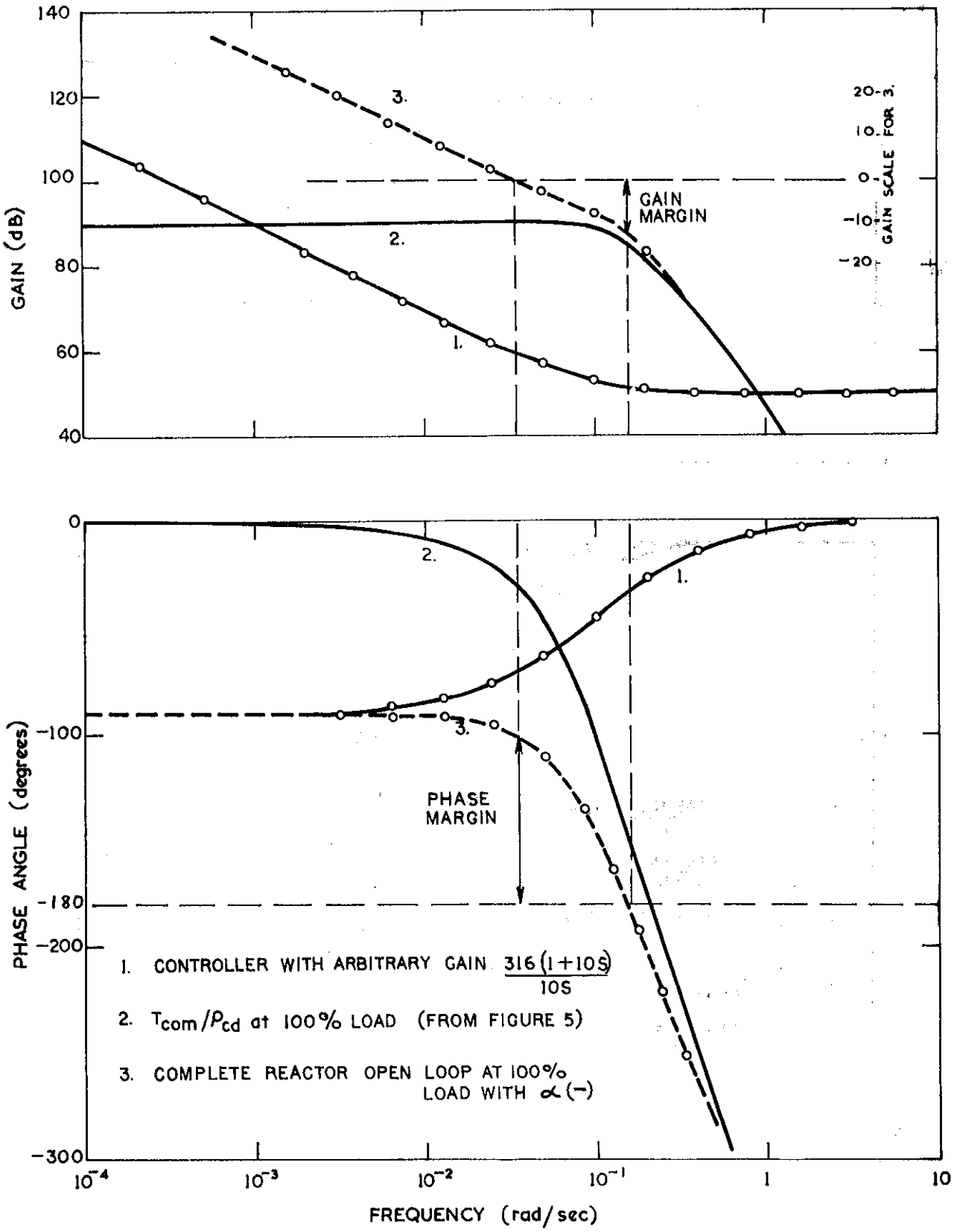

FIGURE 6. FREQUENCY RESPONSE OF REACTOR OUTLET GAS TEMPERATURE CONTROL LOOP

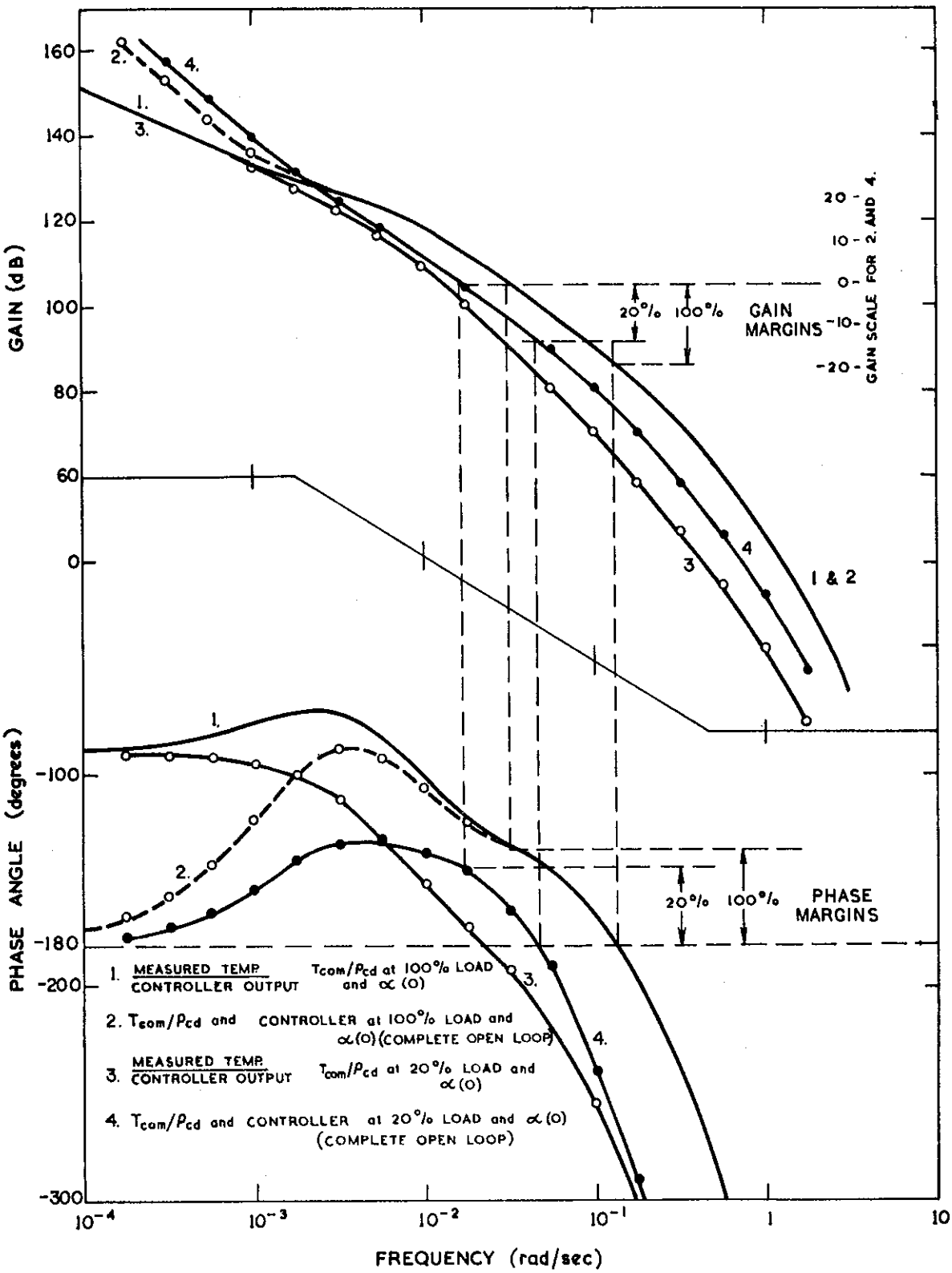

FIGURE 7. FREQUENCY RESPONSE FOR REACTOR OUTLET GAS TEMPERATURE CONTROL LOOP

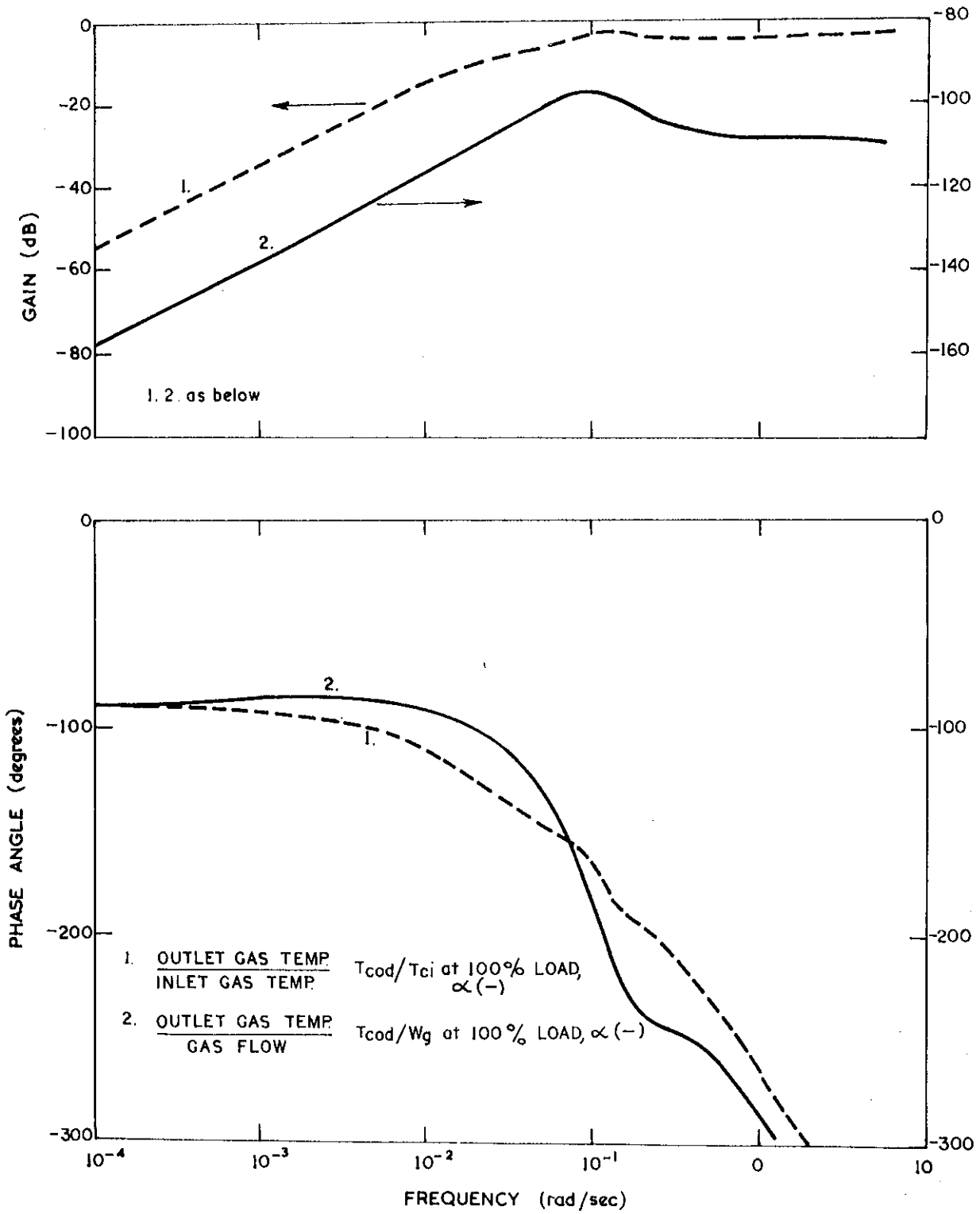

FIGURE 8. CLOSED LOOP FREQUENCY RESPONSE OF REACTOR OUTLET GAS TEMPERATURE CONTROLLER

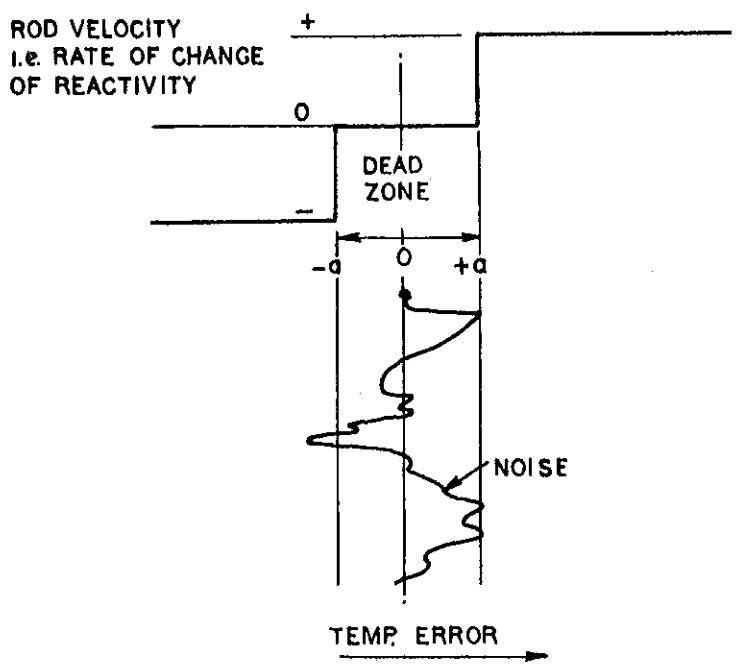

(a) STATIC CHARACTERISTIC OF NON-LINEAR ROD DRIVE

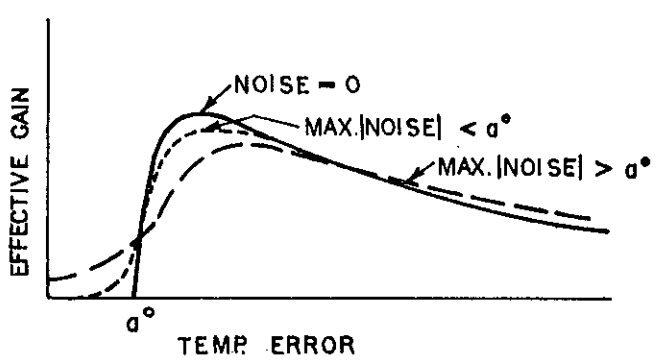

(b) DESCRIBING FUNCTION OF (a)

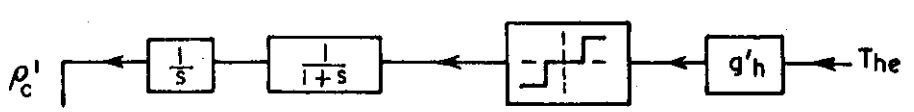

(c) BLOCK DIAGRAM OF NON-LINEAR ROD DRIVE

FIGURE 9. NON-LINEAR ROD DRIVE

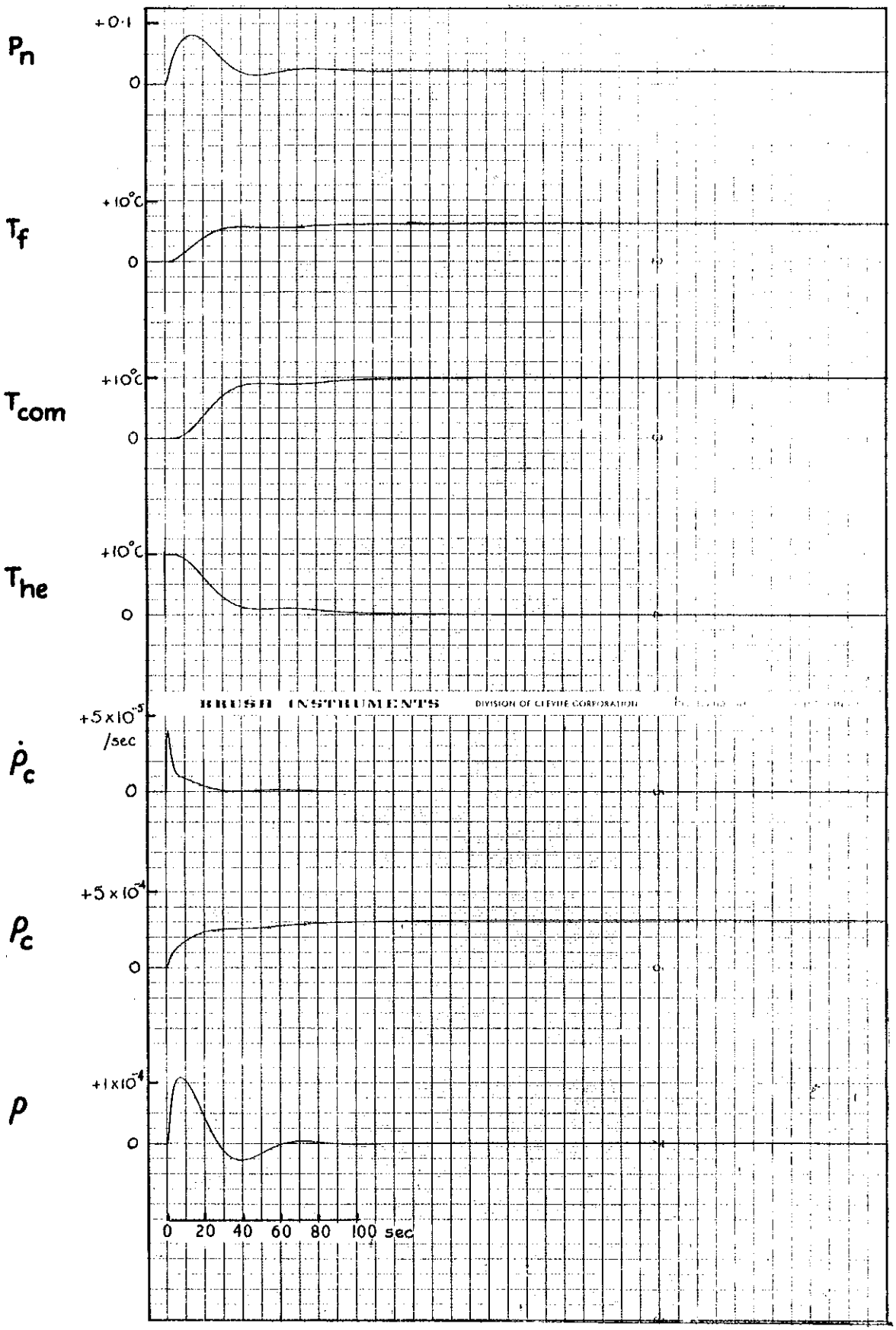

FIGURE 10. RESPONSE OF THE REACTOR AND THE REACTOR OUTLET GAS CONTROLLER TO A 10°C STEP REFERENCE TEMPERATURE T_{hr} (100% load α(-))

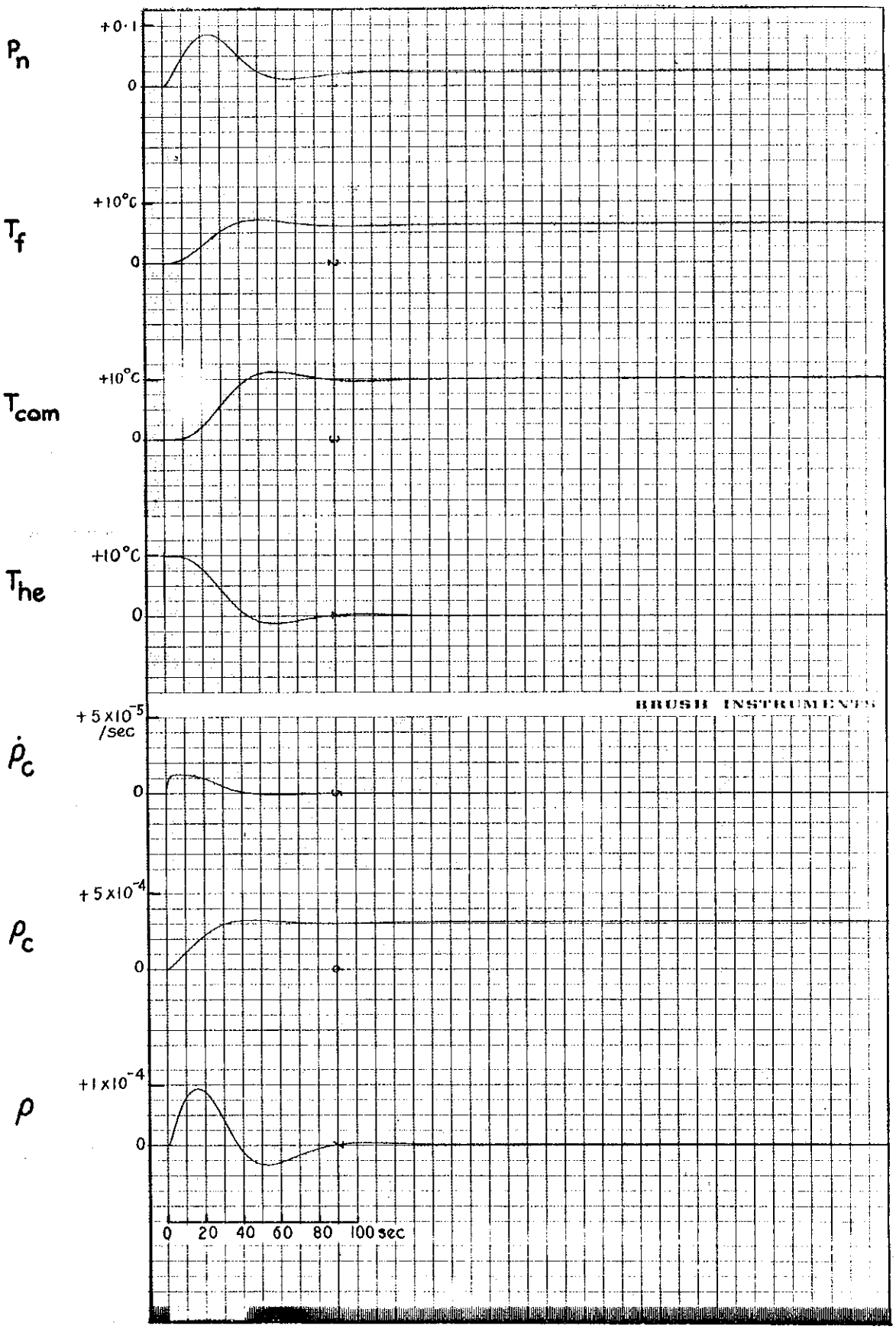

FIGURE 11. RESPONSE OF THE REACTOR WITH A NON-LINEAR CONTROL ROD DRIVE TO A 10°C STEP IN THE REFERENCE TEMPERATURE T_{hr} (100% load, α (-))

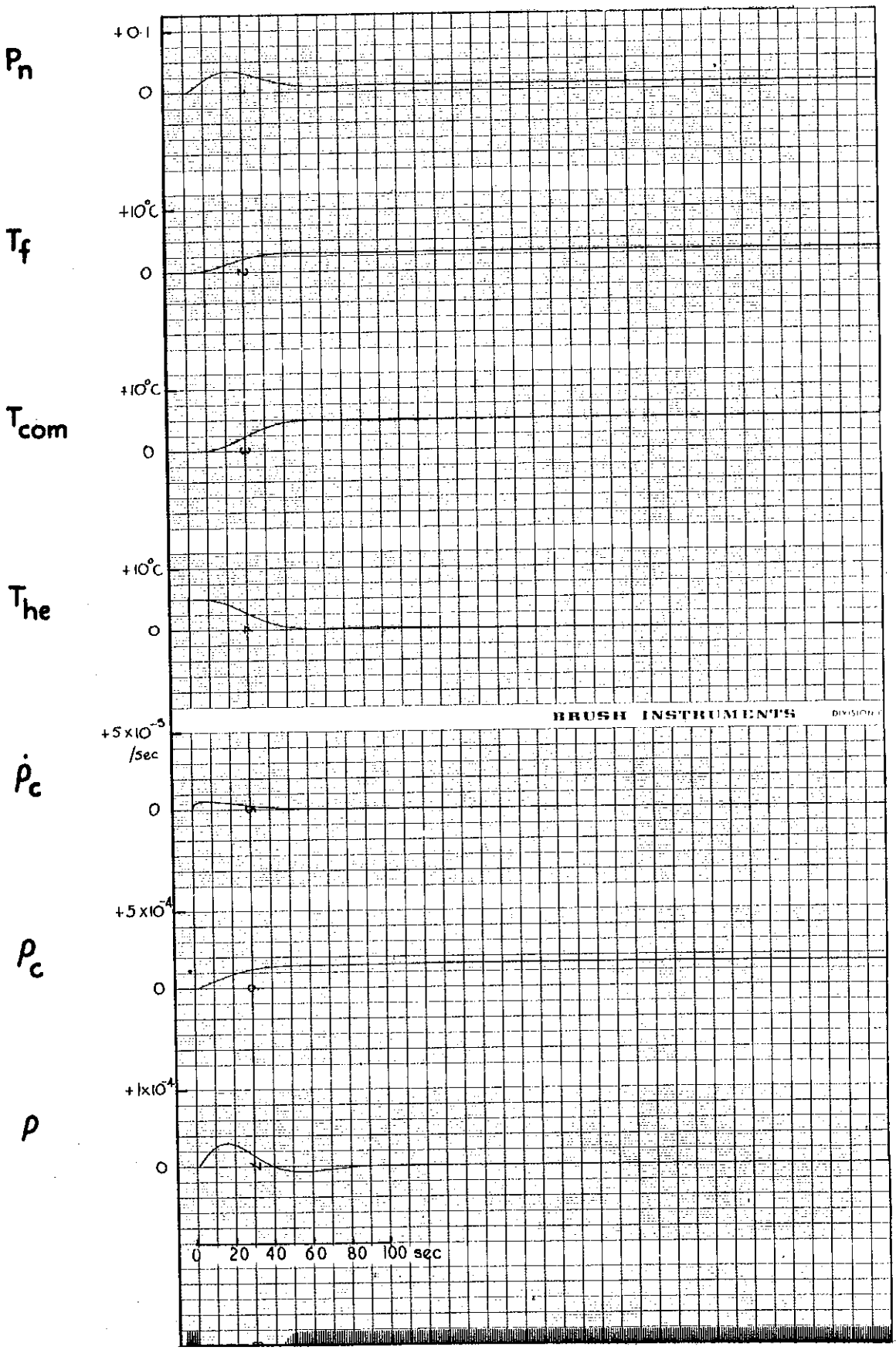

FIGURE 12. RESPONSE OF THE REACTOR WITH A NON-LINEAR CONTROL ROD DRIVE TO A 5°C STEP IN THE REFERENCE TEMPERATURE T_{hr} (100% load, α(-))

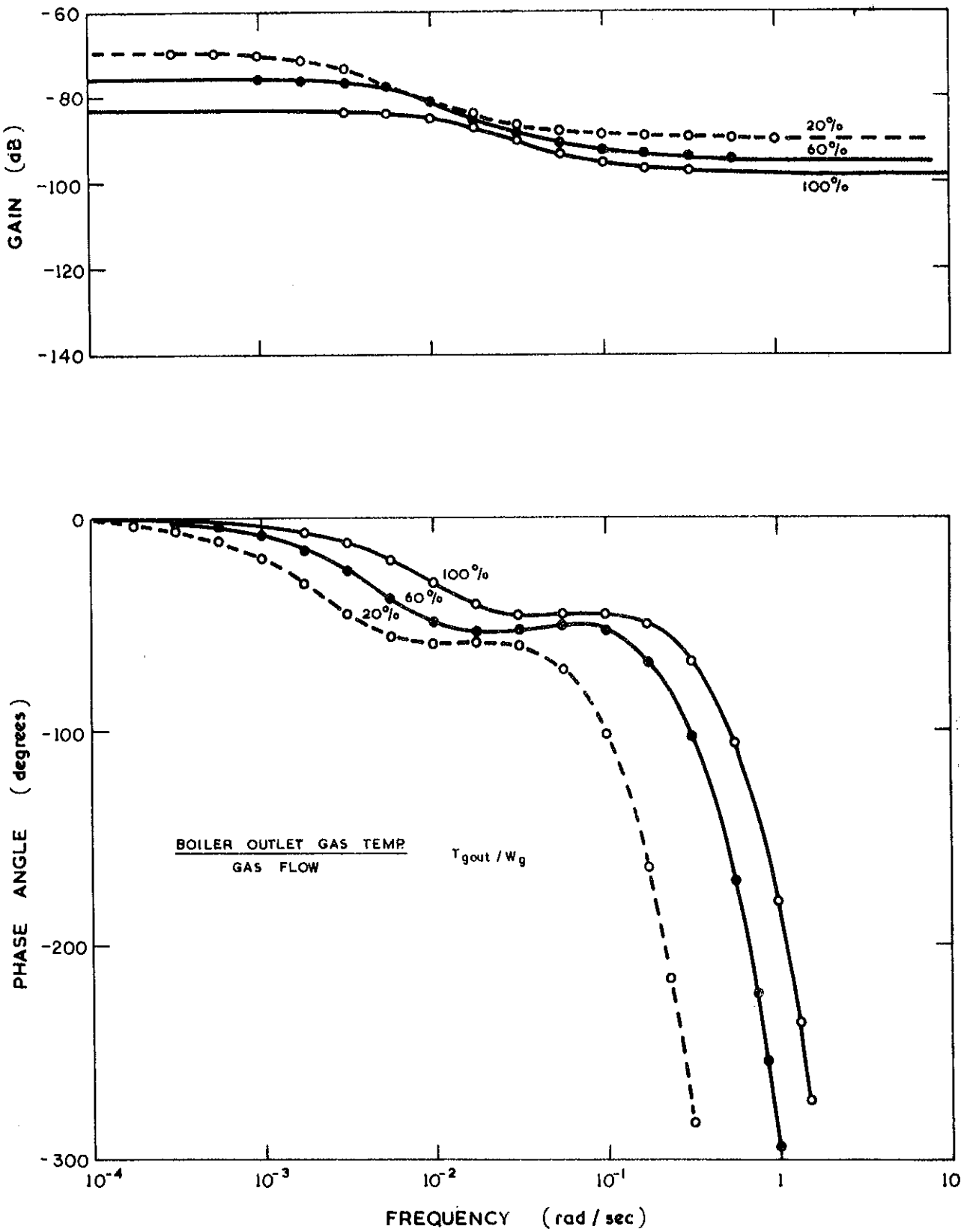

FIGURE 13. FREQUENCY RESPONSE OF BOILER OUTLET GAS TEMPERATURE CONTROL LOOP FOR THREE LOAD LEVELS

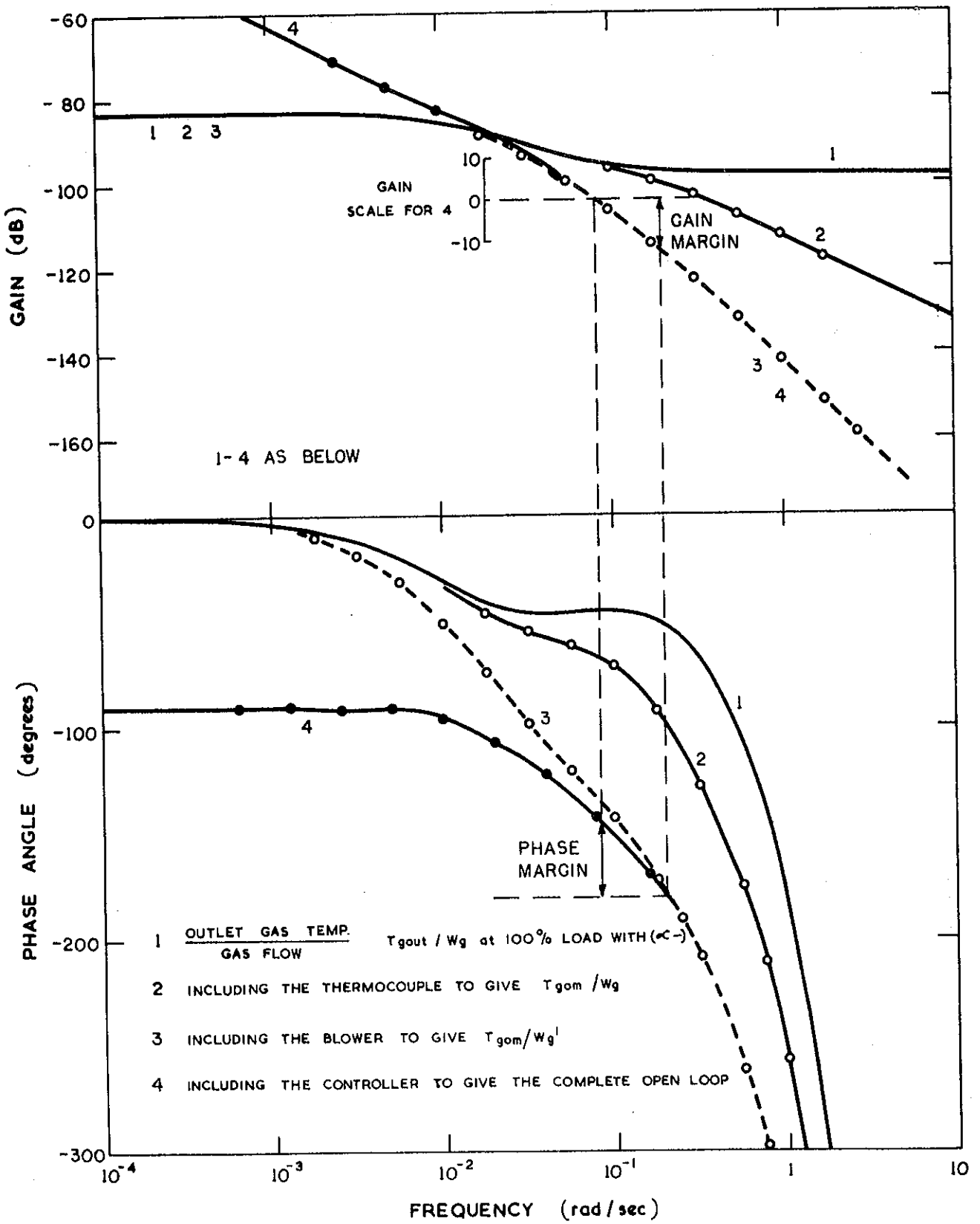

FIGURE 14. FREQUENCY RESPONSE OF BOILER OUTLET GAS TEMPERATURE CONTROL LOOP

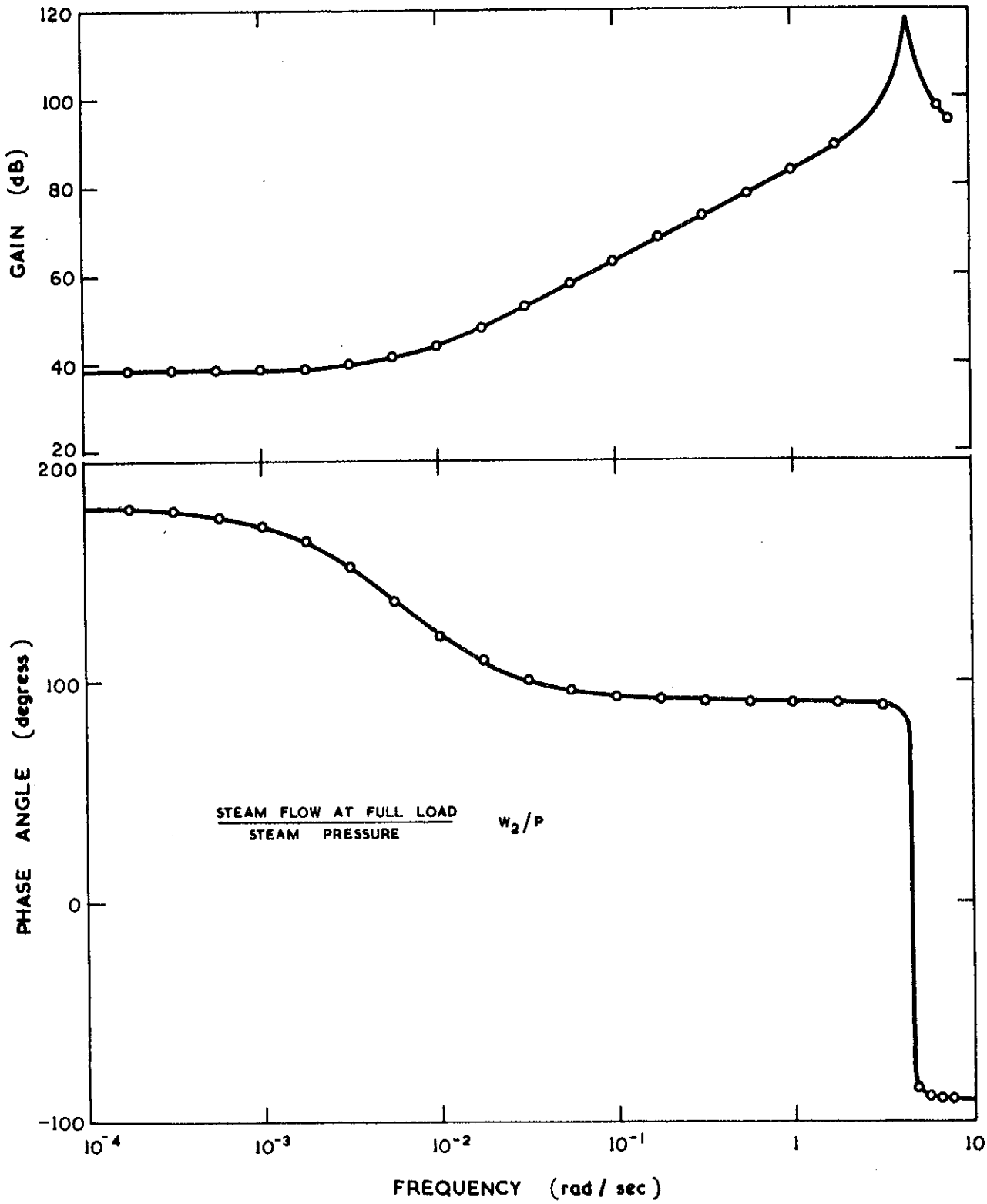

FIGURE 15. FREQUENCY RESPONSE OF THE STEAM DUCT AS SEEN FROM THE BOILER

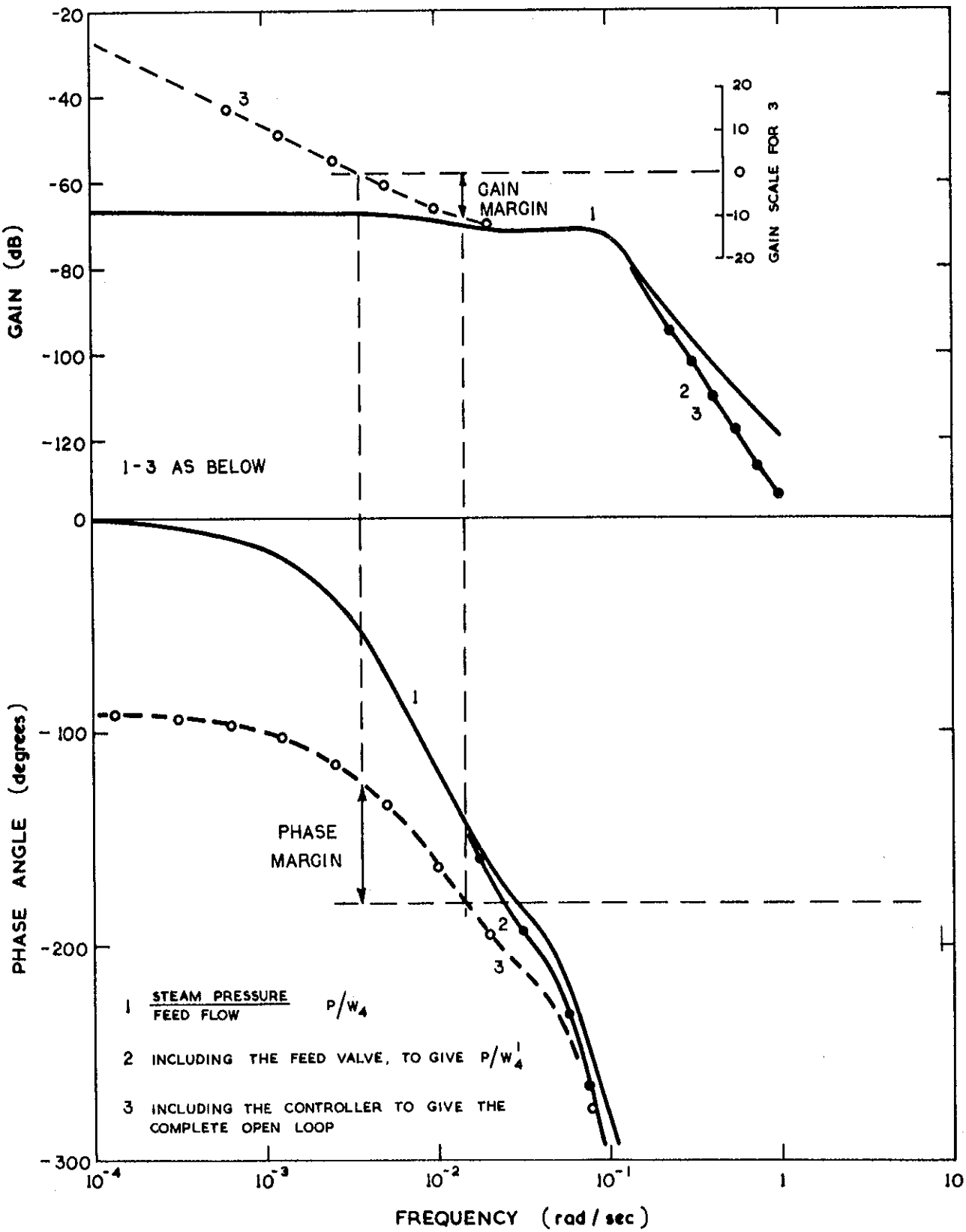

FIGURE 16. FREQUENCY RESPONSE FOR PRESSURE CONTROL LOOP 100 PERCENT LOAD

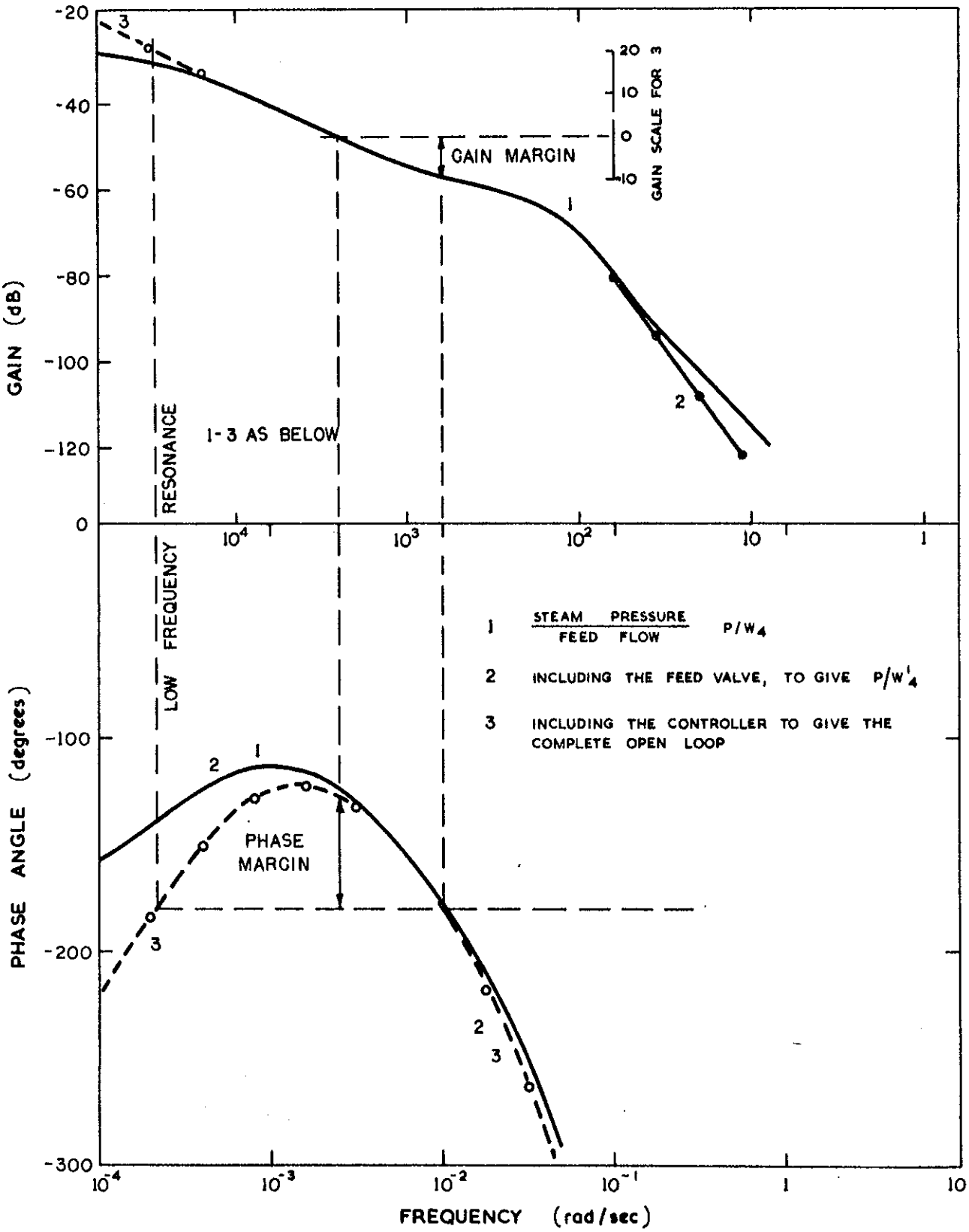

FIGURE 17. FREQUENCY RESPONSE FOR PRESSURE CONTROL LOOP - 60 PERCENT LOAD

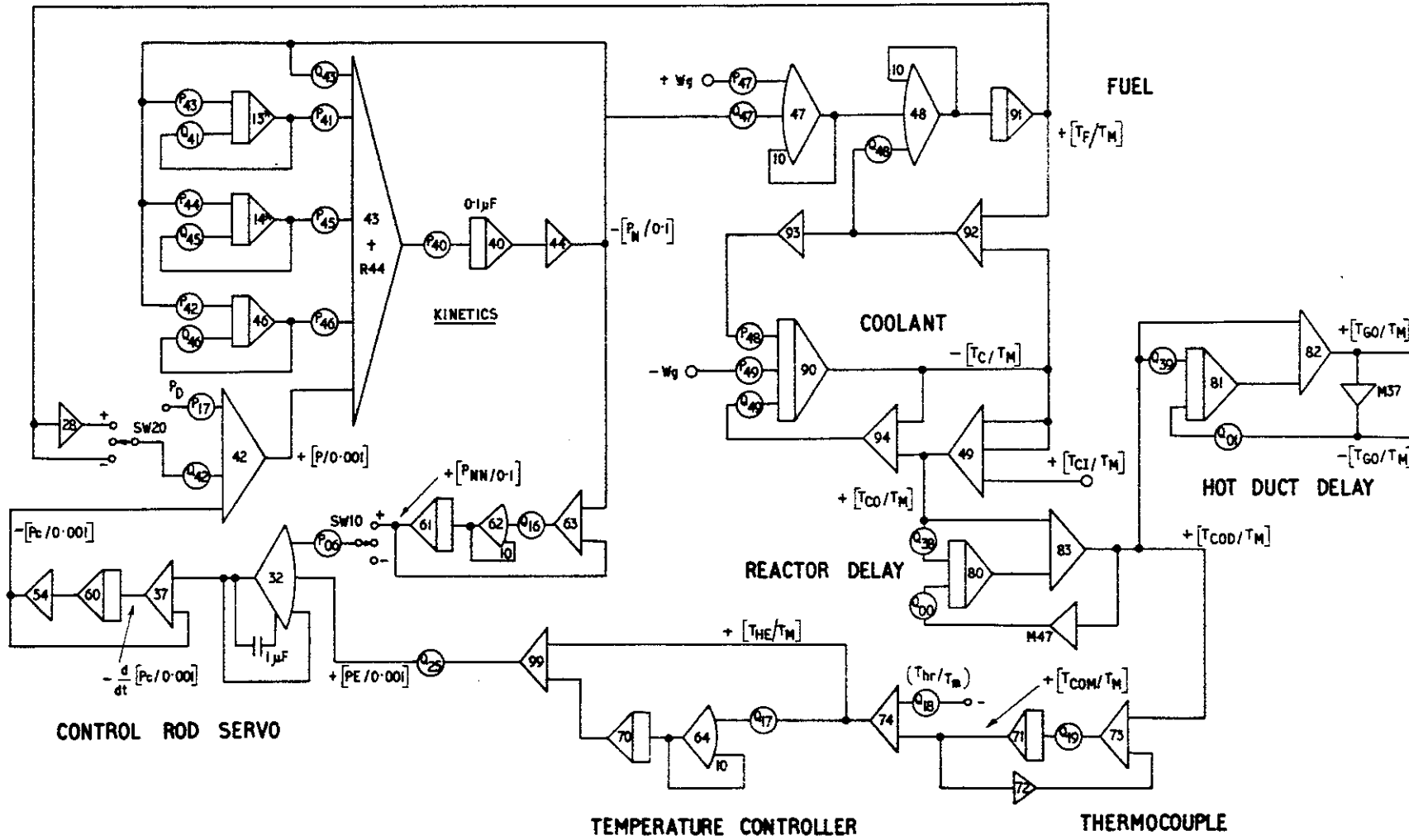

FIGURE 18. ANALOGUE REPRESENTATION OF REACTOR AND GAS CIRCUIT

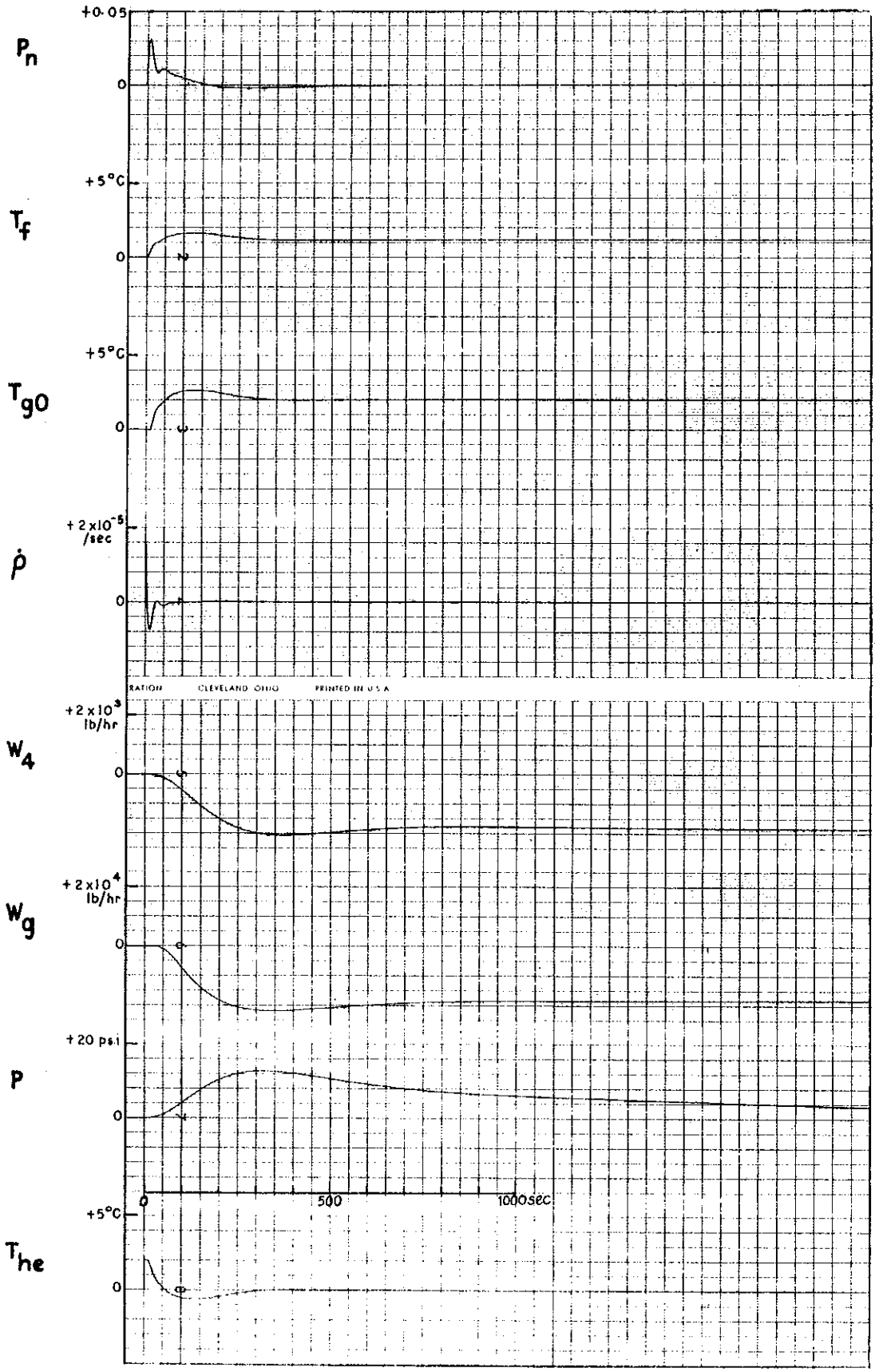

FIGURE 36. SEE TABLE IN SECTION 3.5.2

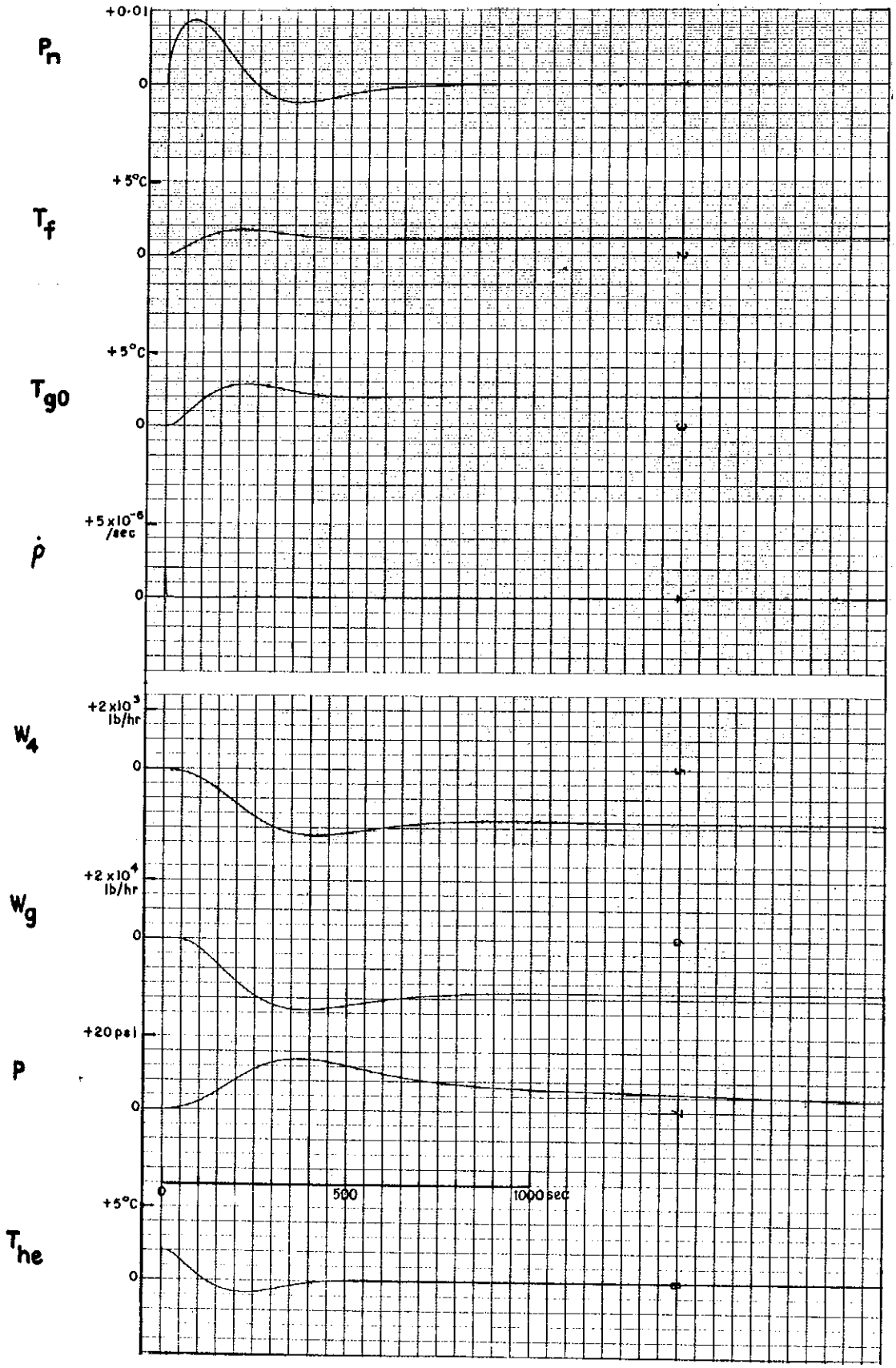

FIGURE 35. SEE TABLE IN SECTION 3.5.2

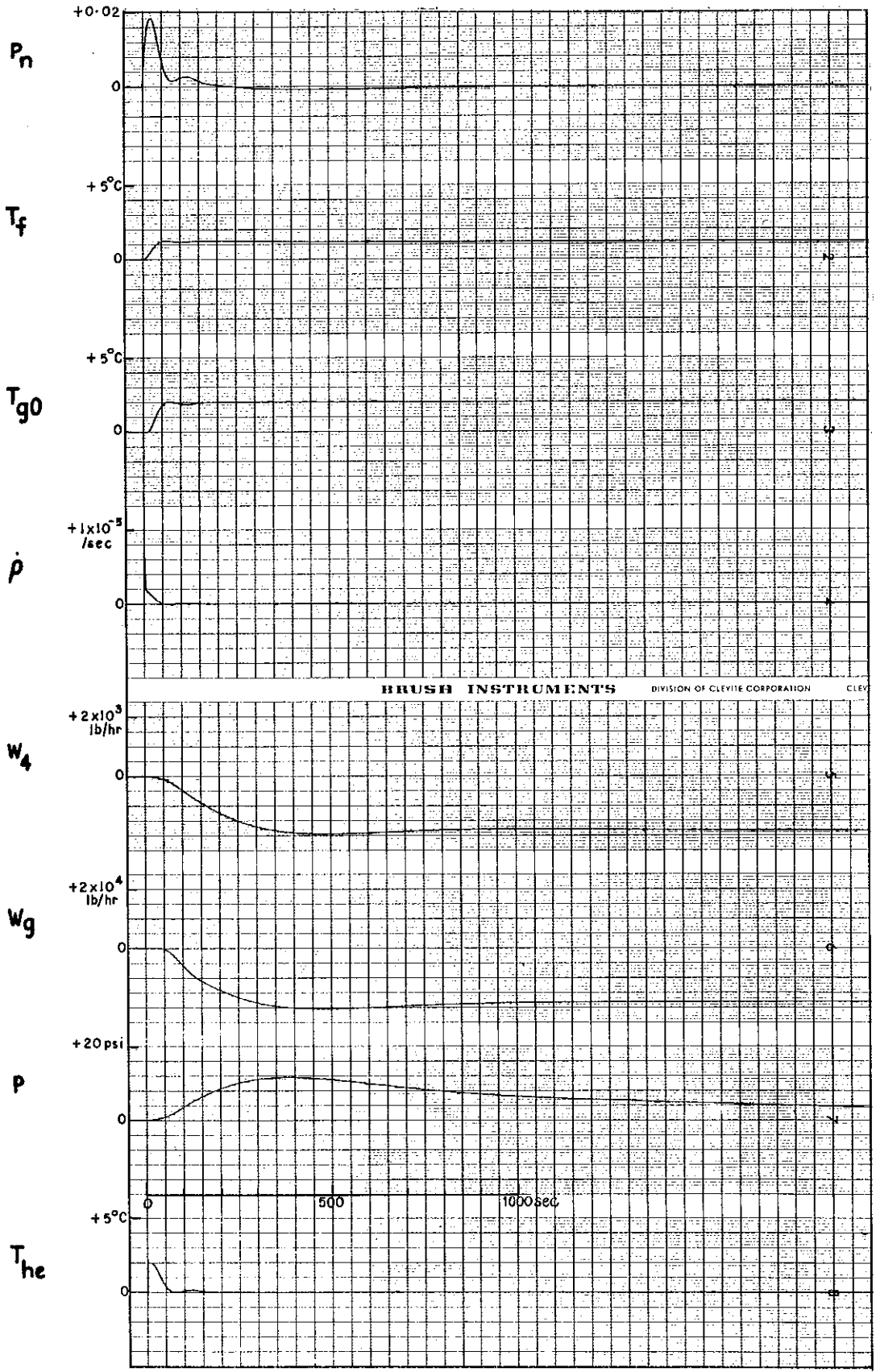

FIGURE 34. SEE TABLE IN SECTION 3.5.2

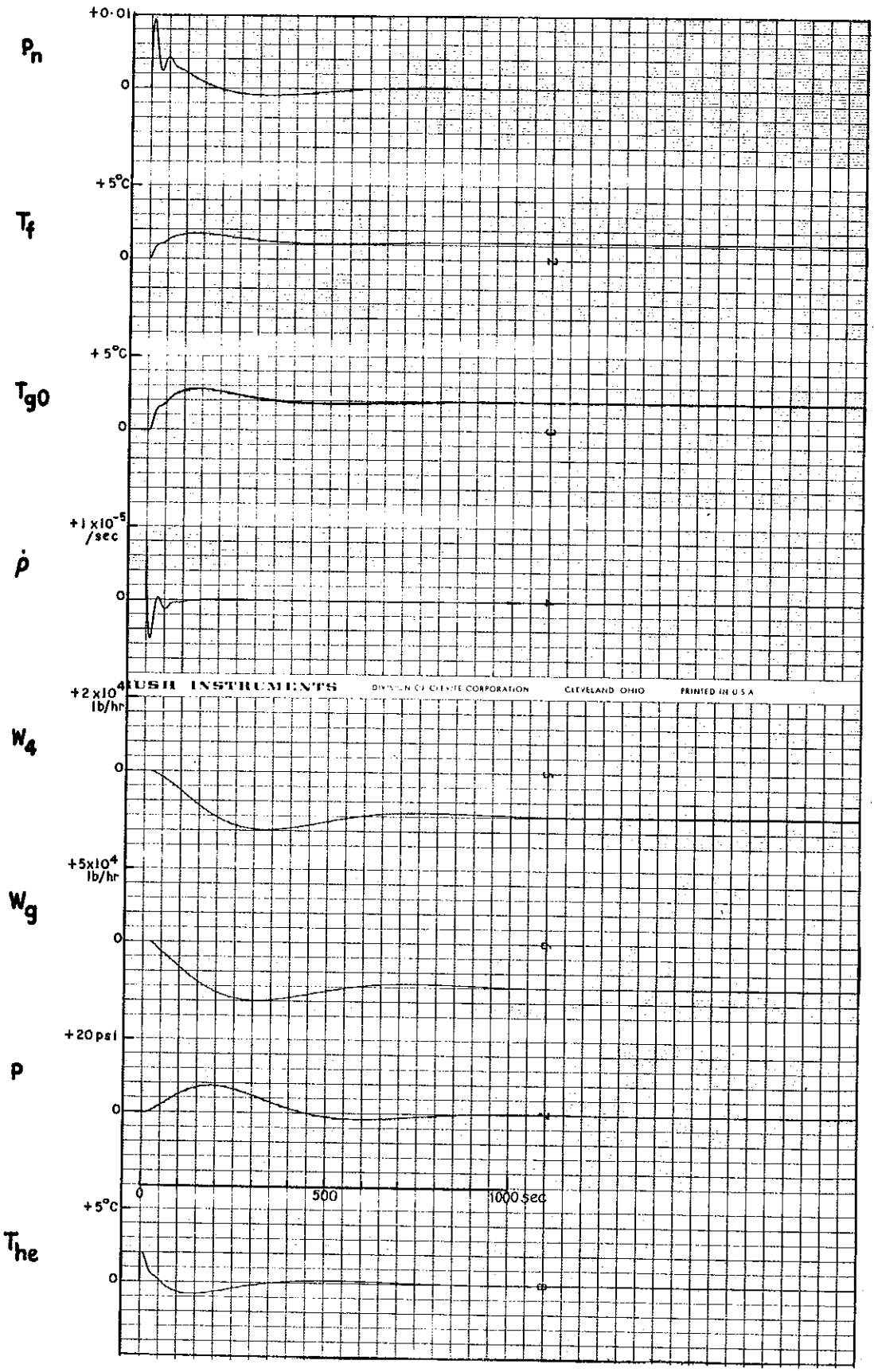

FIGURE 33. SEE TABLE IN SECTION 3.5.2

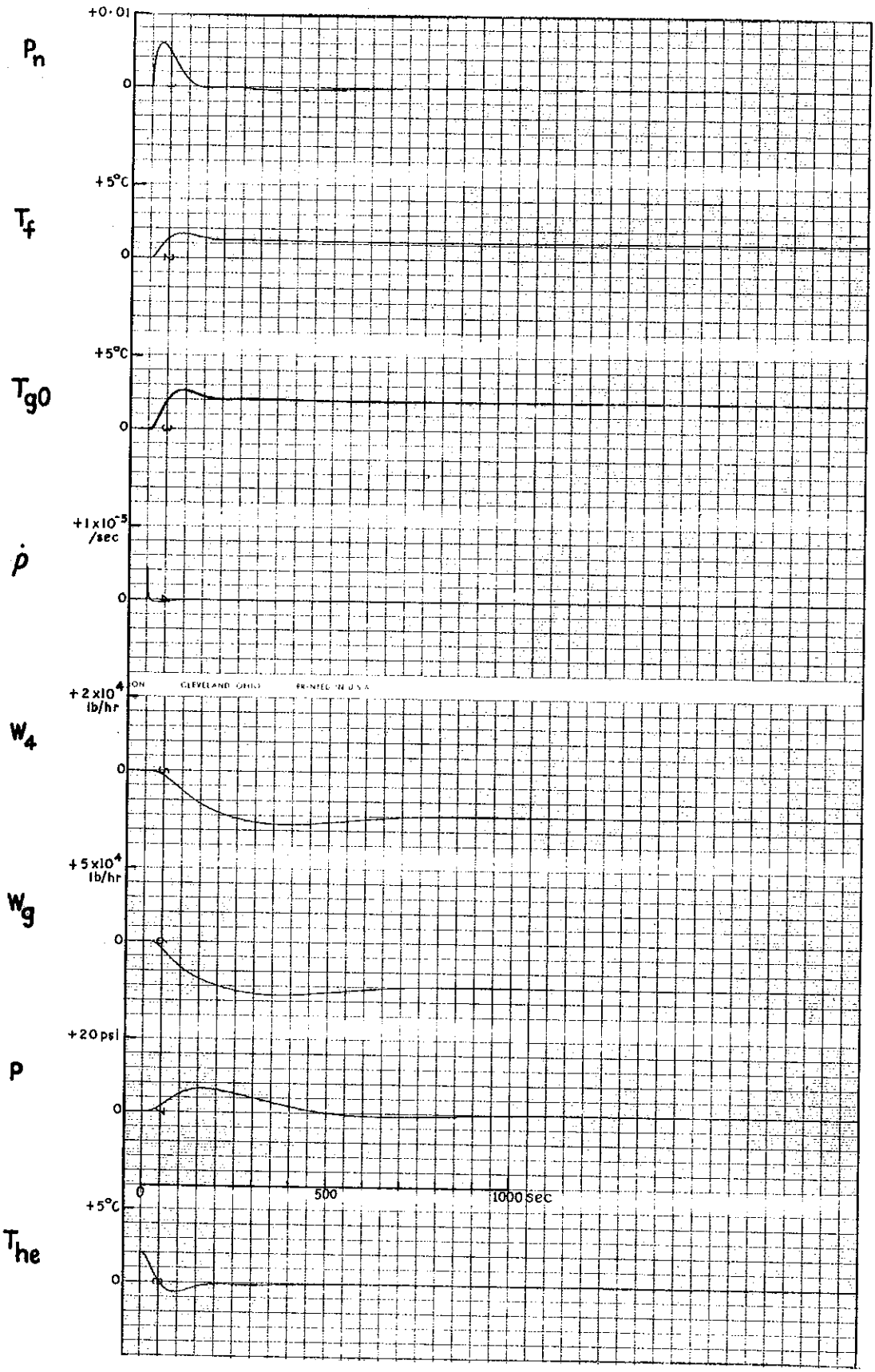

FIGURE 32. SEE TABLE IN SECTION 3.5.2

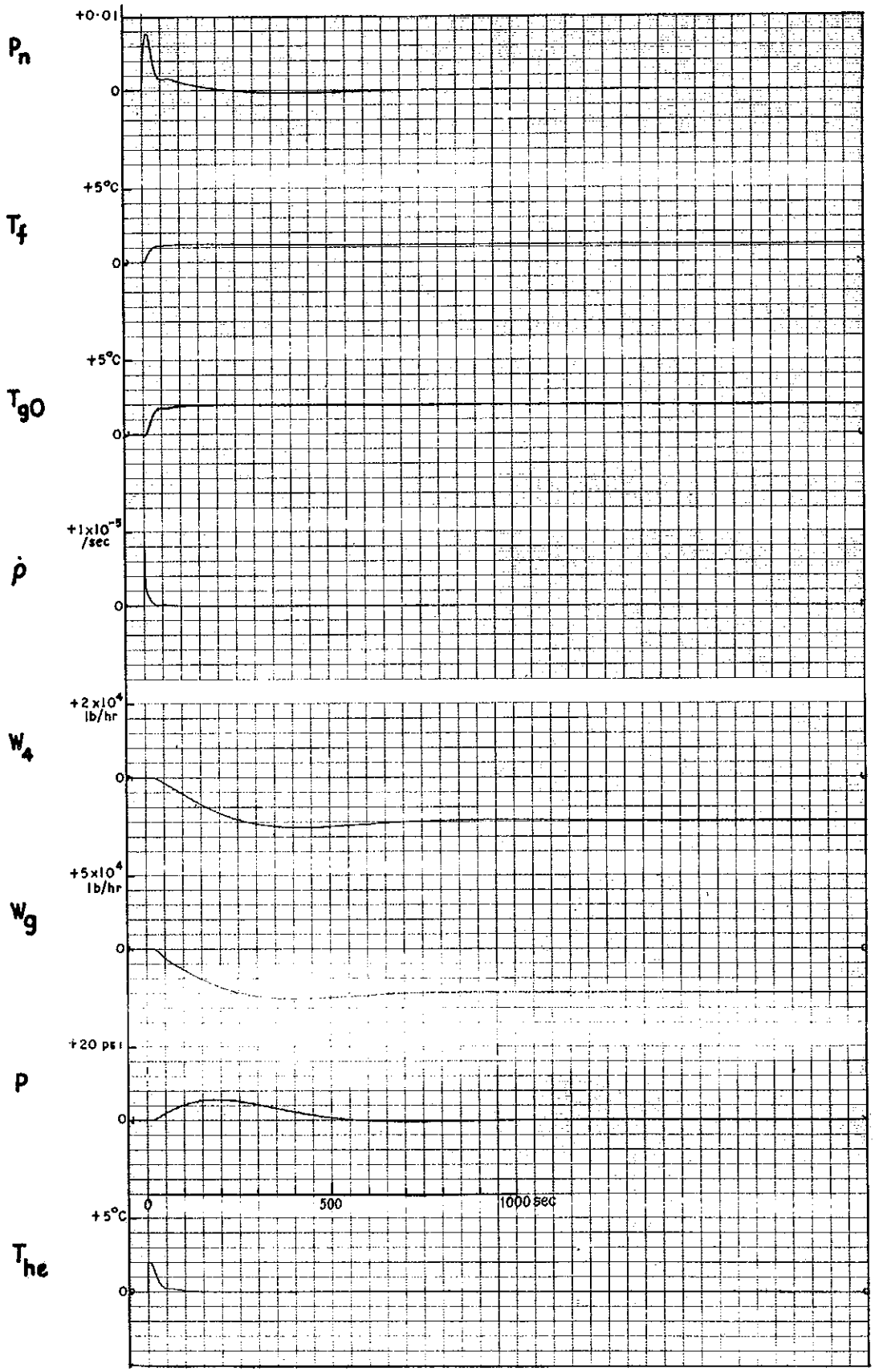

FIGURE 31. SEE TABLE IN SECTION 3.5.2

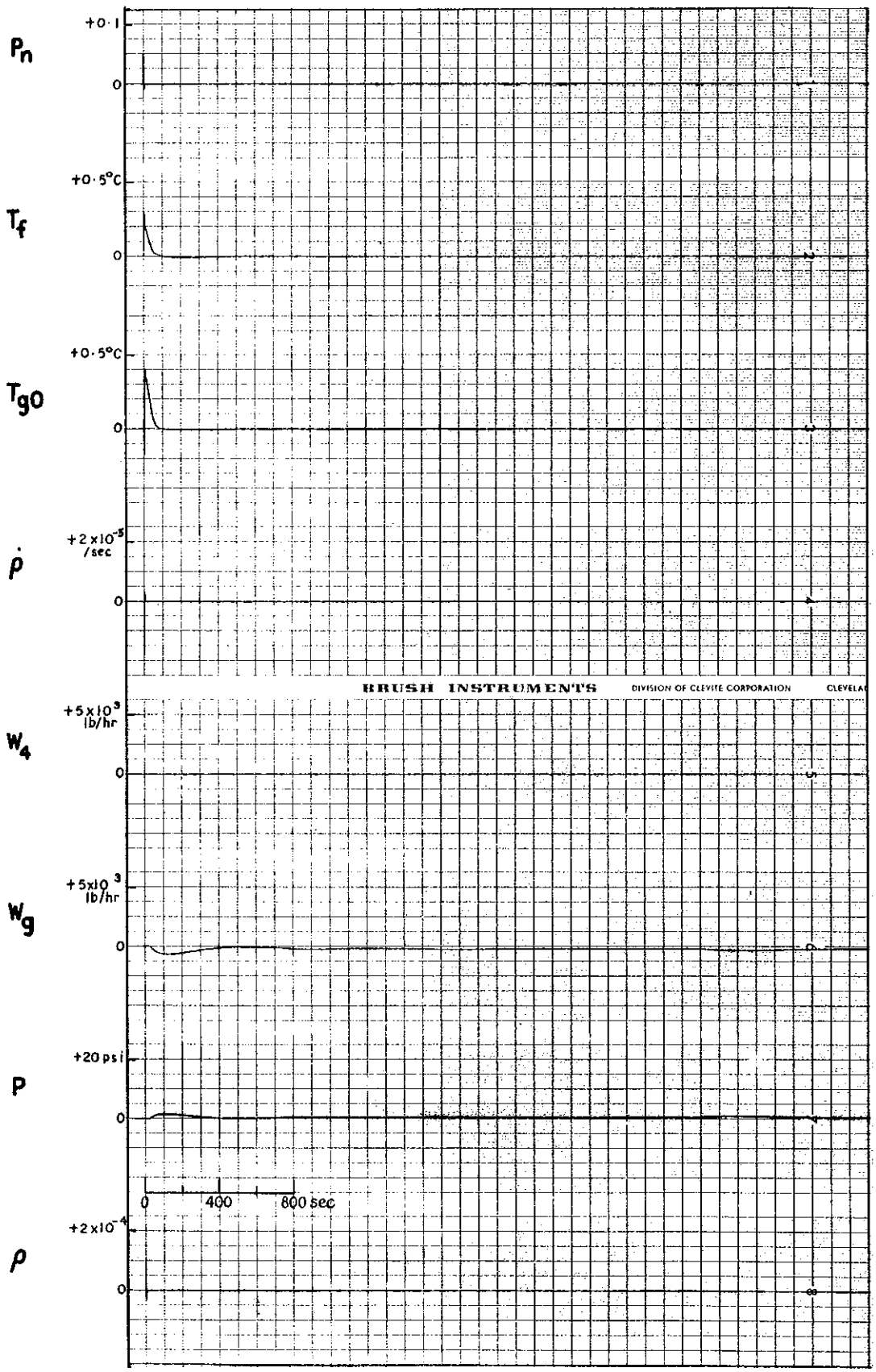

FIGURE 30. SEE TABLE IN SECTION 3.5.2

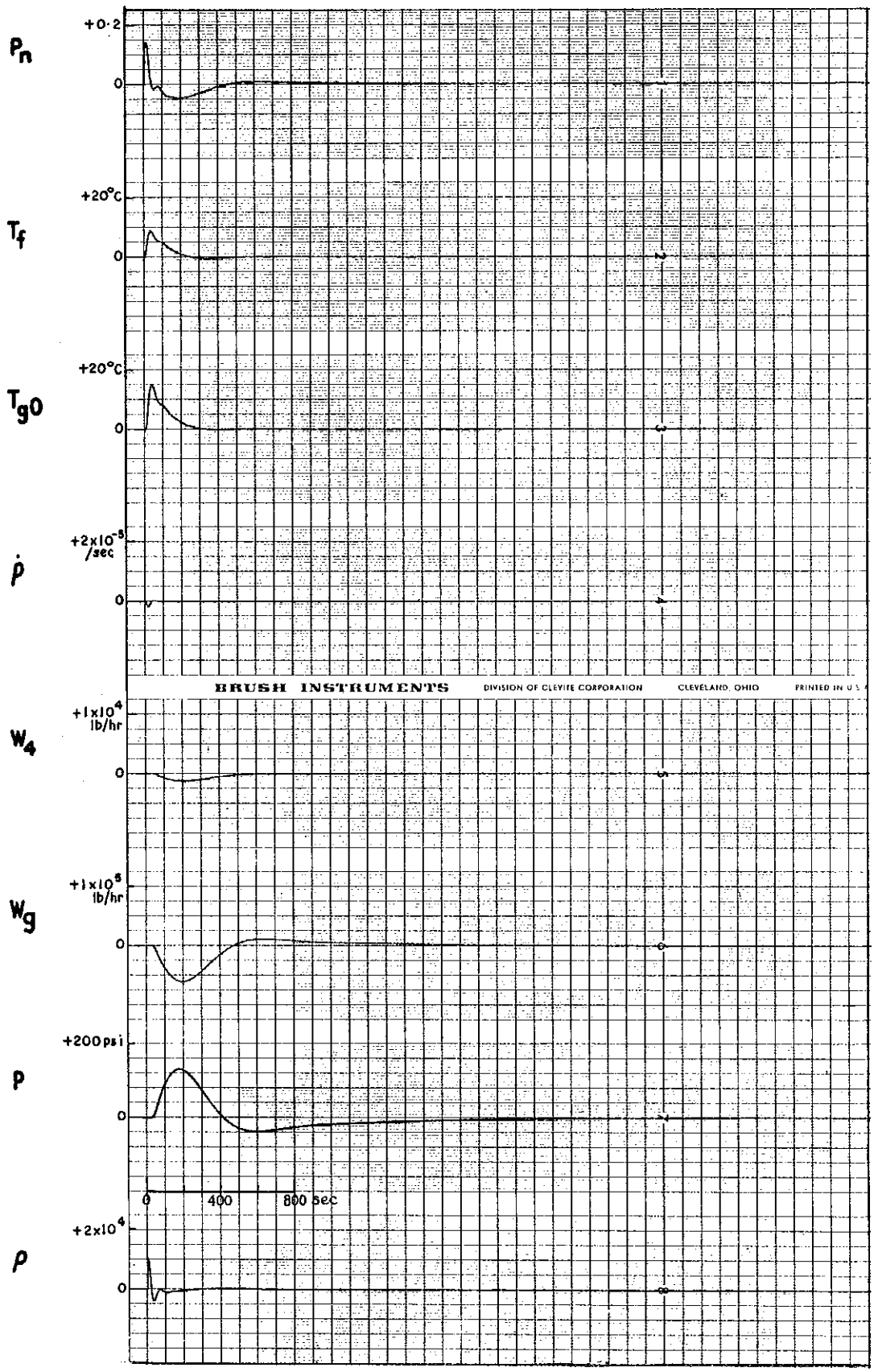

FIGURE 29. SEE TABLE IN SECTION 3.5.2

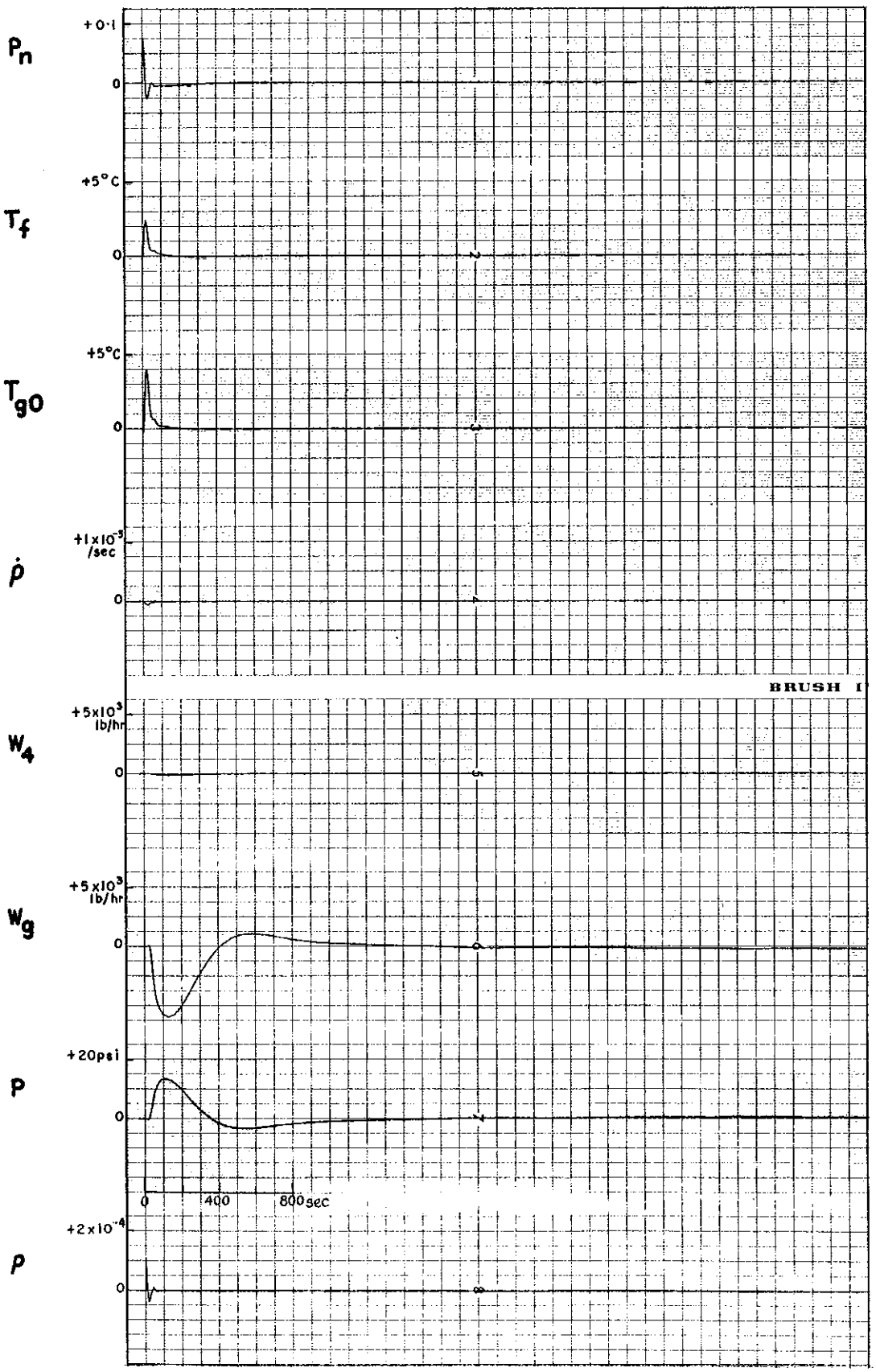

FIGURE 28. SEE TABLE IN SECTION 3.5.2

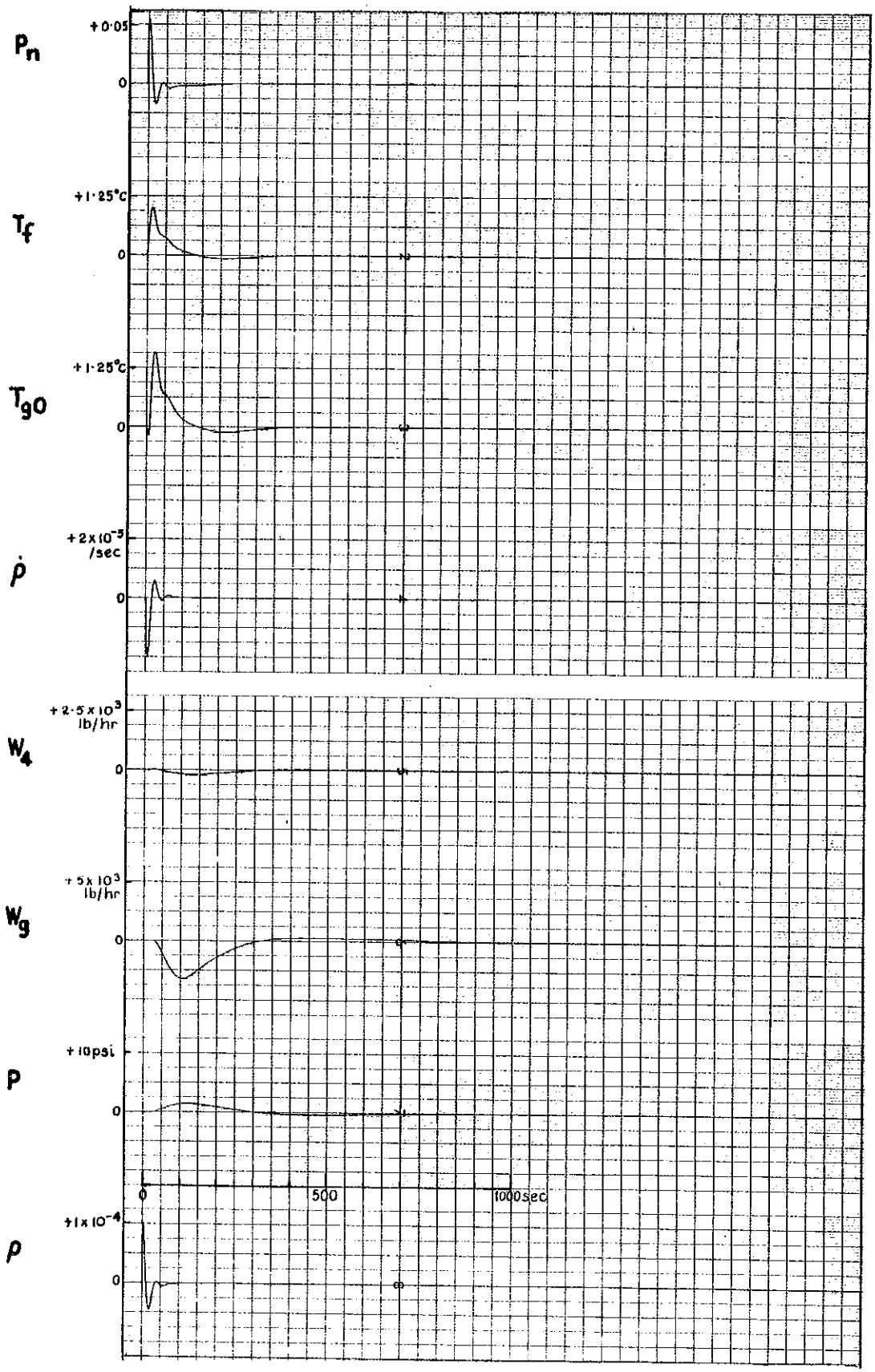

FIGURE 27. SEE TABLE IN SECTION 3.5.2

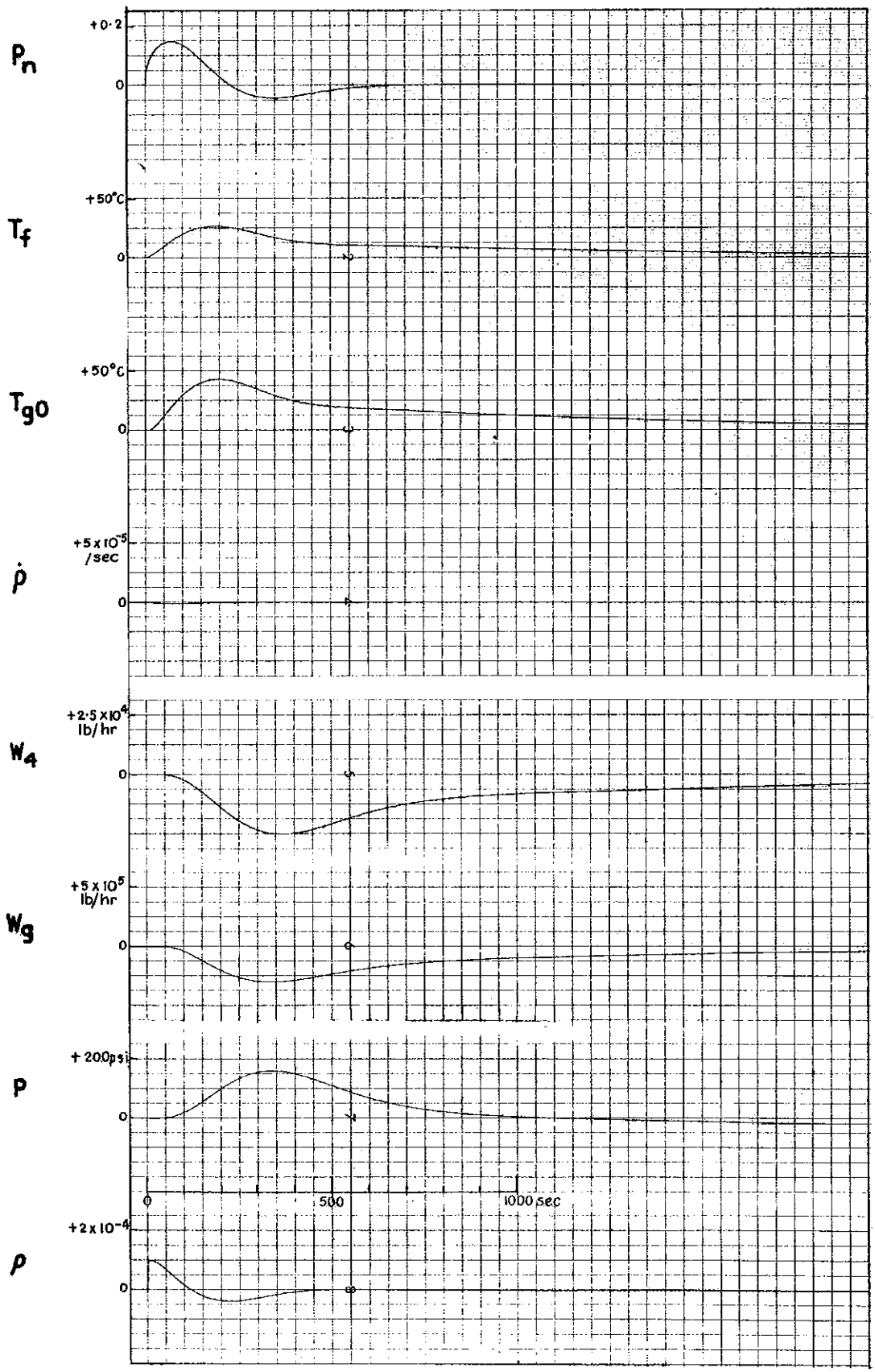

FIGURE 26. SEE TABLE IN SECTION 3.5.2

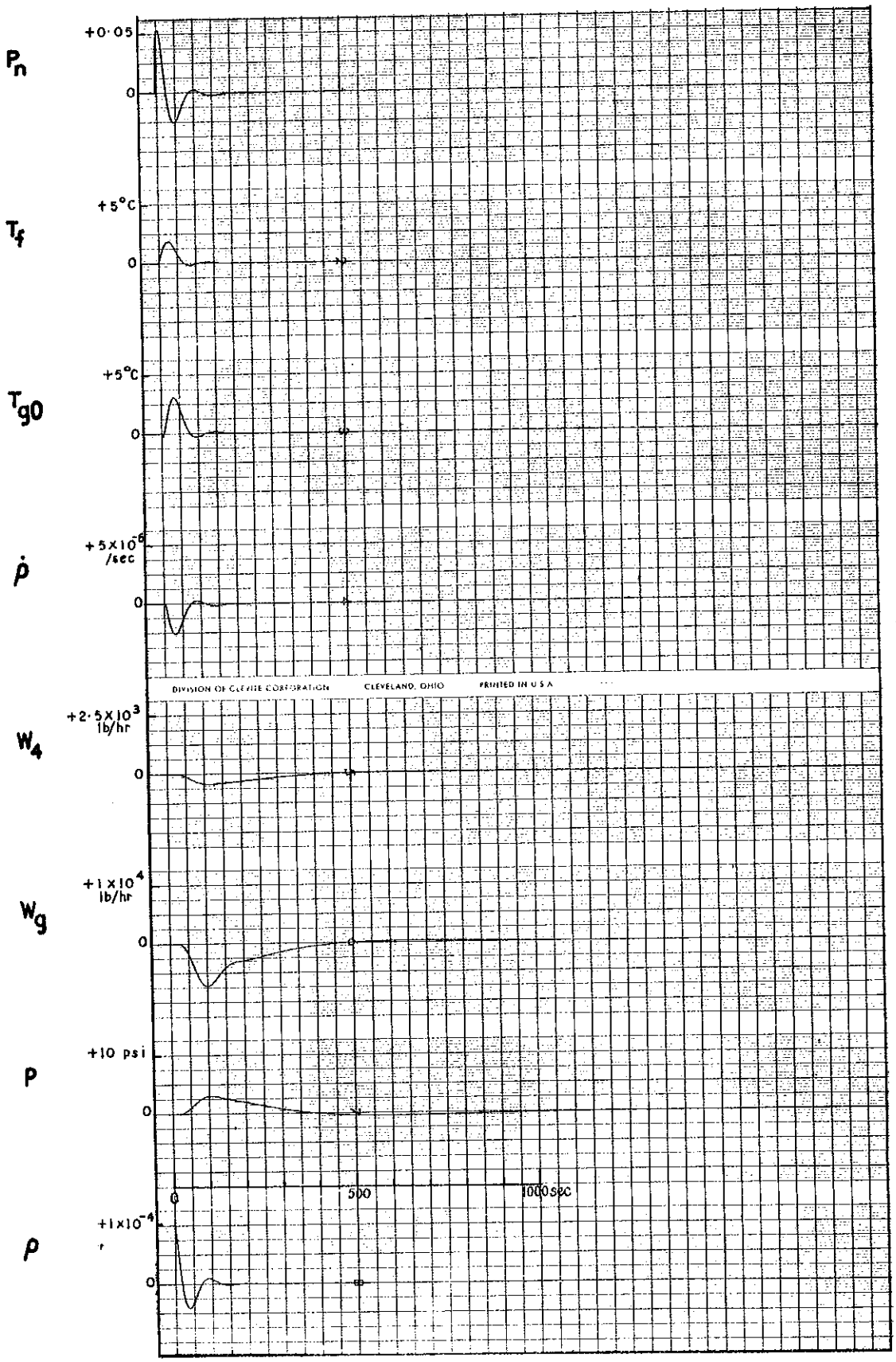

FIGURE 25. SEE TABLE IN SECTION 3.5.2

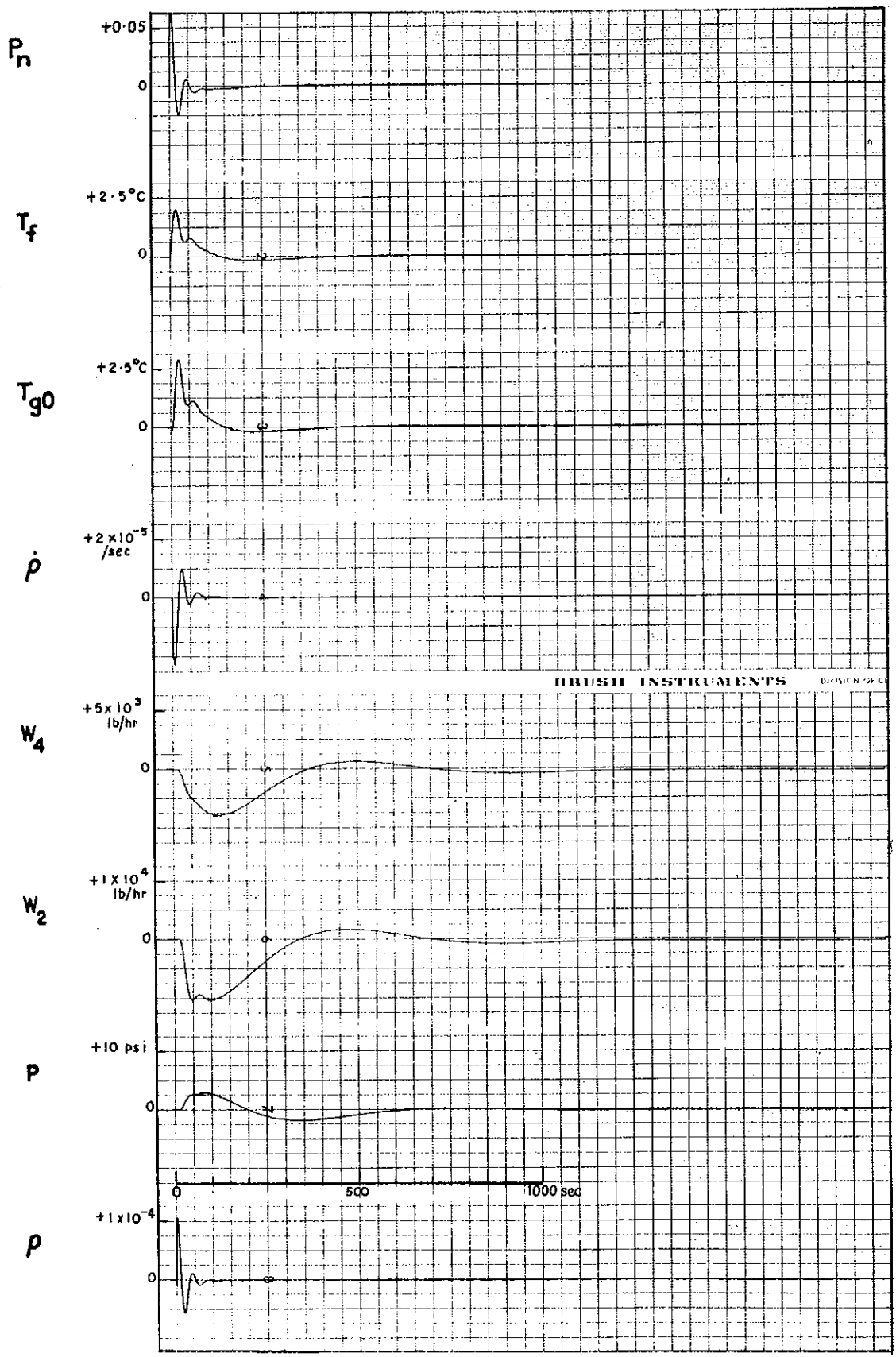

FIGURE 24. SEE TABLE IN SECTION 3.5.2

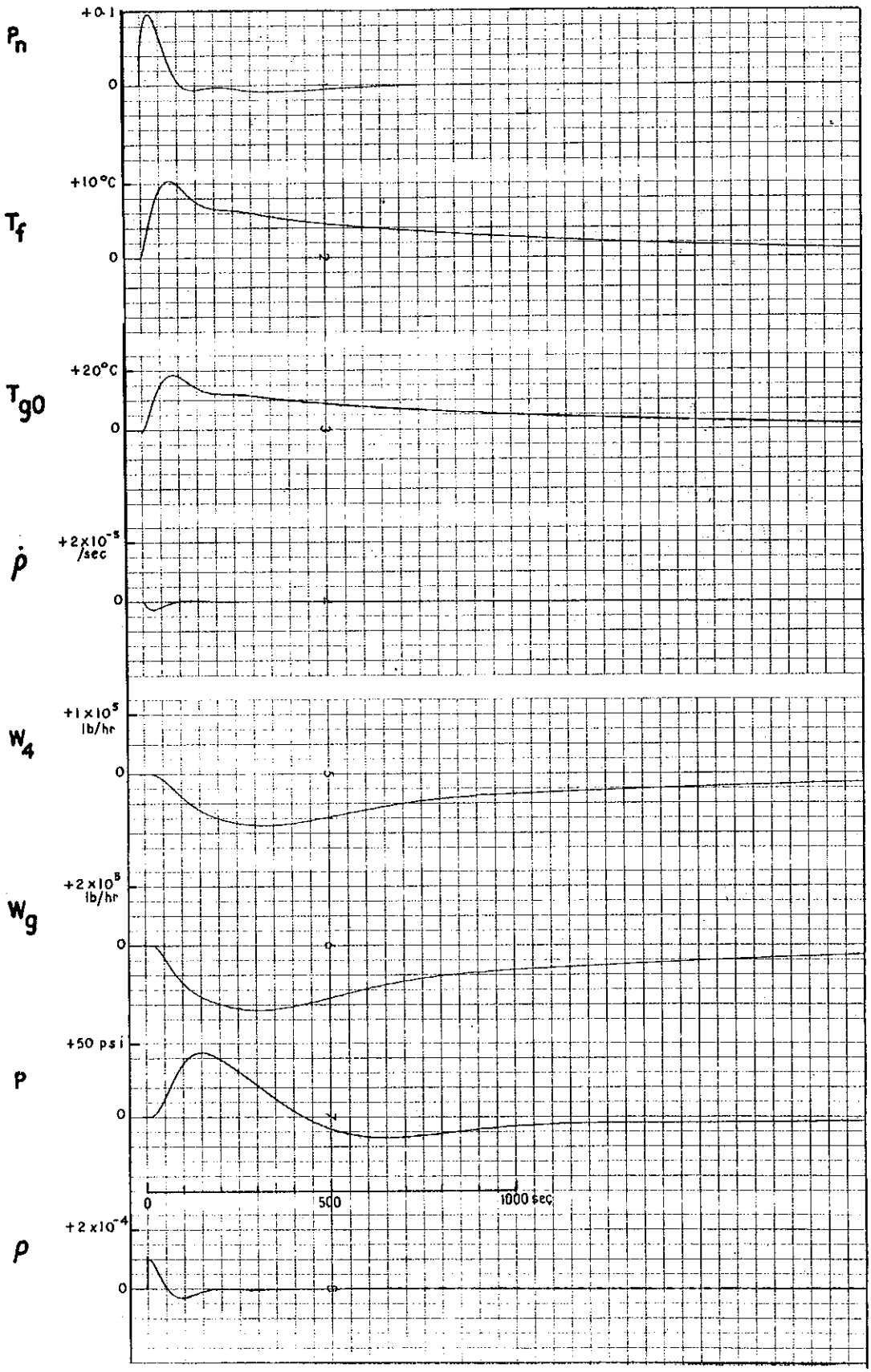

FIGURE 23. SEE TABLE IN SECTION 3.5.2

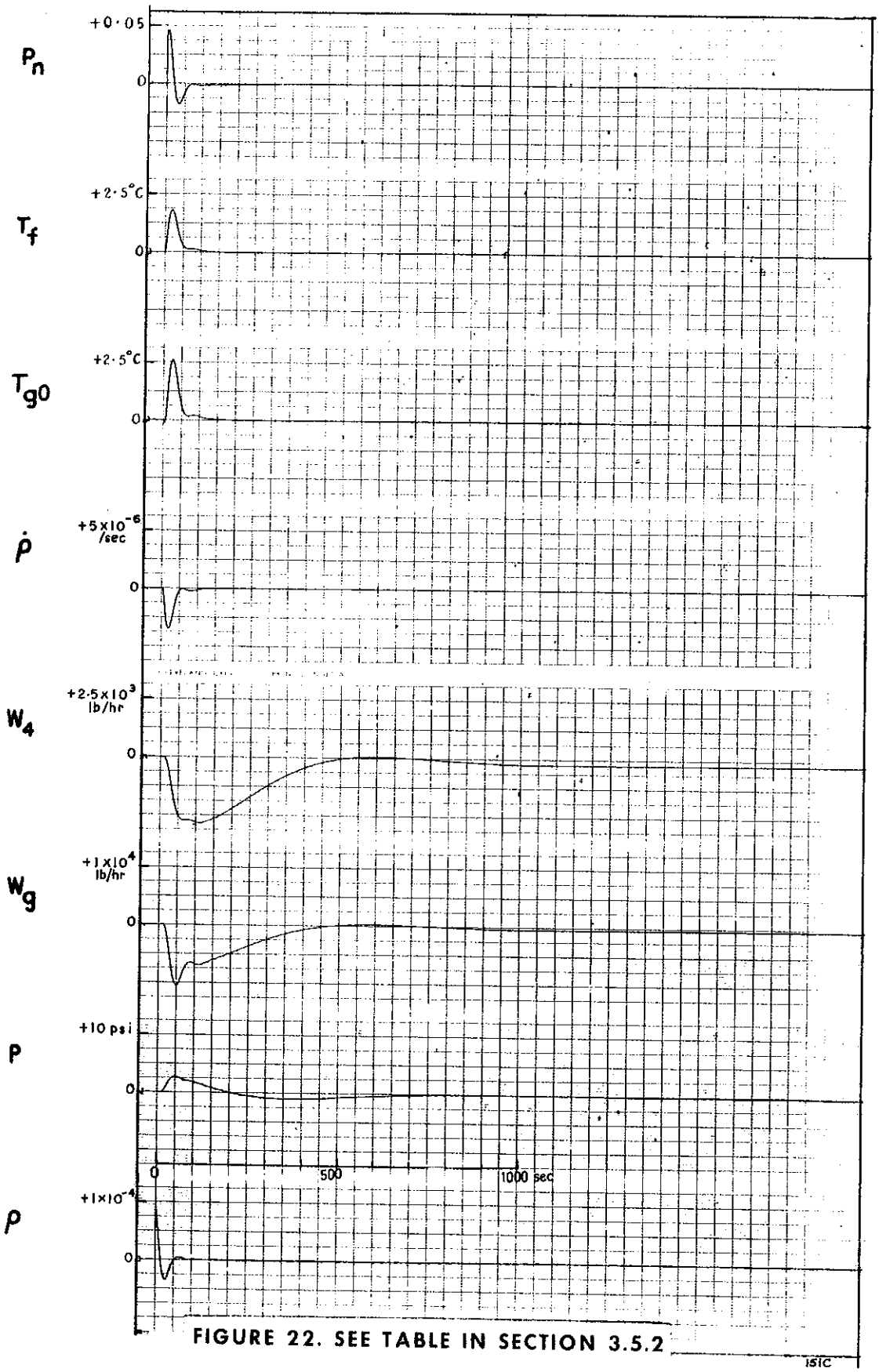

FIGURE 22. SEE TABLE IN SECTION 3.5.2

isic

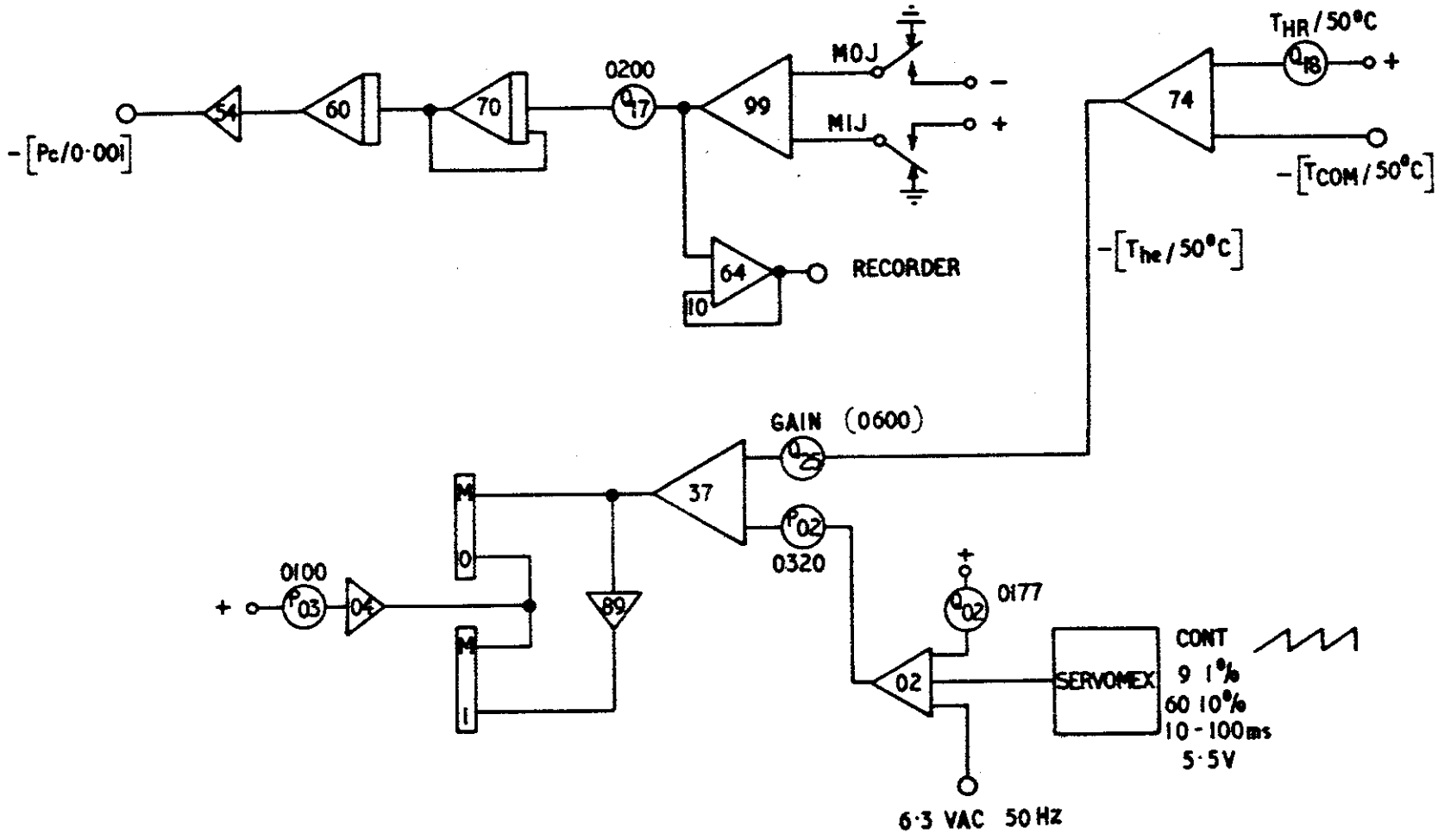

FIGURE 21. ANALOGUE REPRESENTATION OF RELAY CONTROLLER

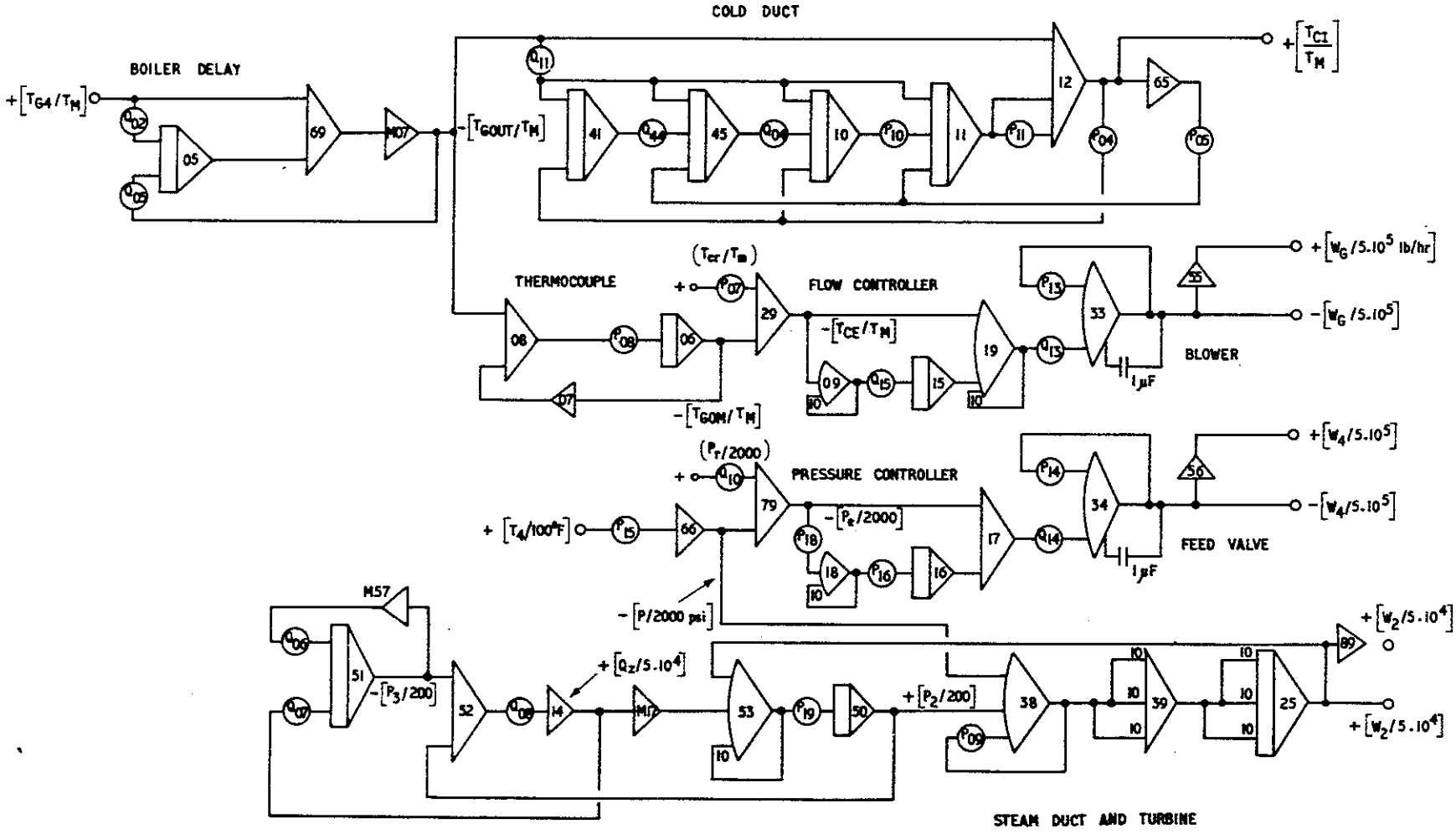

FIGURE 20. ANALOGUE REPRESENTATION OF THE BOILER CONTROLS AND STEAM CIRCUIT

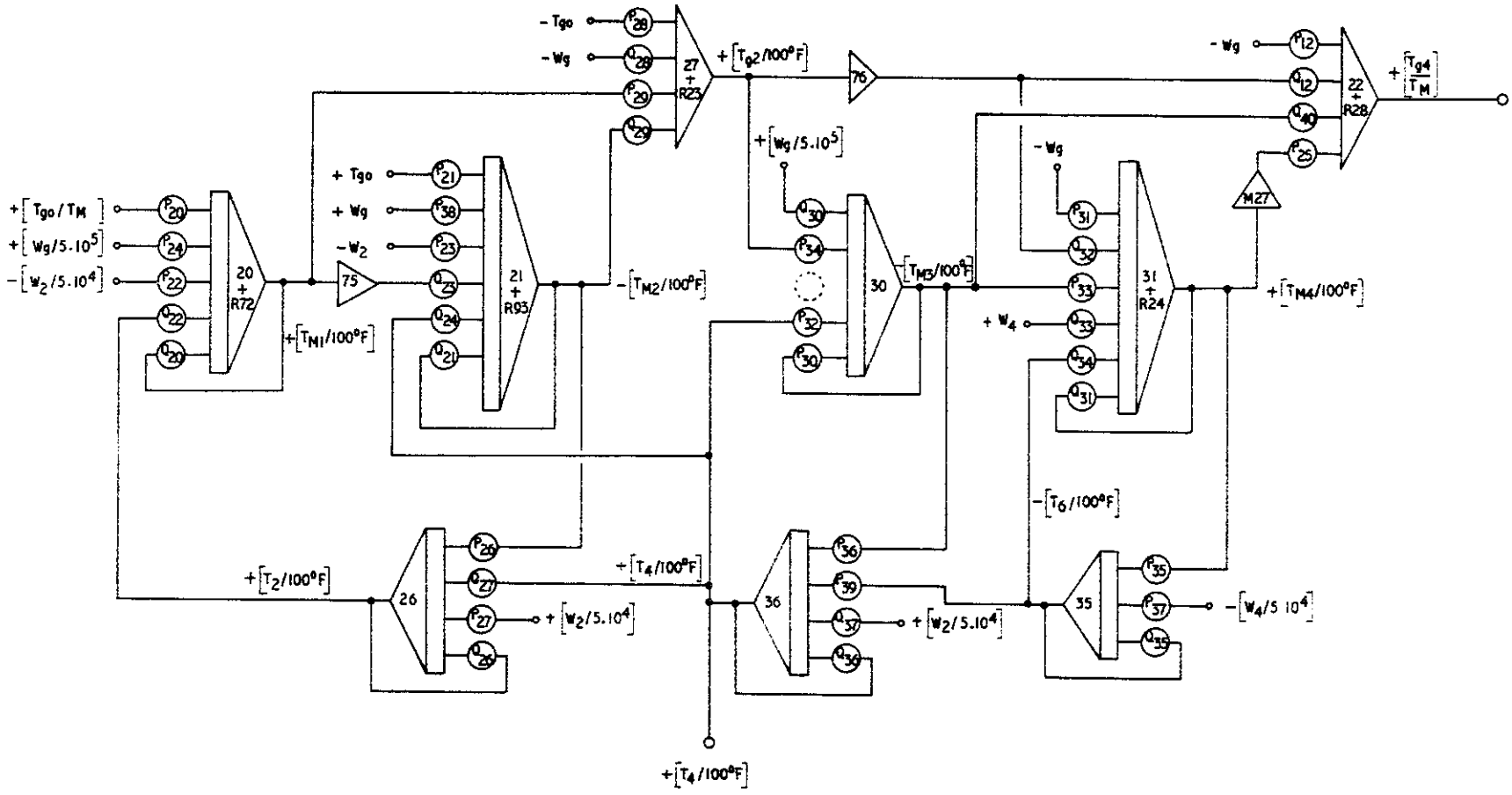

FIGURE 19. ANALOGUE REPRESENTATION OF THE BOILER

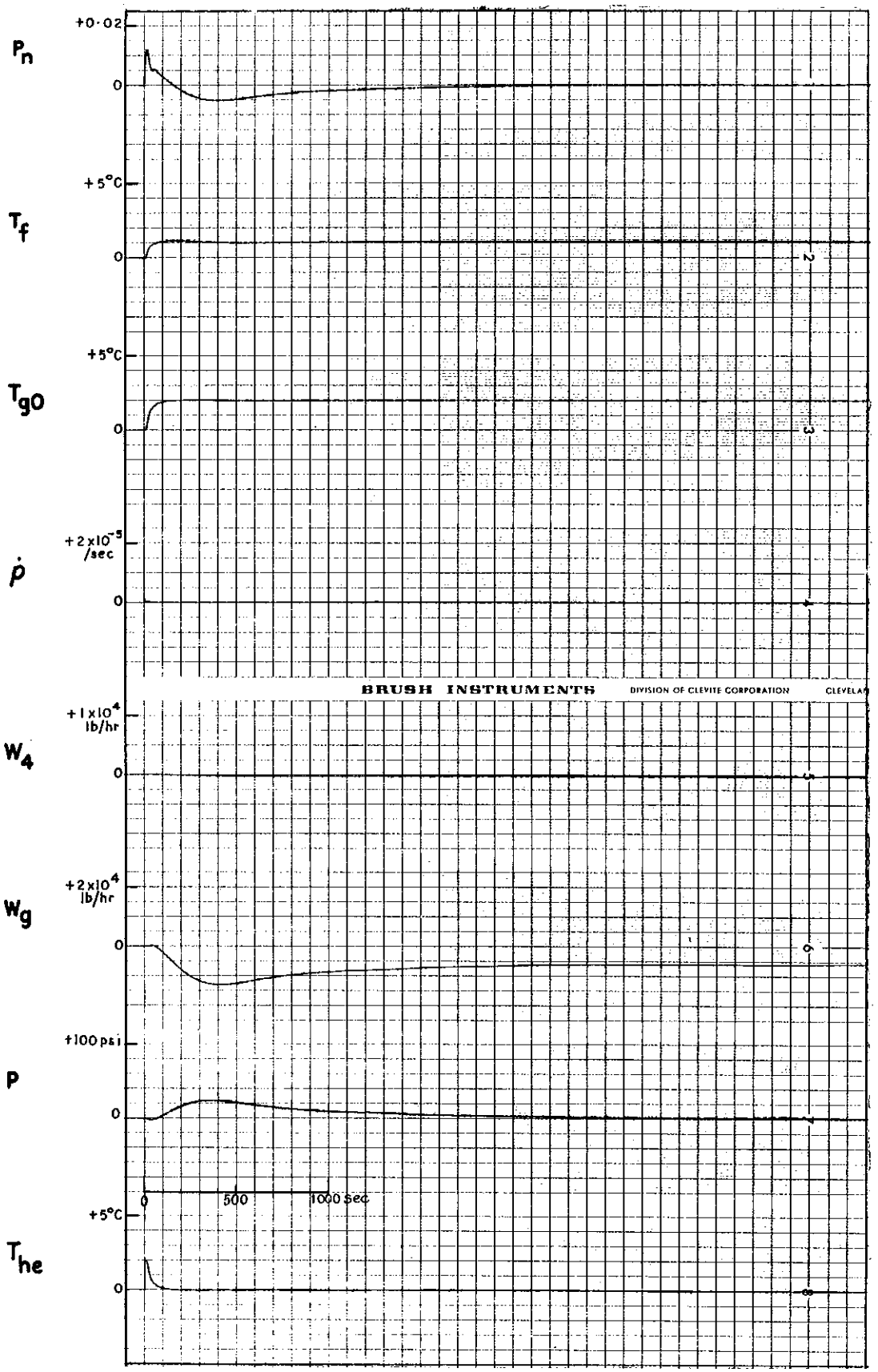

FIGURE 37. SEE TABLE IN SECTION 3.5.2

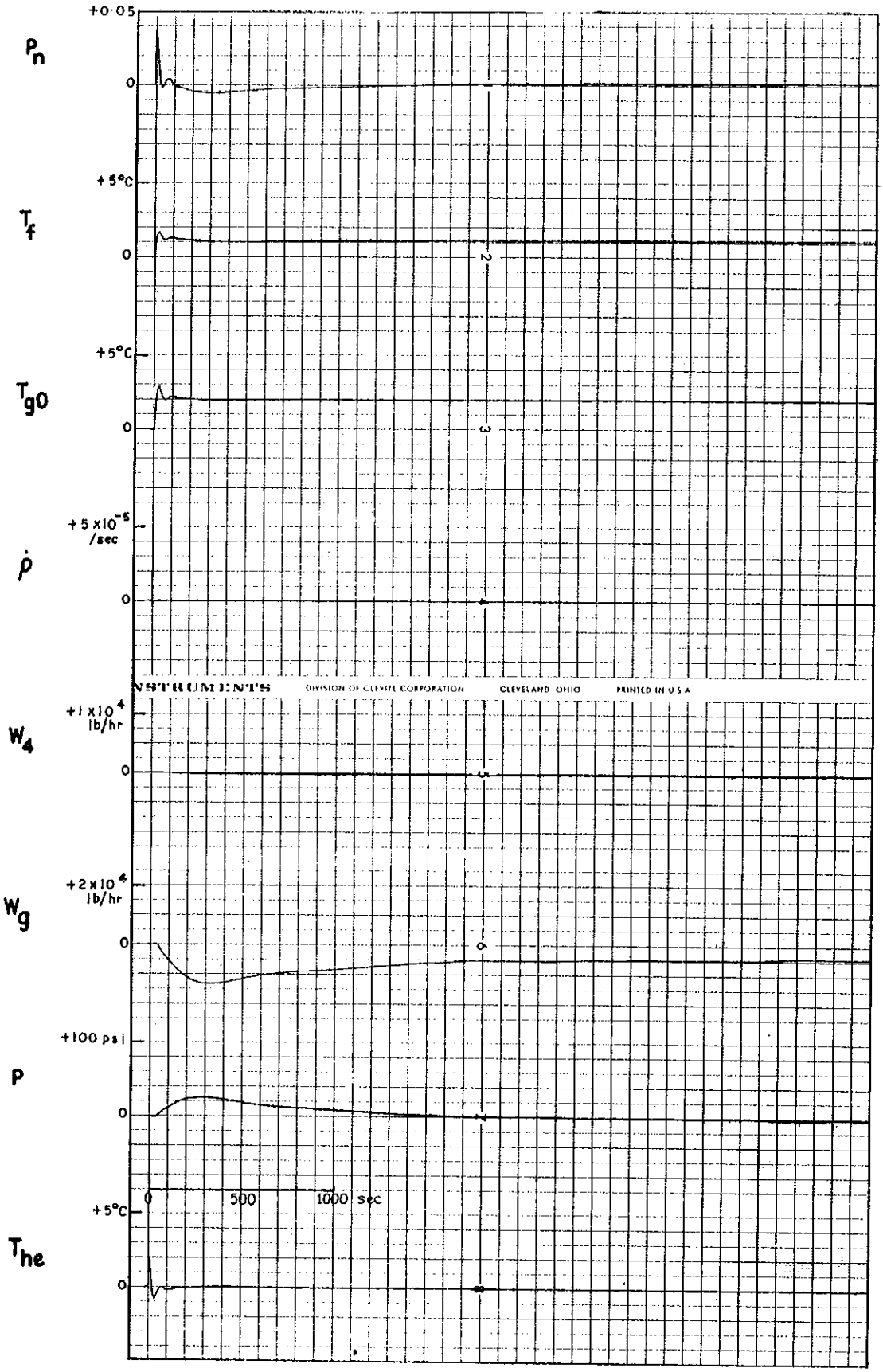

FIGURE 38. SEE TABLE IN SECTION 3.5.2

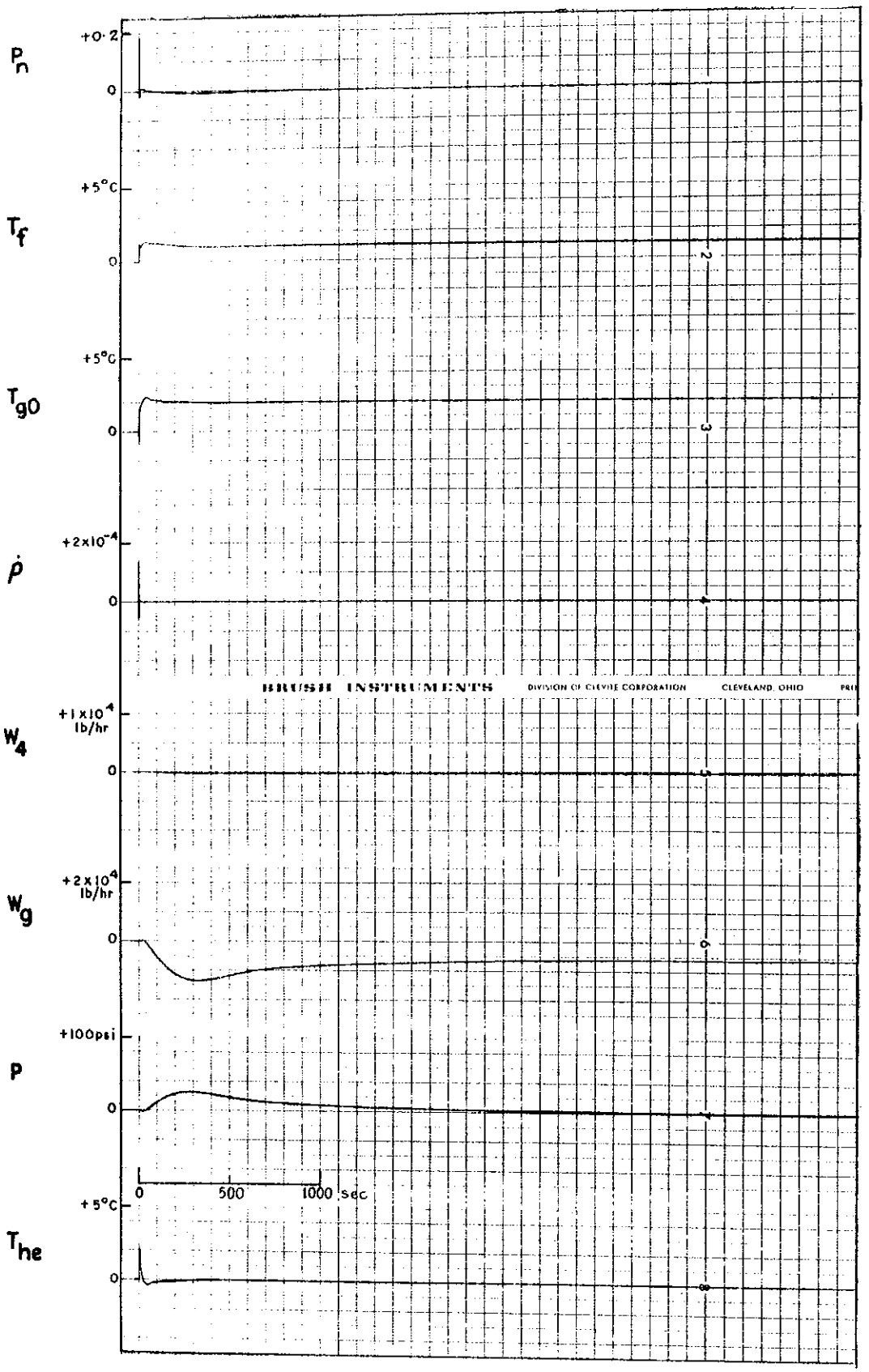

FIGURE 39. SEE TABLE IN SECTION 3.5.2

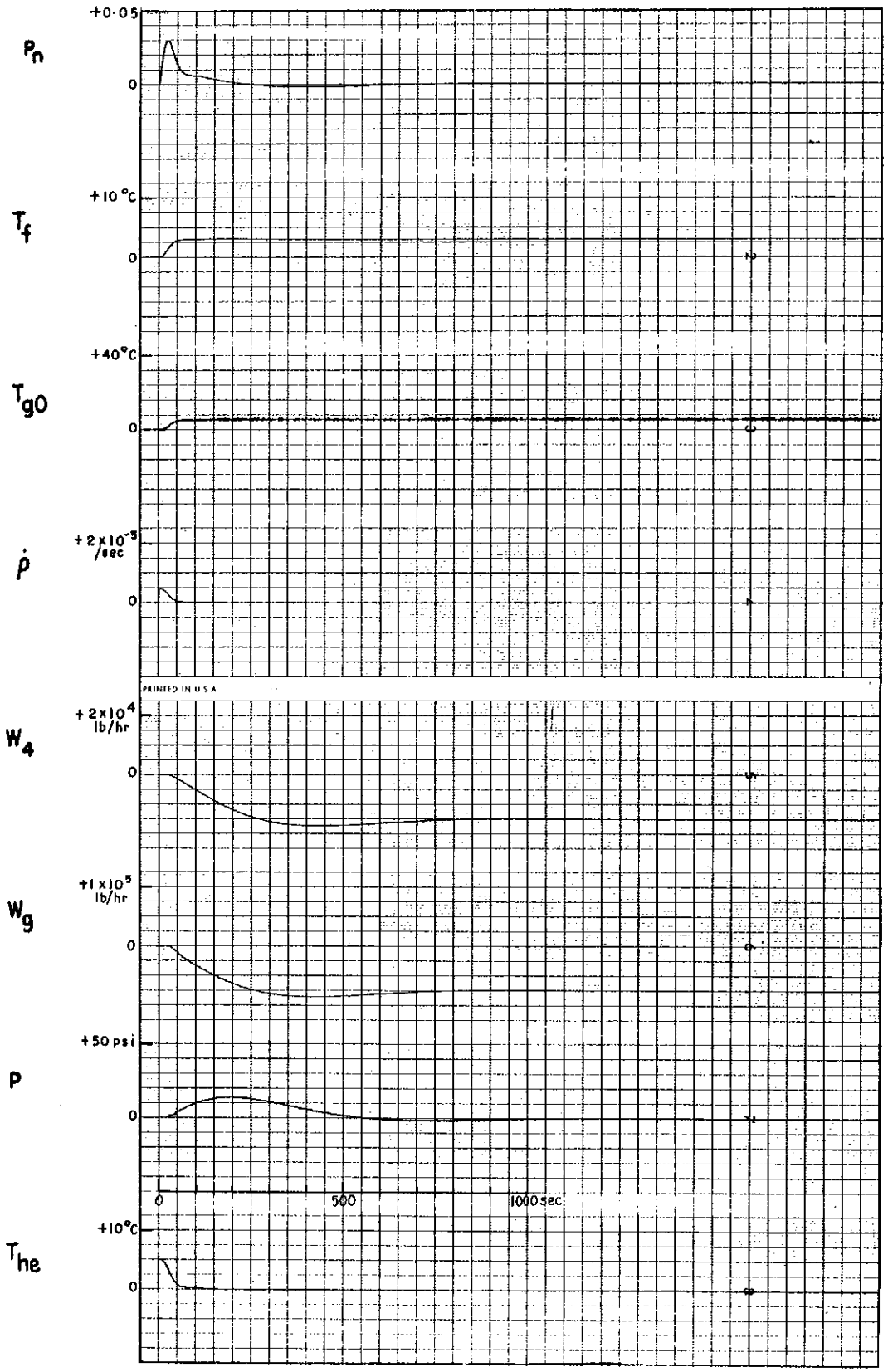

FIGURE 40. SEE TABLE IN SECTION 3.5.2

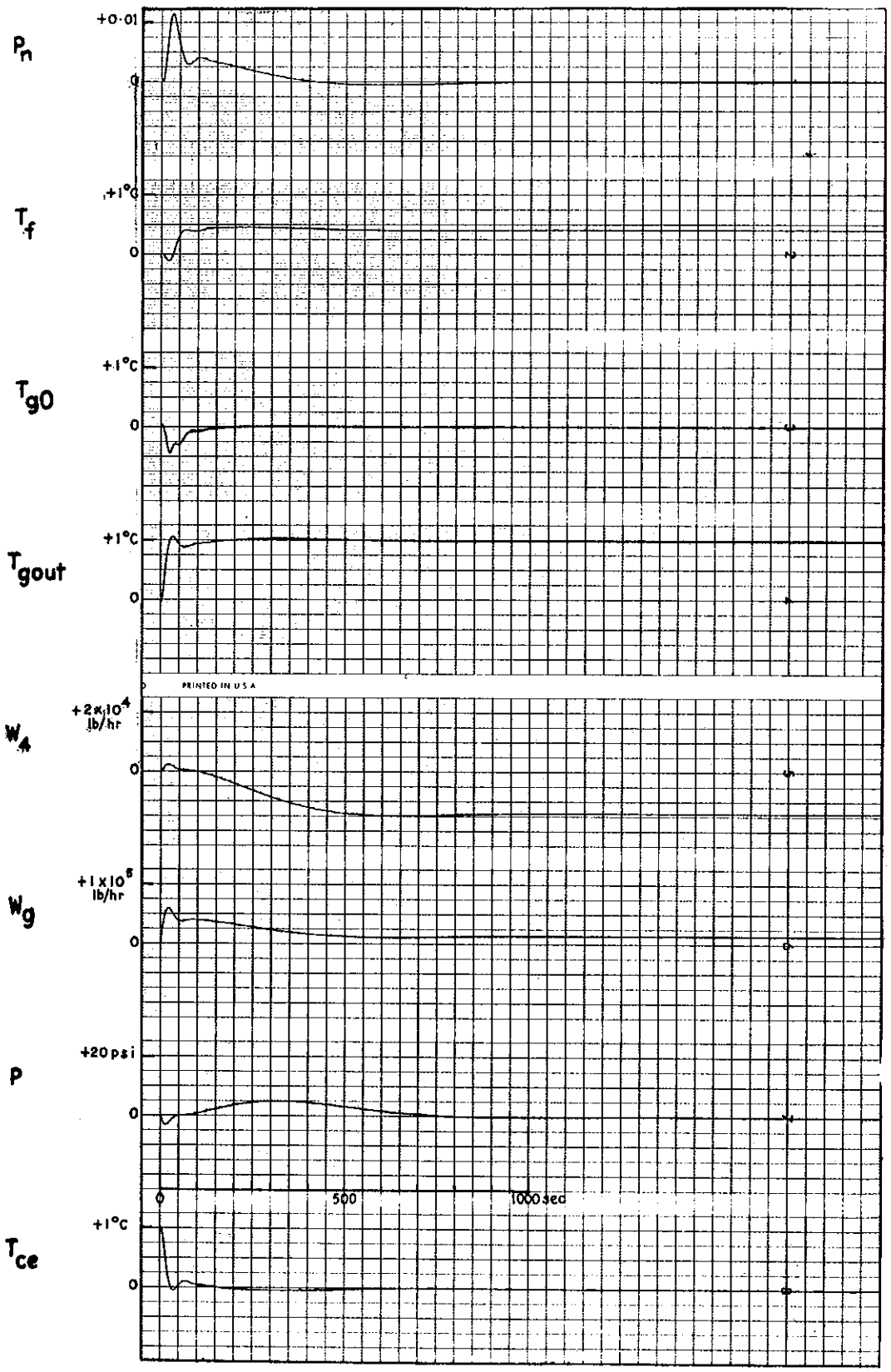

FIGURE 41. SEE TABLE IN SECTION 3.5.2

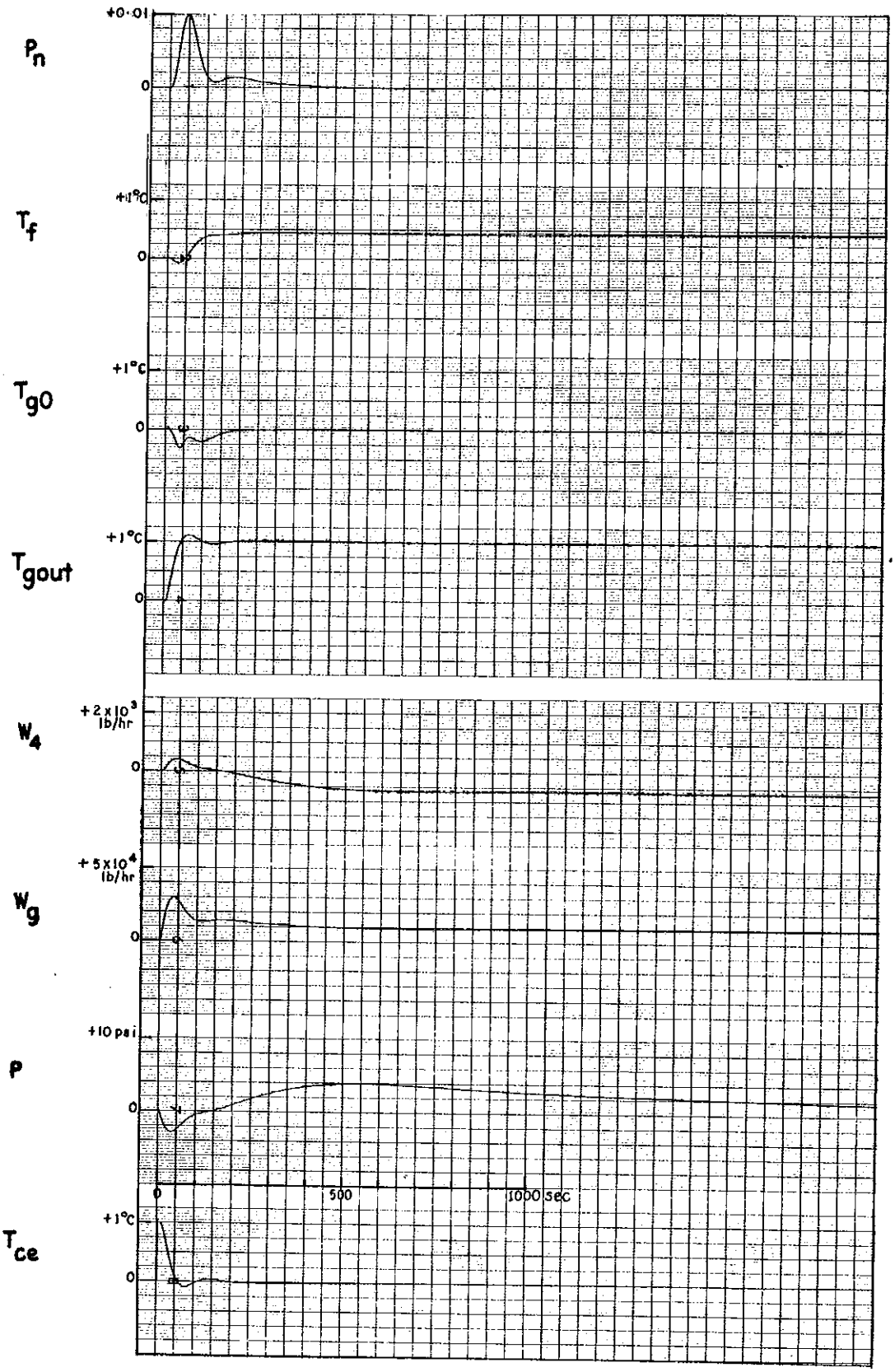

FIGURE 42. SEE TABLE IN SECTION 3.5.2

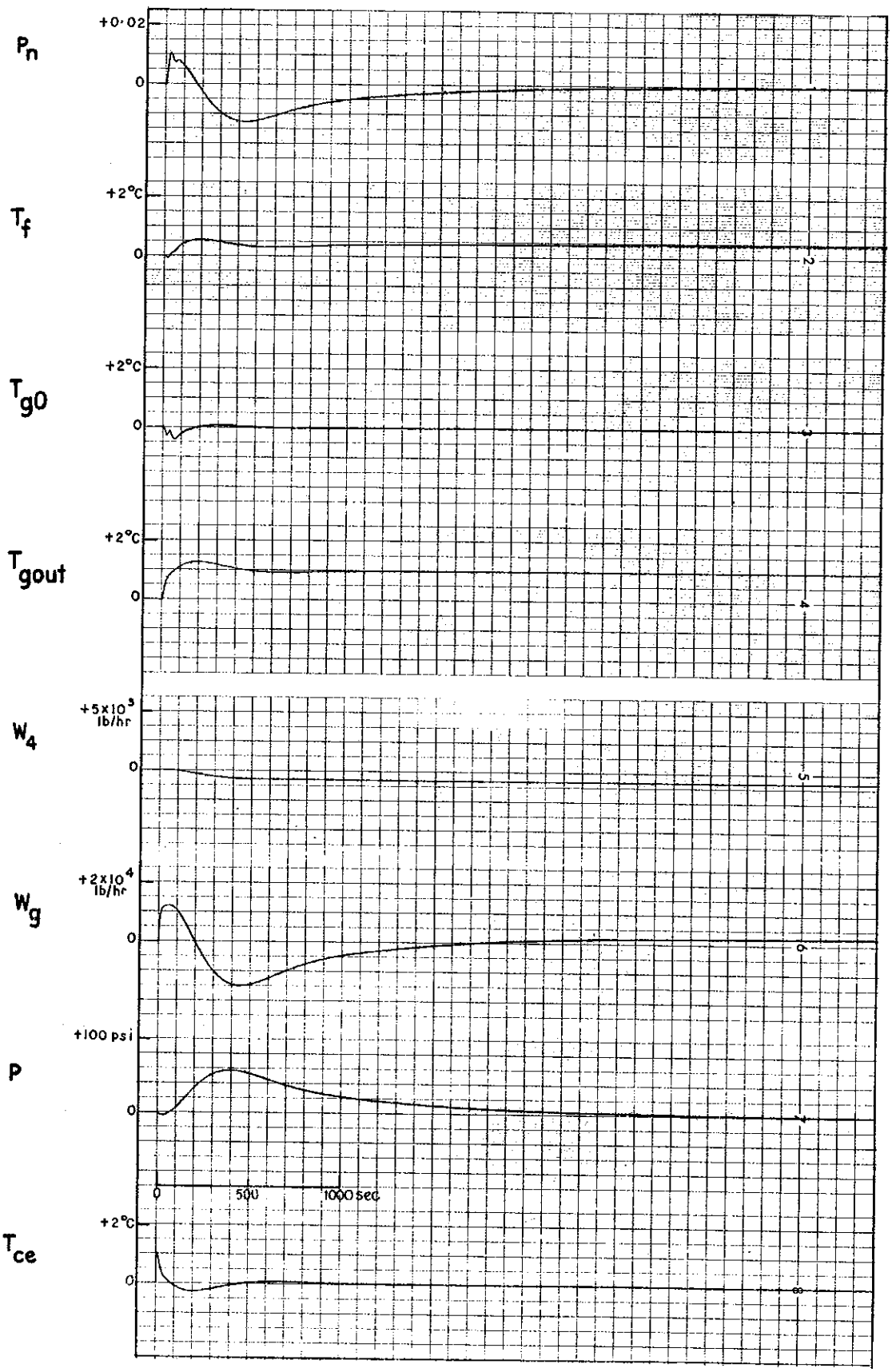

FIGURE 43. SEE TABLE IN SECTION 3.5.2

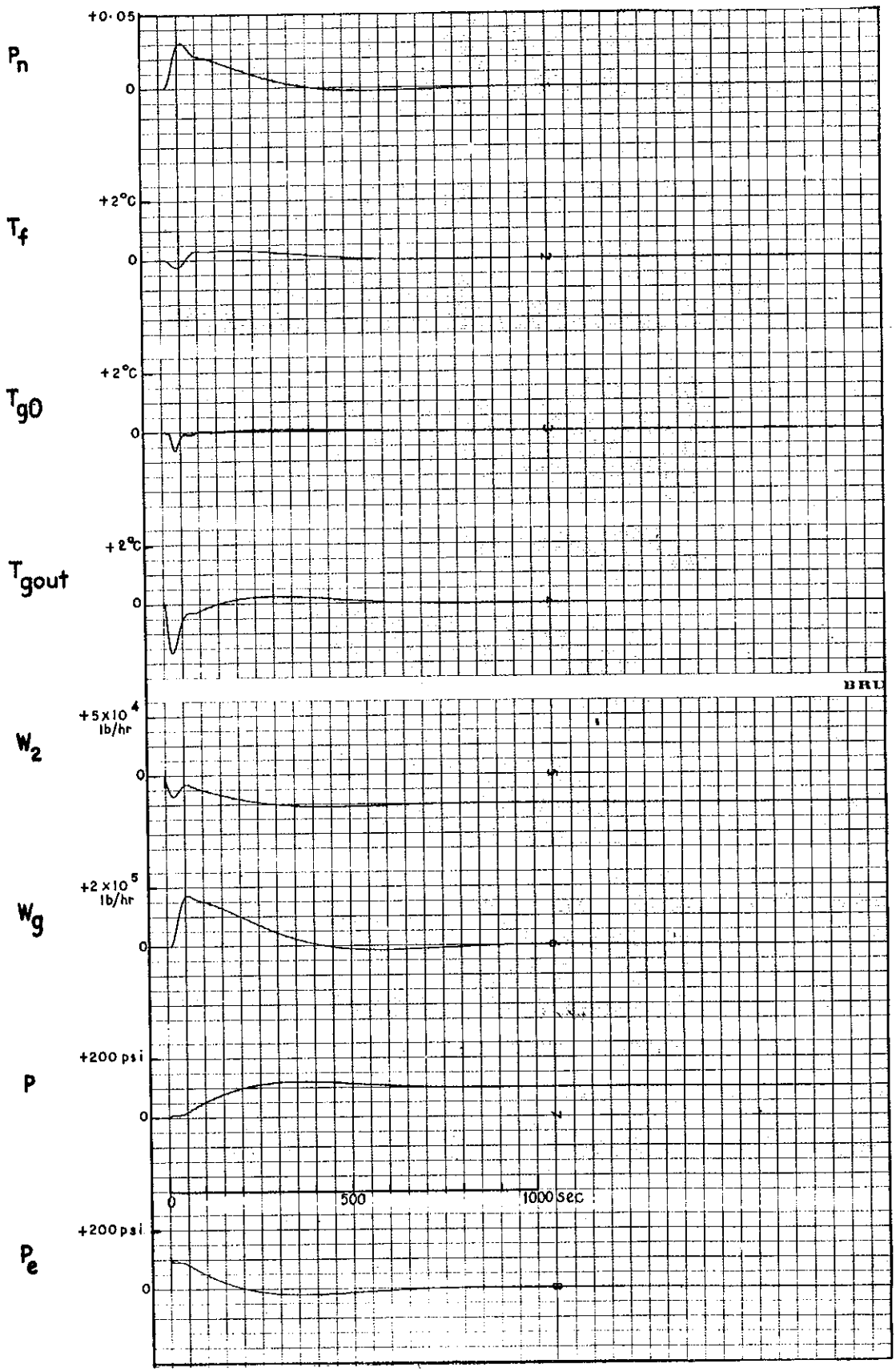

FIGURE 44. SEE TABLE IN SECTION 3.5.2

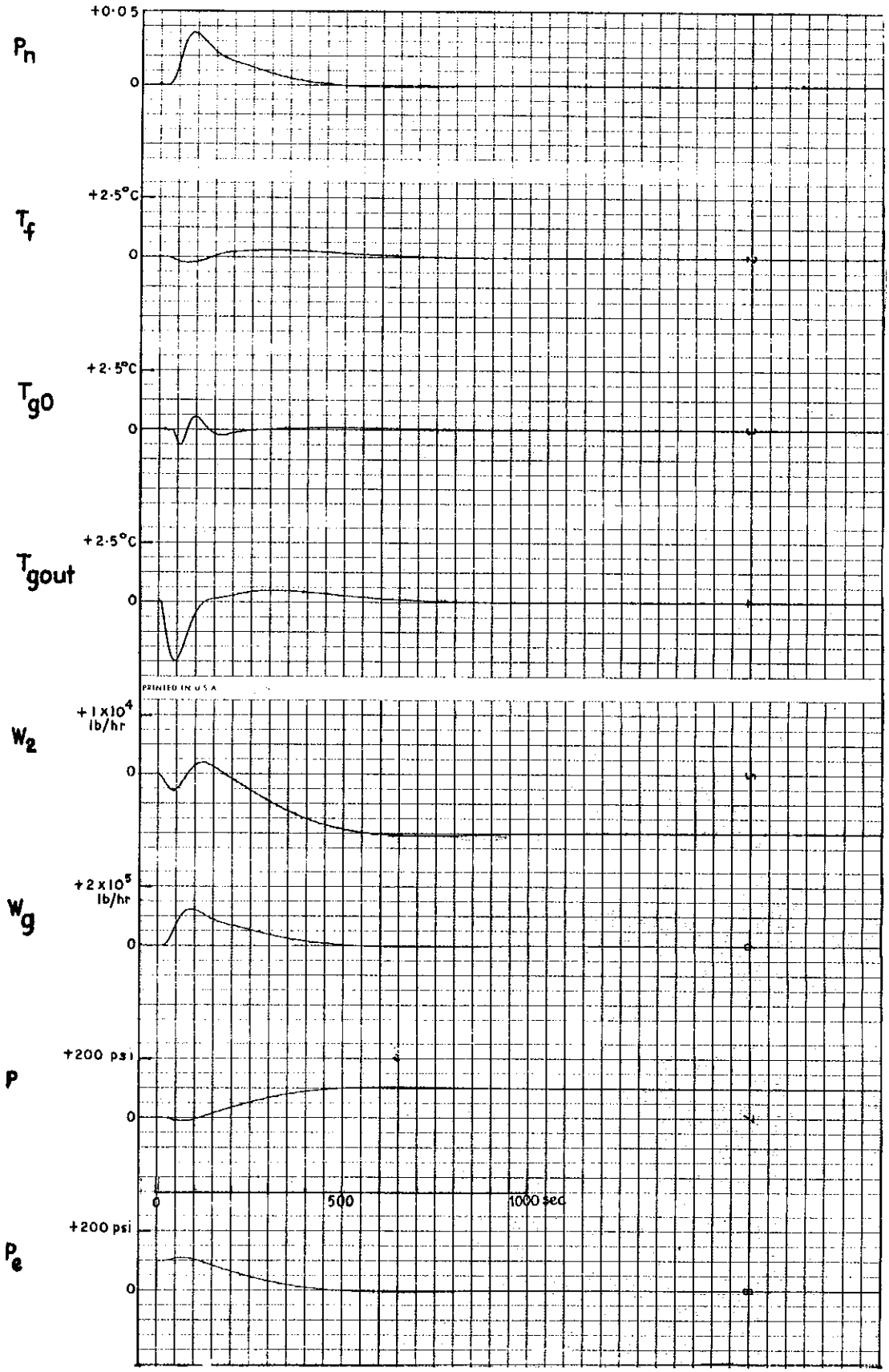

FIGURE 45. SEE TABLE IN SECTION 3.5.2

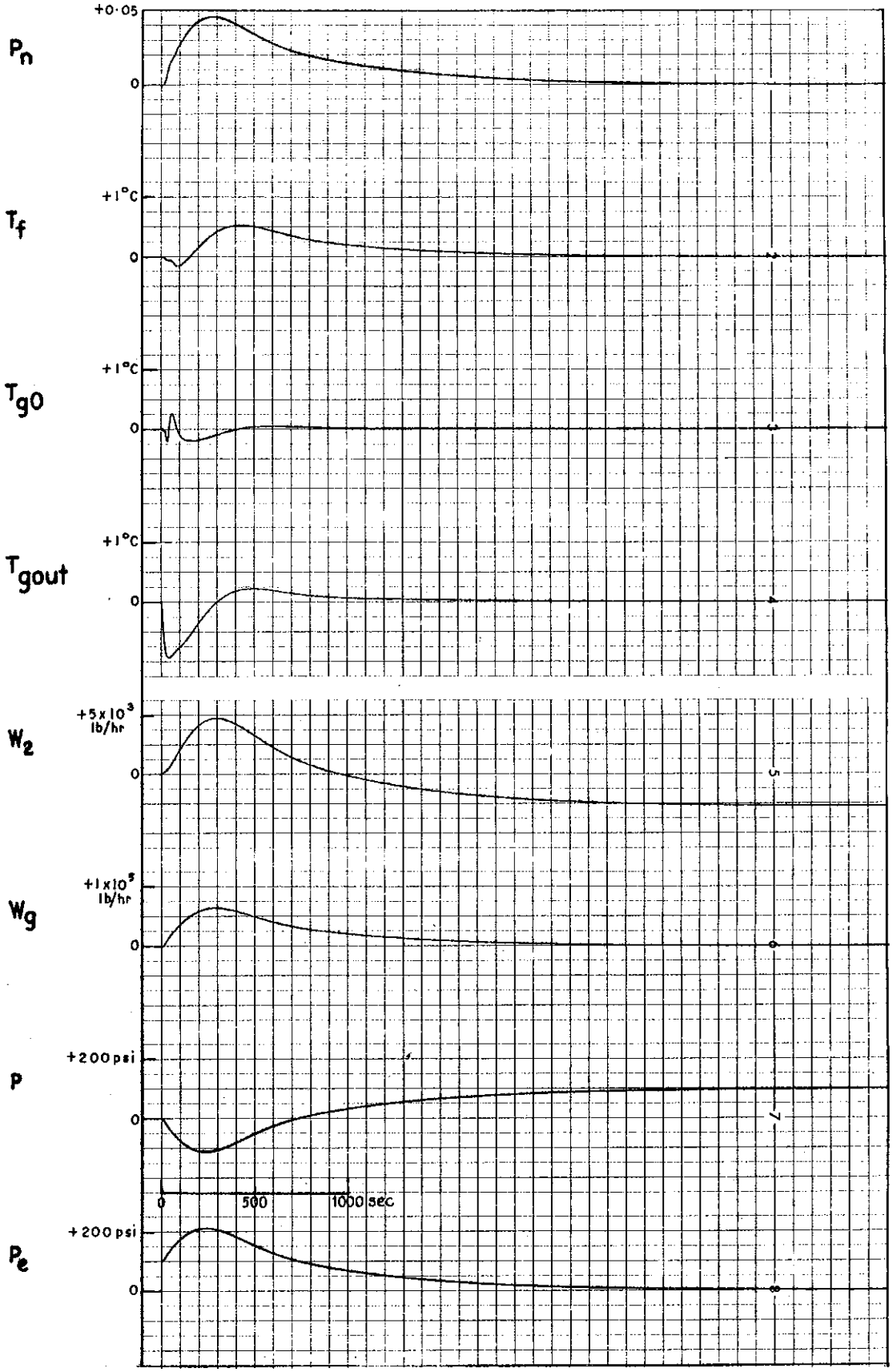

FIGURE 46. SEE TABLE IN SECTION 3.5.2

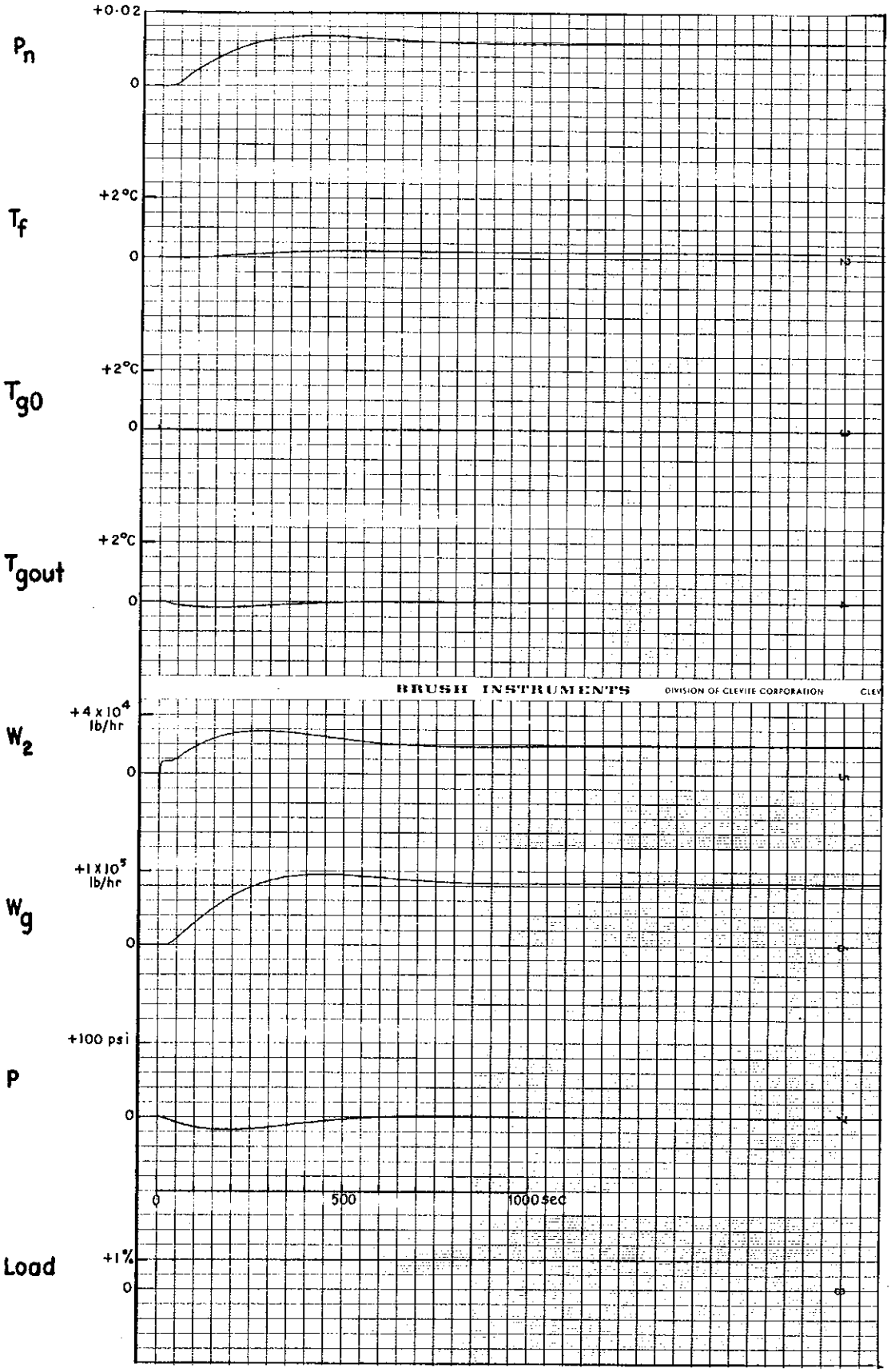

FIGURE 47. SEE TABLE IN SECTION 3.5.2

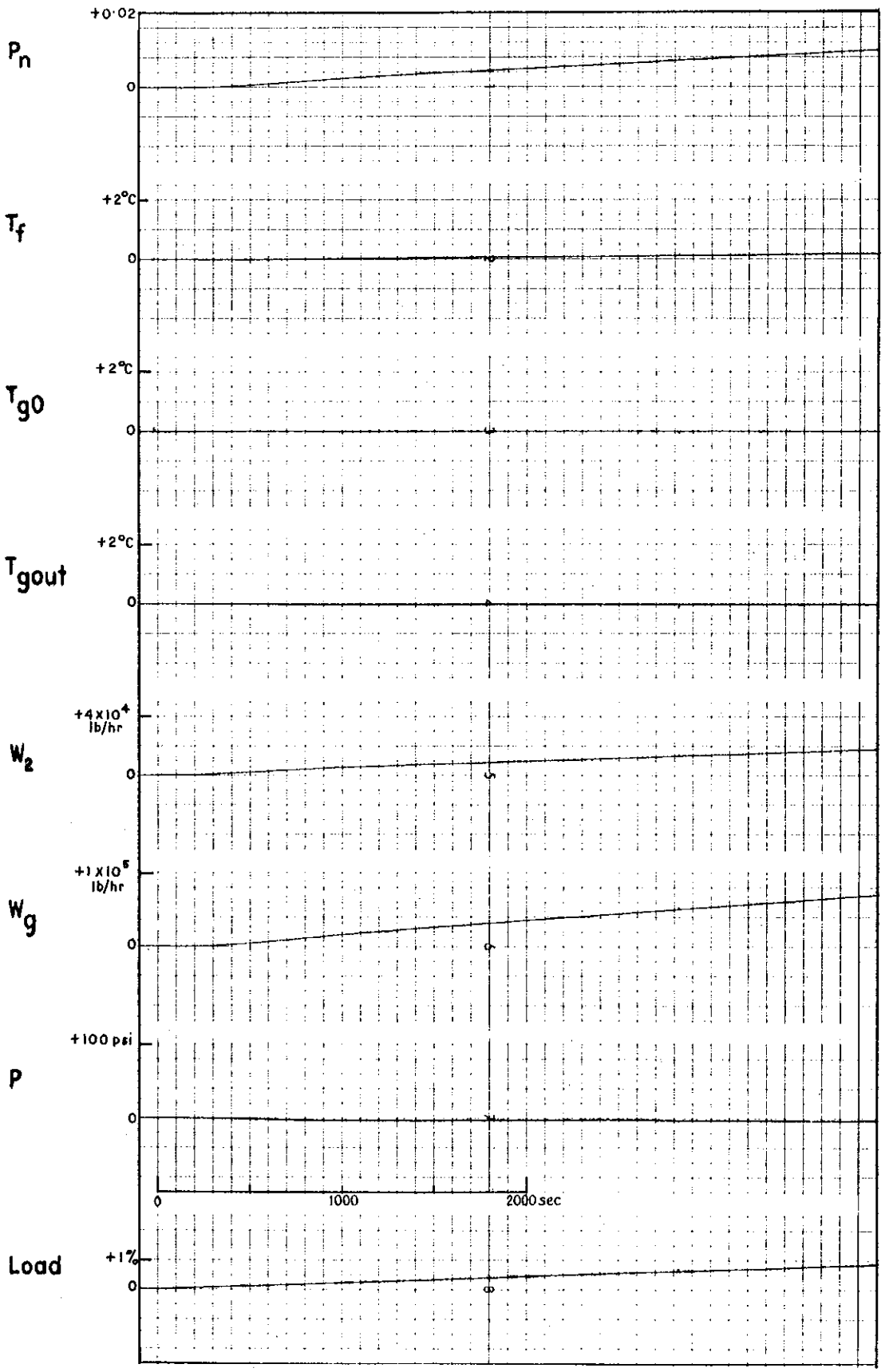

FIGURE 48. SEE TABLE IN SECTION 3.5.2

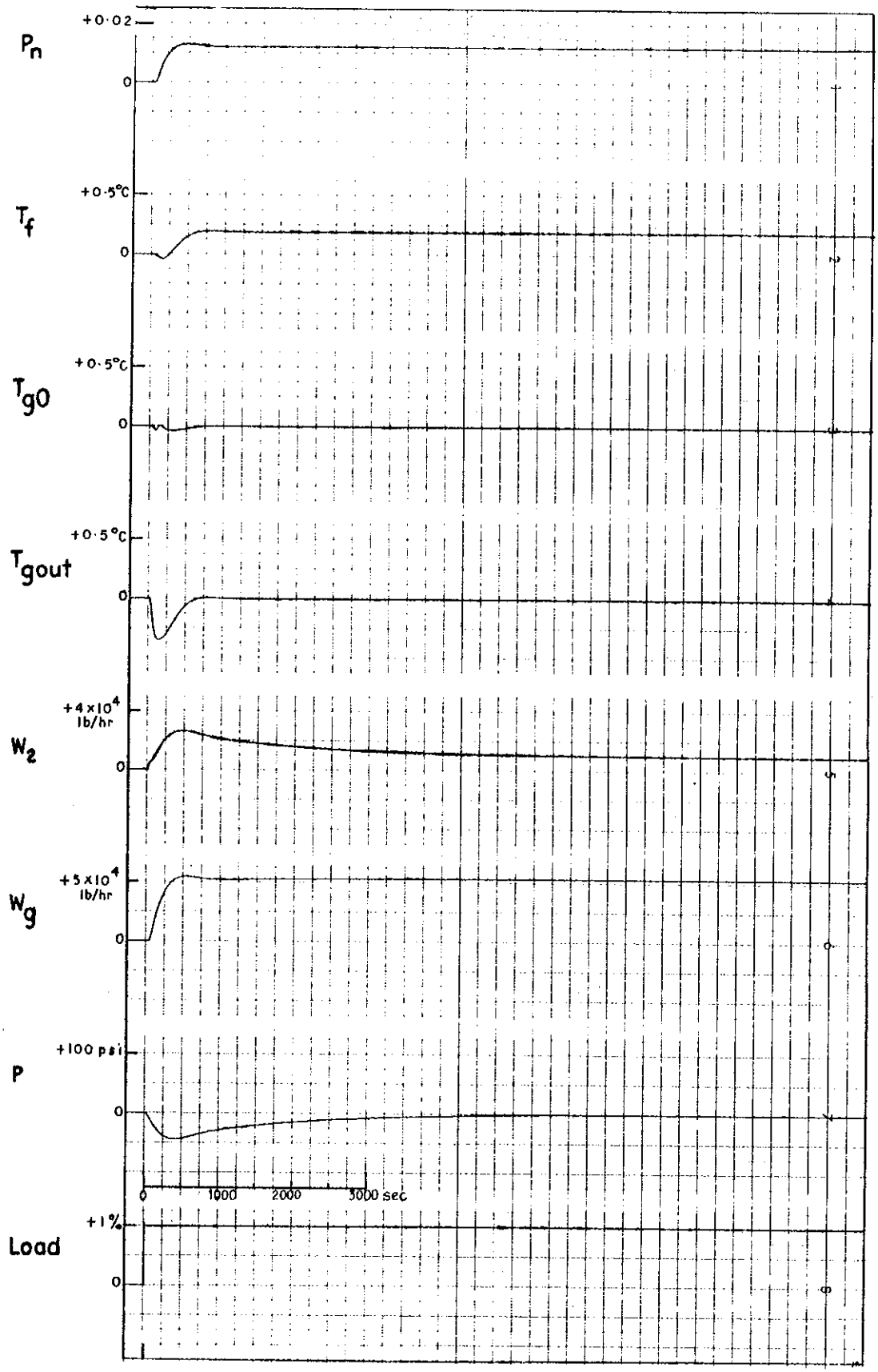

FIGURE 49. SEE TABLE IN SECTION 3.5.2

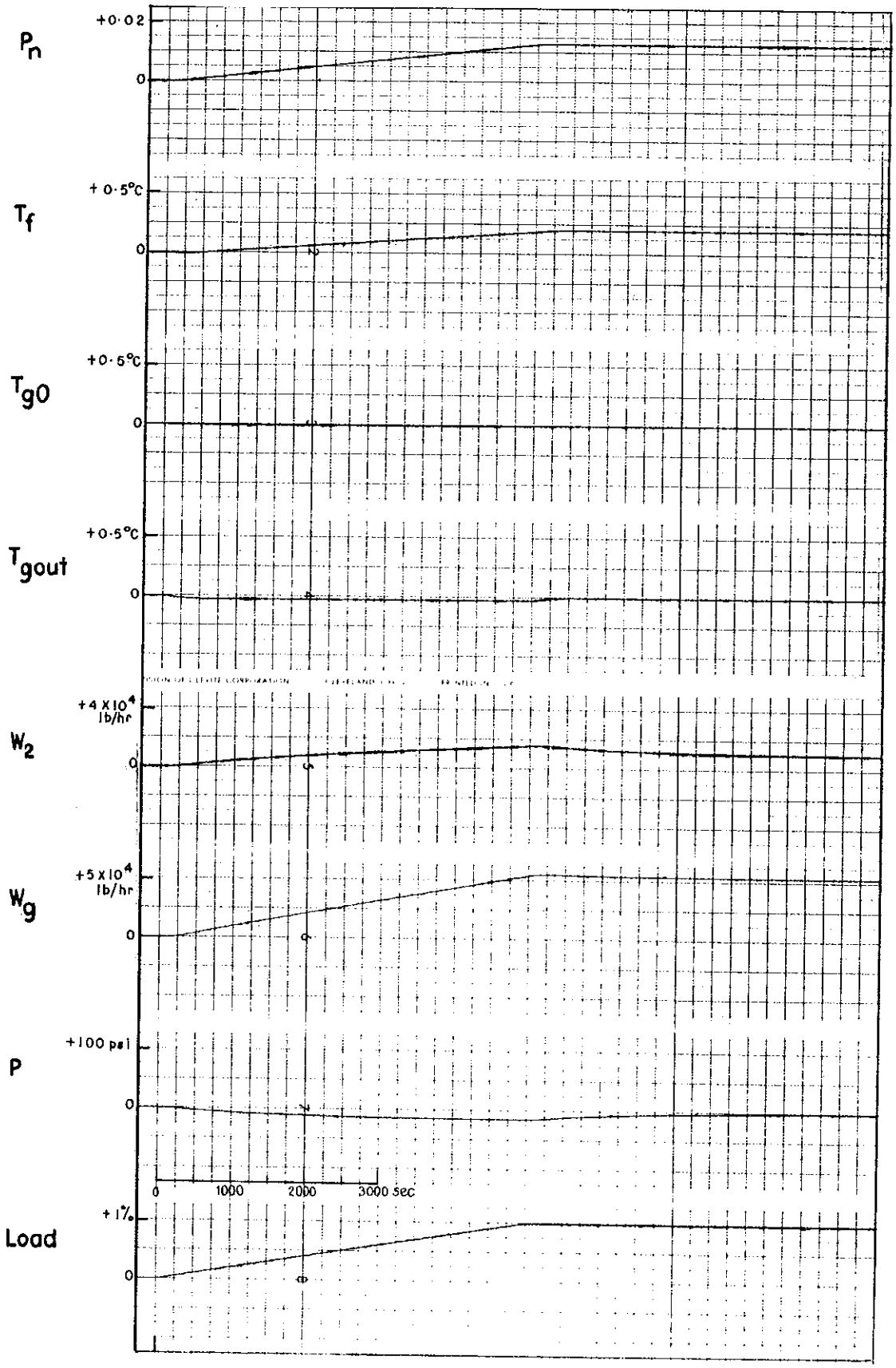

FIGURE 50. SEE TABLE IN SECTION 3.5.2

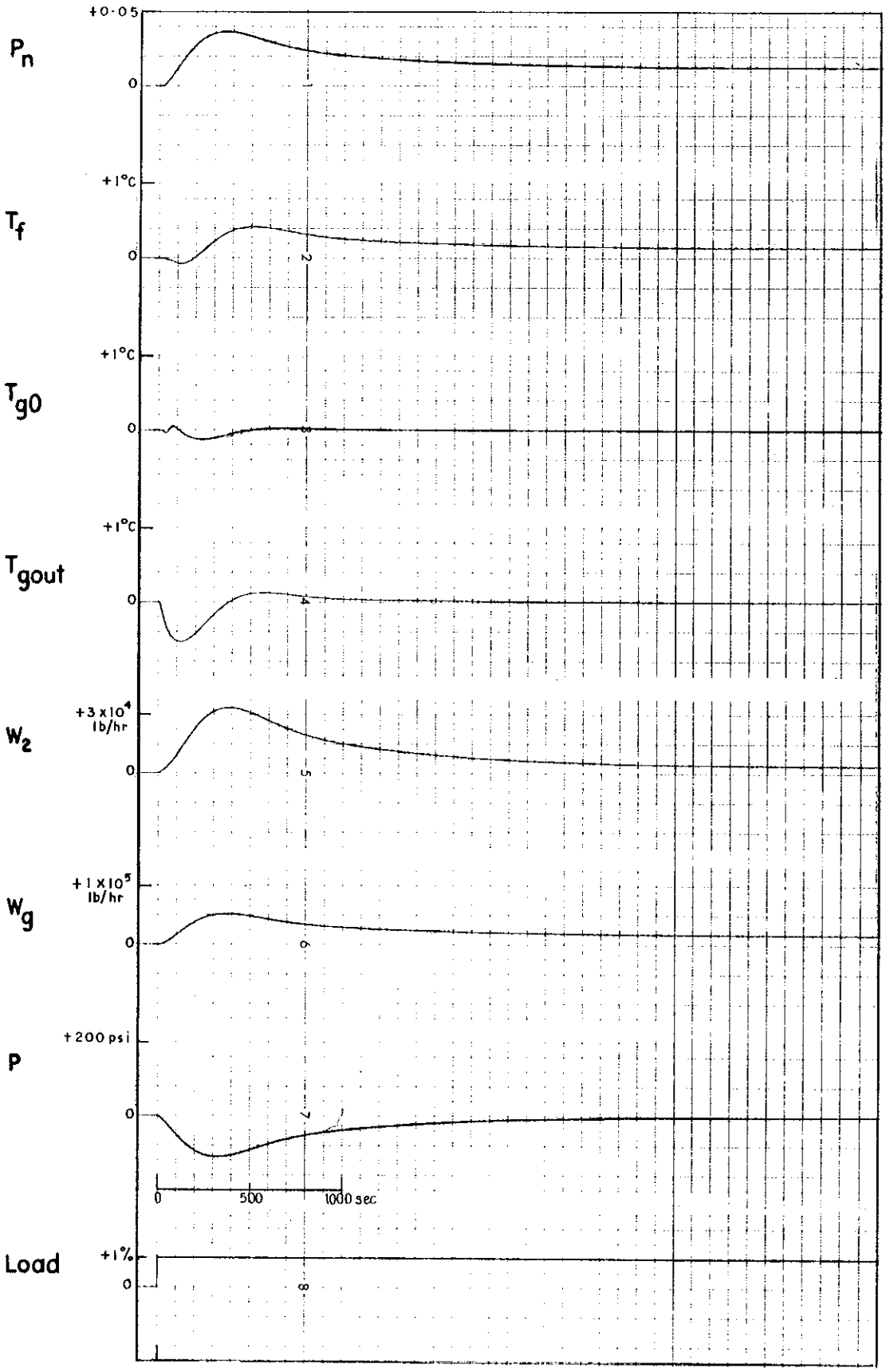

FIGURE 51. SEE TABLE IN SECTION 3.5.2

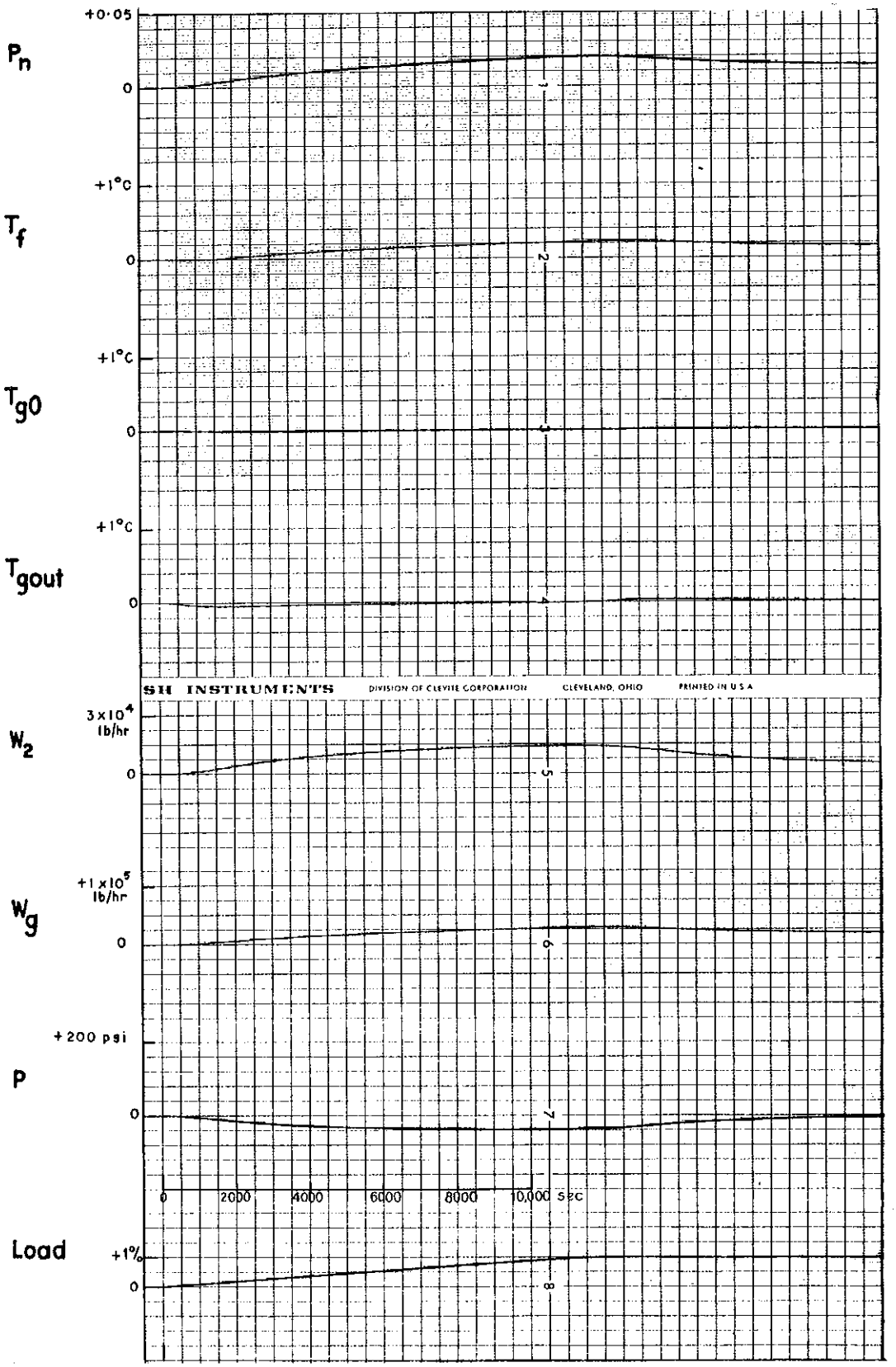

FIGURE 52. SEE TABLE IN SECTION 3.5.2

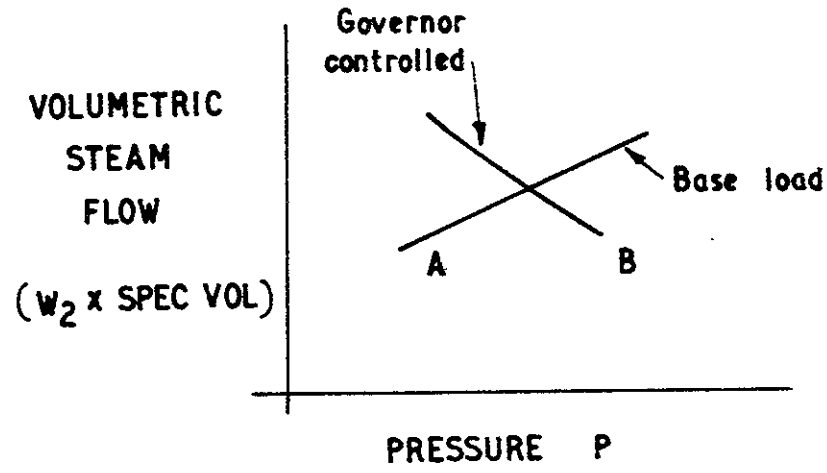

FIGURE 53. STEAM FLOW v. PRESSURE FOR A BASE-LOAD AND A GOVERNOR-CONTROLLED TURBO-ALTERNATOR

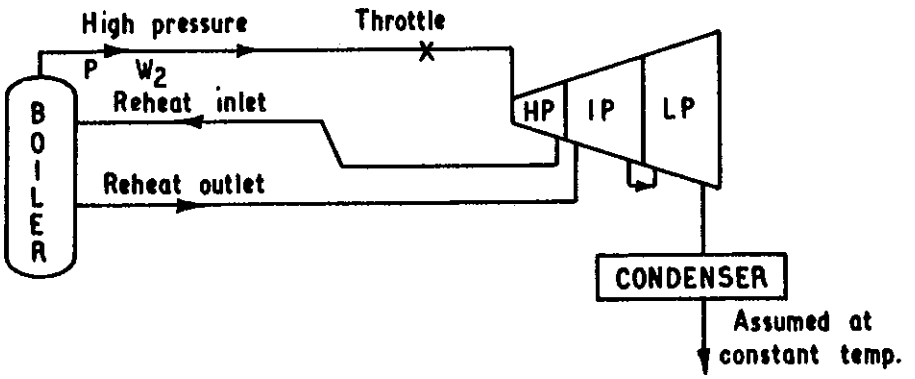

(a) SCHEMATIC LAYOUT OF STEAM CIRCUIT

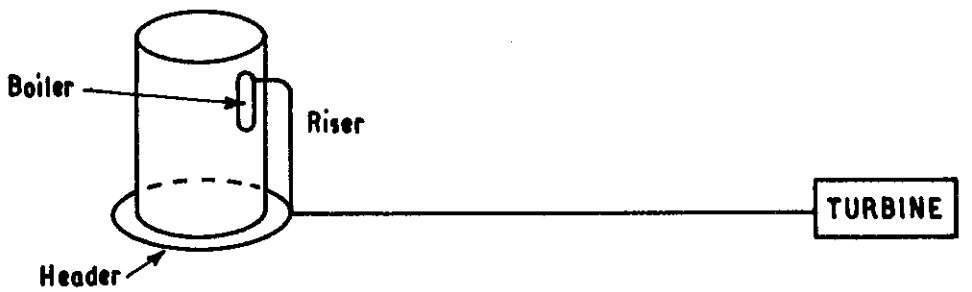

(b) ARRANGEMENT OF STEAM DUCTS

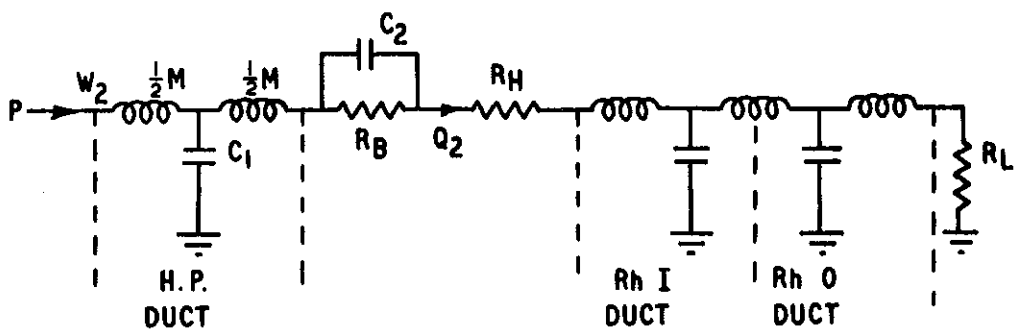

(c) EQUIVALENT CIRCUIT FOR THE STEAM SYSTEM OF (a)

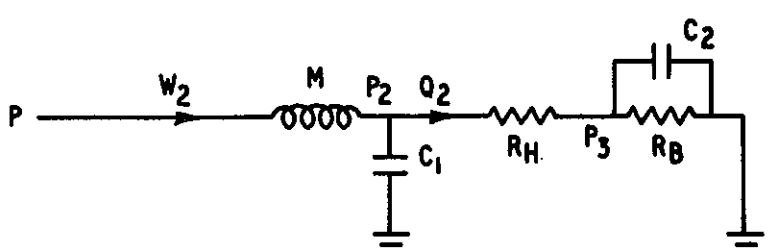

(d) SIMPLIFIED EQUIVALENT CIRCUIT

FIGURE 54. SIMPLIFIED REPRESENTATION OF THE STEAM CIRCUIT

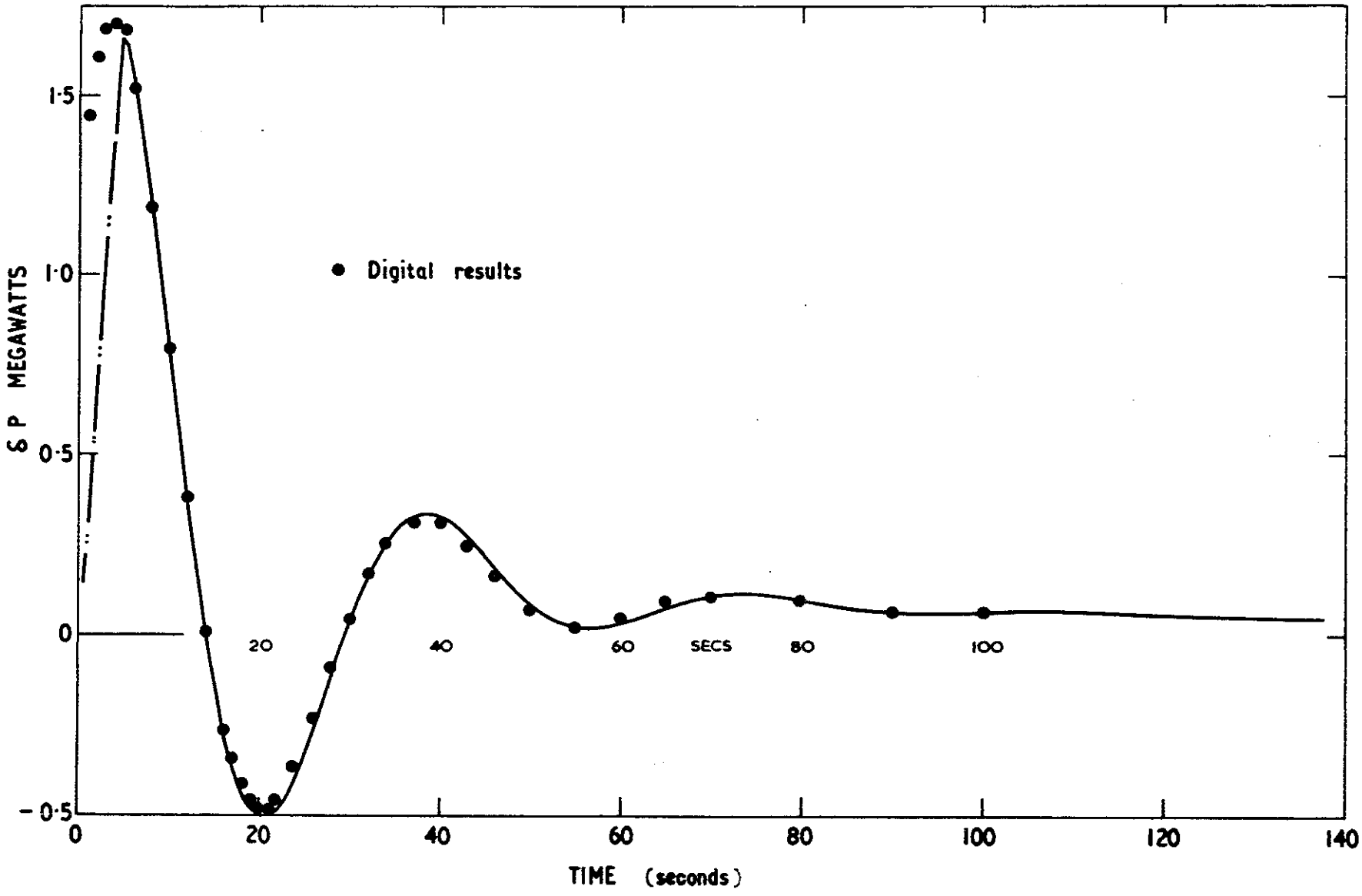

FIGURE 55. REACTIVITY STEP APPLIED TO THE REACTOR KINETICS, HEAT TRANSFER AND FLUX FEEDBACK CIRCUIT, 60 PERCENT LOAD, (α+)